The Hong Kong Polytechnic University
Department of Applied Biology and Chemical Technology

MEASUREMENT OF ATMOSPHERIC HYDROCARBONS AND AIR QUALITY IN HONG KONG

A thesis submitted in partial fulfillment of
the requirements for the degree of

Master of Philosophy

by

Cheung Tsz-fai Vincent, BSc(Hons.)

1998

Abstract of thesis entitled "Measurement of Atmospheric Hydrocarbons and Air Quality in Hong Kong" submitted by Mr. Cheung Tsz-fai Vincent for the degree of Master of Philosophy at The Hong Kong Polytechnic University in August 1998.

A dedicated air sampling and gas chromatographic analysis system was built to measure parts-per-trillion (pptV) to parts-per-billion (ppbV) levels of non-methane hydrocarbons (NMHCs) at a coastal rural background air monitoring station in Hong Kong. The accuracy of analysis was successfully validated by inter-laboratory comparison of calibrated NMHC standards and ambient air samples provided by Dr. D.R. Blake, Department of Chemistry, University of California (Irvine), U.S.A.

C_2-C_6 non-methane hydrocarbons (NMHCs) were measured at the Hong Kong Polytechnic University Regional Air Monitoring Station for the period October, 1995 to March, 1997 on a near daily basis. The annual total C_2-C_6 NMHC concentrations showed a clear high-winter and low-summer seasonal variation trends, though pollution episode days due to influence of micro-meteorological conditions were occasionally observed throughout the year. Monthly averages of total C_2-C_6 NMHC concentrations were in the range of 10 - 50 ppbC (on per carbon basis), with alkanes accounting for 60% of the total concentration, which are typical of the NMHC levels reported for rural/non-urban environments with emissions originating from anthropogenic sources.

The seasonal variation of NMHCs is attributed to the dominant influence of outflow of Asian continental air masses in the winter, and inflow of Pacific maritime air masses in the summer. The origin of air masses reaching Hong Kong was analyzed and classified by 10-day back trajectory calculations.

Relatively high levels of measured NMHCs, characterized by a higher % acetylene content, were associated with continental air masses encountered in Hong Kong. The winter NMHC concentrations show very good linear correlations ($r^2 > 0.8$) with acetylene and CO, suggesting that fossil fuel combustion and biomass burning are a major contributory sources of NMHC pollution derived from the outflow of Asian continental air masses. Good linear correlations ($r^2 > 0.8$) were also found between signature NMHC species derived from liquefied petroleum gas (LPG), suggesting the co-occurrence of LPG leakage as another NMHC contributory source.

In summer, the NMHC levels were much lower than that in the winter and showed no clear or very weak correlation among NMHC species of known anthropogenic sources. This was supported by back trajectory analysis that maritime air masses from South and West Pacific Ocean could reach Hong Kong

in the summer months. Thus the composition of C_2-C_6 NMHCs may serve as signature fingerprints of Pacific maritime air masses encountered in Hong Kong.

At the monitoring site, the measured NMHC levels in some occasions could be strongly influenced by the changes in local meteorological conditions. More than 10 folds increase in total NMHC concentration was observed on local episode days when surface winds were sweeping urban pollutants direct onto the air monitoring station.

During cold front days in the winter, the measured total NMHC levels were increased by 2 folds due to the greater anthropogenic emission loading in the continental air masses. The chemical composition and characteristics of the continental air masses vary with time of the cold front period. The surface wind speed increased to 14 m/s or higher, contribution from photochemical "less aged" air masses, as indicated by the highest % content of reactive species like propylene and ethylene, were observable in the associated NMHC measurements.

Our data set is in quantitative agreement with the findings of the NASA Pacific Exploratory Missions (PEM-West A & B) which also observed higher NMHC levels during the late winter and early spring, and lower NMHC levels in the summer and early autumn. The PEM-West A & B studies were aircraft-based measurements with flight path stretching a large part of Western Pacific (north to Japan, and south to Singapore and Indonesia), but only of limited time span. In contrast, our data set is more comprehensive in providing information on meteorological, micro-meteorological, estimation of emission sources and time span effects on pollution levels at Hong Kong and its neighboring regions.

TABLE OF CONTENT

LIST OF TABLES

LIST OF FIGURES

ACKNOWLEDGMENT

Words cannot be expressed in how I am indebted to Dr. C.W. Tsang, my chief supervisor, for his guidance and support in this project.

I would like to thank Dr. T. Wang and Dr. K.S. Lam, my co-supervisors, for all the wonderful opportunities and freedom they granted me throughout my graduate career in the Hong Kong Polytechnic University.

It is very difficult to adequately express my appreciation to Mr. Li Ping, who has been working in solving problems, whether in personal matters and research difficulties, and sharing his learned experience. I am very proud and honored to have him as my friend.

I would also like to thank

Prof. M. Anson, Dean of Faculty of CLU and the coordinator of this project, for his support in my work;

Prof. K.Y. Wong for his the kind help in this project;

Dr. Donald R. Blake, Department of Chemistry, University of California-Irvine, for the kind support in the inter-laboratory experiment and sampling equipment, and the invaluable discussion and encouragement in my project;

Dr. James P. Greenberg, National Center for Atmospheric Research, for the supply of sampling canisters;

Dr. Patrick B. Zimmerman, National Center for Atmospheric Research, for his helpful discussion in my project;

Dr. Joyce Harris, Climate Monitoring and Diagnostic Laboratory, National Oceanic and Atmospheric Administration, for the kind help in supplying the back trajectories

All technical staff in the Department of Applied Biology & Chemical Technology, Department of Civil & Structural Engineering, and Hong Kong Telecom for their technical assistance and support, and station maintenance.

Finally, I would like to acknowledge the support of the Research Committee of the Hong Kong Polytechnic University for the funding of this project.

SECTION I: BACKGROUND

1. *Introduction*

1.1. Brief Description of the Atmosphere

The atmosphere is a thin layer of gases that covers Earth's surface. It nurtures life on Earth by providing a reservoir of gases, including oxygen for respiration and carbon dioxide for plant photosynthesis. It provides nitrogen for nitrogen-fixing bacteria and ammonia-manufacturing plants to produce chemically-bound nitrogen, an essential component of life molecules. It also moderates and stabilizes Earth's temperature and serves as a protective blanket to absorb damaging ultraviolet radiation from the Sun and cosmic rays from outer space.

One of the important functions of the atmosphere is to remove pollutants by atmospheric purification processes including chemical degradation, wet and dry deposition, and the uptake by the oceans and Earth. These processes stabilize the atmosphere by cycling the gaseous constituents between the atmosphere, the vegetation, the oceans, and the biological organisms. Although the Earth's atmosphere is huge and has an enormous ability to resist and correct for detrimental change, human activities can have a significant impact on it because of the over-burdening of the atmospheric purification processes. The adverse effects of this practice include damage to vegetation and materials,

shortening of human life, and alternation of the characteristics of the atmosphere.

Industrialization and modernization causes the expansion of energy production and industry, which consumes vast amounts of raw materials and produces a large quantity of pollutants. Biomass and fossil fuels burning, tropical forest destruction, and spread of animal grazing and agriculture, release large quantities of carbon dioxide and greenhouse gases into the atmosphere. The significant effects are global warming and substantial climatic change. The use and release of chlorofluorocarbon (CFC) compounds as refrigerant fluids and propellants results in stratospheric ozone depletion, permitting more harmful ultraviolet radiation to reach Earth's surface. Transportation practices nowadays have a great reliance on automobiles, and vehicle emission is a significant source of air pollutants in most urban locations. One of the important consequence of air pollution is photochemical smog formation, which is a serious environmental problem that poses significant hazards to living things and materials.

In order to assess the effect man-made emissions may have on the atmosphere as a whole, systematic research in atmospheric chemistry is essential to have a detailed understanding of the photochemical reactions of these pollutants, the predominant removal mechanisms, and the effects of their reaction products. Apart from that, the study of atmospheric chemistry can play a key role in identifying these pollution problems and contribute to

environmental preservation, such as imposing suitable measures and controls to the pollution sources, switching to alternate energy sources, and increasing use of energy conservation measures.

With accelerated industrial and economic growth, anthropogenic hydrocarbon emissions from the Asia continent is expected to increase rapidly in the coming years. They will become a growing factor affecting the distribution and dispersion of atmospheric trace gas pollutants and oxidants in the Pacific Rim, and globally in the long term. However, there is a lack of data reports on the NMHC levels and associated photochemical studies in this Western Pacific region. In response to this urgent need and growing concern about air quality in Hong Kong, a background air monitoring station was established by the Hong Kong Polytechnic University in 1993 with the aim of conducting research towards the understanding of basic air quality and atmospheric chemistry in this region. The present study is part of the research effort conducted by the research team at the air monitoring station, with focus on the measurement and interpretation of nonmethane hydrocarbon (NMHC) data collected at the Station.

1.2. Study of Hydrocarbons

1.2.1. Characteristics of Hydrocarbons

Much of the reactive carbon entering the atmosphere is in the form of nonmethane hydrocarbons (NMHCs). They have an enormous complexity in

chemical compositions, with more than 10^3 species in the atmosphere, including saturated compounds (alkanes), unsaturated species with one carbon-carbon double bond (alkenes) or two double bonds (alkadienes), acetylene type compounds (alkynes), and benzene derivatives or aromatic compounds (arenes). The amount produced, in the range of 500-1000 Teragram per year, is comparable to or even larger than that of methane, the simplest and the most abundant hydrocarbon in the atmosphere[1].

Hydrocarbons are important atmospheric constituents both biologically and chemically. Biologically, they serve as a carbon source for terrestrial micro organisms, plant hormones (e.g. ethylene), pheromones, and a contributing factor in controlling plant selection and grazing pressure through vegetation palatability. They also play an important role in tropospheric chemistry. They influence atmospheric acidity because products of their oxidation, such as peroxy radicals, facilitate the oxidation of sulfur and nitrogen oxides to sulfuric and nitric acids. On a global scale, hydrocarbon oxidation leads to products such as carbon dioxide (CO_2) and ozone (O_3), which absorb outgoing infrared radiation and thus can contribute to global warming. Carbon monoxide (CO), which is also a product of hydrocarbon oxidation, is not a primary greenhouse gas; however, it can affect climate change indirectly through its reaction with atmospheric hydroxyl (OH) radical. Increases in CO will reduce OH levels. Since the OH is the major sink for methane, the reduction in OH leads to

accumulation of this hydrocarbon, which is one of the more important greenhouse gases in the troposphere.

NMHCs are derived from both anthropogenic and natural sources, and are source specific. The atmospheric lifetimes of the NMHCs can range from a few hours to several months (See Table 1.1). With different contributors and vastly different photochemical reactivities, and the change in the spectrum of the concentrations in different species during their residence in the atmosphere, they are expected to develop large gradients of mixing ratios between the source regions and the remote troposphere. When the NMHC data are combined with back trajectory analysis, they provide estimation on the relative age of air masses and the characterization of the anthropogenically induced chemical signatures in the atmosphere. Data collected are also used as the basis for source apportionment[2] and the input to atmospheric models for studies of pollutant interactions in order to establish regulatory control strategies.

The degradation of NMHCs is by oxidation reaction with OH, O_3. NO_3 and other oxidants[3] and the initial products are aldehydes and oxygenated organic radicals. They are also noteworthy as an important source of atmospheric carbon monoxide[4,5].

1.2.2. Emission Sources of Methane & NMHCs

NMHCs are organic pollutants with both anthropogenic and natural sources. They are released in all anthropogenic activities with the use or transfer of energy. Also there are large natural emissions from terrestrial and oceanic sources. Common anthropogenic sources in industrialized countries include emissions from transportation and stationary fuel combustion, refining and transportation of gasoline, natural gas production and seepage, forest fires, open burning, and incineration. Biomass burning is an added component in less developed part of the world. For natural sources, two major types are identified: oceanic and plant emissions. The oceanic sources of NMHCs have been investigated in seawater[6,7,8] and found that alkanes and alkenes are significantly supersaturated in seawater compared to their atmospheric burden. Attempts to quantify both anthropogenic and natural sources of NMHC for the United States and the world have been conducted in a number of studies[9,10,11,12,13].

Sources of individual hydrocarbon species in the global atmosphere, both anthropogenic and natural, were based on estimates from available emission inventories[5,9,10,11,12,13,14,15,16,17], extrapolations of fuel usage, data collected in the industrial world[11,12,17,18], and determination from field and laboratory studies[8,19,20,21,22,23,24].

Table 1.1 : Estimated Atmospheric Lifetimes of Selected Nonmethane Hydrocarbons (NMHCs)

Species	OH Rate [a]	Lifetimes (Days) [b]
Ethane	0.27	78
Ethyne	0.90	23
Propane	1.15	18
Benzene	1.23	17
i-Butane	2.34	9
n-Butane	2.54	8
i-Pentane	3.90	5
n-Pentane	3.94	5
n-Hexane	5.61	4
Toluene	5.96	3
Ethene	8.52	2
Propene	26.3	0.8
1-Butene	31.4	0.7
1-Pentene	31.4	0.7
Isoprene	101	0.2

Rate constants for NMHCs taken from *Atkinson* [1990].

[a] Units, 10^{-12} x k(298)

[b] Lifetimes of hydrocarbons are calculated by comparison with the CH_3CCl_3 lifetime of 5.7 years, *Prinn*, [1992].

Acetylene and ethylene are well-known signature compounds for fossil fuel combustion[25], and acetylene is a near exclusive product of automobile emissions (100% from car exhaust, See Table 1.2), and therefore most commonly used as a tracer of vehicle emissions in urban areas. A biomass burning source of 2 to 4 Tg/yr (Teragram per year) and auto emission source of 1 to 2 Tg/yr is estimated[1]. However, a global biomass emissions of 0.7 Tg/yr is also reported[26]. Only a small oceanic source (<0.1 Tg/yr) has been identified[1].

Among the NMHCs, ethane is the most stable, having a lifetime of 78 days (refer to Section 1.2.4). The biomass burning source of ethane is estimated to be 4-5 Tg/yr. Ethane source from oil combustion and natural gas emissions is estimated to be 2-3 Tg/yr. Oceanic source of nearly 1 Tg/yr can also be calculated. Direct biogenic emissions from plants and vegetation cannot be presently calculated but may be significant. Global emission inventory for ethylene was estimated to be 35 Tg/yr (range 18-45 Tg/yr)[1], of which 74% is natural and 26% anthropogenic. About 10% (2-3 Tg/yr) is attributed to oceanic sources.

Propane is not emitted from either the combustion or evaporation of fossil fuel[27]. Biomass burning, natural gas emissions, and oceanic emissions are thought to be the three major sources for propane, with estimated emissions of 1.5-2.5 Tg/yr, 1-2 Tg/yr, and 0.5-1.0 Tg/yr, respectively. Alternate (biogenic)

sources of propane has been suggested to account for the relatively high global concentration of propane at 15-20 Tg/yr.

Combustion is a major source of propylene. Emissions from automobiles and biomass burning are estimated to be about 1.5 and 5 Tg/yr, respectively. The oceanic source of propylene is calculated to be 2-3 Tg/yr.

For butanes and pentanes, they are nearly exclusive products of combustion, natural gas emissions, with minor oceanic sources. In addition, the butanes as well as propane are possible source from leakage of liquefied petroleum gas (LPG)[25], arousing a major concern in many cities because of the common usage of LPG as domestic fuel for cooking and heating[25]. Benzene and toluene are also products of fuel combustion, and also from biomass burning.

The source specificity of the NMHCs allows them to be used as tracers of atmospheric transport[28,29] and to characterize the sources and distributions of this complex group of chemicals. In practice, the NMHCs measured at a monitoring site are derived from a multitude of emission sources. As an example, the estimated results for two urban centers, Los Angeles (USA) and Sydney (Australia) are shown in Table 1.2 for reference

Table 1.2 : Percentage Contribution of Various Sources of Hydrocarbons in (a) Los Angeles, USA and (b) Sidney, Australia

Compound	Location	Car Exhaust	Gasoline spillage	Gasoline evaporation	Natural gas	Industrial processes	Solvents
Ethane	a	7.9	-	-	90.9[a]	-	-
	b	18.2	-	-	82.2	-	-
Propane	a	-	-	3.6	96.4[a]	-	-
	b	1.2	-	7.9	26.6	64.4	-
n-Butane	a	24.0	7.0	40.5	28.2[a]	-	-
	b	14.6	9.3	59.3	4.0	12.8	-
Isobutane	a	16.3	3.5	33.3	46.9[a]	-	-
	b	11.4	6.1	56.2	4.3	22.0	-
n-Pentane	a	47.5	13.3	23.3	15.9[a]	-	-
	b	26.6	24.2	43.7	1.7	-	2.9
Isopentane	a	37.5	14.0	37.3	10.7[a]	-	-
	b	22.6	22.3	53.6	0.9	-	0.9
2-Methylpentane	b	31.1	29.8	21.8	0.8	-	15.7
3-Methylpentane	b	33.1	30.4	20.4	0.8	-	17.3
n-Hexane	b	32.9	28.3	15.0	1.3	-	22.6
n-Nonane	b	7.6	6.5	-	-	-	85.1
n-Decane	b	18.1	8.7	-	-	-	73.1
Ethene	b	98.9	-	-	1.4	-	-
Propene	b	49.9	-	-	0.3	49.8	-
1-Butene		67.3	3.3	29.4	-	-	-
Isobutene	b	77.4	2.6	17.7	-	-	-
trans-2-Butene	b	23.3	10.6	65.8	-	-	-
cis-2-Butene	b	22.7	11.3	63.9	-	-	-
Acetylene	a	100	-	-	-	-	-
	b	100	-	-	-	-	-
Benzene	b	77.0	17.8	6.0	-	-	-
Toluene	b	38.7	16.3	1.7	-	-	43.0
Ethylbenzene	b	45.4	17.5	1.1	-	-	33.7

[a] includes both natural gas emanating from the ground before processing and commercial natural gas.

1.2.3. Role of NMHC in Photochemical Smog

One of the significant atmospheric functions of the NMHCs is that they are one of the important ingredients in the chemical processes that produce photochemical smog on the urban and regional scale. While uncertainties remain in the understanding of tropospheric photochemistry, the basic set of reactions leading to ozone production has been identified.

In the atmosphere, ozone is formed by the reaction:

$$O + O_2 + M \rightarrow O_3 + M \qquad \text{[Equation 1]}$$

Most of the atomic oxygen is formed by the photodissociation of nitrogen dioxide:

$$NO_2 + h\nu \xrightarrow{\lambda<440nm} NO + O \qquad \text{[Equation 2]}$$

Nitric oxide reacts with ozone, regenerating NO_2:

$$NO + O_3 \rightarrow NO_2 + O_2 \qquad \text{[Equation 3]}$$

Other species can compete with ozone, e.g., peroxy radicals (RO_2):

$$NO + RO_2 \rightarrow NO_2 + RO \qquad \text{[Equation 4]}$$

Peroxy radicals are formed by degradation of hydrocarbons. The degradation process includes the attack by OH radical and addition of molecular oxygen:

$$RH + OH \rightarrow R + H_2O \qquad \text{[Equation 5]}$$

$$R + O_2 \rightarrow RO_2 \qquad \text{[Equation 6]}$$

Natural concentration level of OH is partly sustained by the photolysis of ozone and reaction with water vapor:

$$O_3 + h\nu \xrightarrow{\lambda<320nm} O(^1D) + O_2 \qquad \text{[Equation 7]}$$

$$O(^1D) + H_2O \rightarrow 2OH \qquad \text{[Equation 8]}$$

Aside from the above-mentioned reactions, other secondary reactions are involved in the complex reaction scheme involving NMHCs, NO_x and O_3. For example, degradation of hydrocarbons also leads to the formation of aldehydes, which are important intermediate species in the photochemical reaction chains. Aldehydes are dissociated by solar radiation and thus are important sources of radicals. Peroxyacetyl nitrate (PAN) can be formed from acetaldehyde in reaction with OH:

$$CH_3CHO + OH \rightarrow CH_3C(O) + H_2O \qquad \text{[Equation 9]}$$

$$CH_3C(O) + O_2 + NO_2 \rightarrow CH_3C(O)O_2NO_2 \qquad \text{[Equation 10]}$$

Internal combustion engines used in automobiles and trucks produce reactive hydrocarbons and nitrogen oxides, two of the three major ingredients for smog formation. Under certain favorable meteorological conditions, photochemical smog would be formed that causes damage to materials and vegetation, and poses health hazards to human.

1.2.4. Atmospheric Lifetimes

The atmospheric behavior of trace species is to a large extent dictated by their lifetimes. The major destruction process of the NMHCs are oxidative reaction with hydroxyl (OH) radicals (Equation 5 & 6) and to a lesser degree with O_3[3]. This is because photolysis of NMHC is not possible as they do not absorb UV radiation, or removal by dry or wet deposition as they are relatively insoluble. The lifetime of an NMHC can be defined as

$$\tau = \left\{k_{OH}[OH] + k_{O_3}[O_3]\right\}^{-1} \qquad \text{[Equation 11]}$$

where k_{OH} and k_{O3} are reaction rates with OH and O_3, respectively. However, as the OH concentrations (also O_3) have a strong seasonal and latitudinal dependence[30], the lifetimes of NMHC are a strong function of season and geography.

Estimated atmospheric lifetimes of NMHCs, for example, propane, ethylene, and ethane, can vary from hours, days, to months, respectively (see Table 1.1).

1.3. NMHC Measurement Challenge

Research in tropospheric chemistry pushes measurement techniques to their limits. The primary obstacle is that chemist generally must deal with incredibly low concentrations of atmospheric species, so that the detection and analysis of these species and their reaction products would be quite difficult. Instruments must also be developed to detect species at such low concentrations ranged from parts-per-million by volume (1 ppm = $1x10^{-6}$ v/v) down to parts-per-trillion (1 ppt = $1x10^{-12}$ v/v) or less. Separation of that many different compounds in air sample requires quite sophisticated analytical techniques.

Accurate analysis of NMHCs down to the parts-per-billion by volume (ppbV) concentrations requires specialized and dedicated sampling systems, with special attention to a number of technical problems. There may be destruction of species by reaction with O_3, NO_2 and/or artifact formation during sampling. Sample contamination or wall loss (or gain) in contact with container surfaces, especially over extended storage periods lasting several days to months are also possible. Improper and incomplete identification of chromatographic peaks are common due to the lack of GC-MS confirmation. The chromatographic separation may be insufficient, resulting in incorrectly identified and overlapping peaks. There is also a lack of uniformly available stable standards at low (ppb or ppt) concentrations for system and FID detector response factor calibration.

The methodologies used to determine the atmospheric concentration of hydrocarbons include the three distinct steps of collection, chemical identification (speciation), and detection. The three phases are of roughly equal importance. If sample integrity is not maintained during collection, the result will not reflect true ambient conditions. Separation of the air matrix into individual components is clearly a requirement for meaningful analysis, and without sensitive and precise detectors, quantitation is not possible.

1.3.1. Collection

Procedures commonly used to collect vapor-phase organic compounds include whole-air, cryogenic, adsorption, and derivation methods. For the analysis of ambient NMHCs at ppbV to sub-ppbV levels, whole-air sampling in a stainless steel container is commonly used. Rigid metal containers are easy to clean, less prone to leakage, and better for shipping samples from field sites to an analytical laboratory. The most widely used are electropolished stainless steel canisters in which whole air samples are collected at pressures of 30-100 psig. A variety of hydrocarbon species has been demonstrated to be stable in the canisters but departures can occur[31], which may be related to the specific electropolishing, preconditioning, and sampling procedures used by specific investigators, or the ozonolysis reaction occurred in the cryogenic sampling process. Experimental evidence indicates that O_3 itself is generally destroyed relatively quickly in stainless steel vessels and hence poses less of a problem when whole air samples are collected in canisters.

Cryogenic collection utilizes a glass, Teflon, or stainless steel trap cooled to subambient temperatures. A liquid argon or liquid oxygen cooled trap quantitatively retains all of the nonmethane organic compounds but permits the passage of nitrogen and most of the oxygen in ambient air. This separation is important because a big plug of nitrogen or oxygen flushed onto a capillary column will disrupt the initial portion of the chromatogram. However, O_3 and water can cause problems. When O_3 is concentrated in the cryogenic trap and subsequently warmed up and transferred the content of the sample loop to the gas chromatographic column, ozonolysis reactions will occur that can destroy the olefins. Therefore O_3 scavengers, such as potassium carbonate or sodium sulfite, are sometimes used to remove the O_3 from the airstream prior to sampling. However, in the present study, O_3 were found to be destroyed within a short period of sampling and storage in the electropolished stainless steel canisters, therefore the O_3 scavengers were not needed in our sampling procedure.

1.3.2. Speciation and Detection

The most common practice for the analysis of NMHC employs gas chromatography (GC) equipped with flame ionization detector (FID), although gas chromatography/mass spectrometry (GC-MS) or Fourier transform infrared (FTIR) spectroscopic techniques have been utilized in very limited instances. Typical light hydrocarbons (C_2-C_5) are usually separated both by packed columns

and/or capillary columns, whereas capillary columns are being used for heavier hydrocarbons[19,31].

Temperature programming of the GC column is generally employed to give the desired resolution of the compound peaks. Over the years, separation and the integrity of compounds that pass through the columns have been improved by development of better column packing compounds for packed columns and chemically bonded silicone stationary phases for fused silica open tabular capillary columns. Recent developments include the use of capillary-type columns [e.g. Al_2O_3 porous layer open tabular (PLOT)] for separation of the lower molecular weight hydrocarbon[32].

The PLOT columns are ideal for separating volatile compounds; they have the large surface area and hence high sample capacity needed for separation of these compounds. The new Al_2O_3 PLOT column available from Hewlett-Packard Supplies in 1994/95 was used in our analysis of NMHC in this project. The column provides unique selectivities for cyclopropane, propylene, acetylene, propadiene, and 1,3-butadiene in light hydrocarbon analysis, and resolves impurities in acetylene and propadiene from butane.

The most common detector used is the flame ionization detector (FID) because nearly all of the vapor-phase organic compounds will respond when added to the detector. It has been proven to be the best detection system for

most organic compounds. Its nearly equal carbon response for the C_2-C_5 hydrocarbons greatly facilitates calibration of a GC system because this property allows the determination of the response-versus-concentration curve using a single hydrocarbon or a mixture of a few hydrocarbons, and finally the concentrations of all the hydrocarbons in a complex mixture. They are robust systems and can be transported to and operated at remote field sites. The wide linear range and low detection limit make the FID an ideal detector for quantifying hydrocarbons in the atmosphere.

The use of a single FID response factor for a wide range of NMHCs may lead to errors in quantitation. Intercomparison studies at low concentration synthetic air mixtures of NMHCs are performed only in the US, and only recently in Europe. Sample analysis is cumbersome and usually requires several hours from sample introduction to final tabulation. This renders the analysis of NMHC inherently slow, and therefore difficult to acquire the temporal and spatial resolution required to adequately define the hydrocarbon distribution so that photochemical models of their effects on the chemistry of the atmosphere can be adequately tested. A program of intercomparison of CH_4 analysis was first initiated by APARE laboratories in 1997, but there is no interlaboratory comparison for NMHCs among laboratories in Asia yet.

1.4. Atmospheric Distributions

For the last thirty years, measurements of NMHC have been conducted in urban environments in the United States[33,34,35], the United Kingdom[36], Australia[37,38], and in rural/non-urban environments[33,36,39,40].

Typical concentrations of NMHC in most urban locations are in the range 100-1000 ppbC (parts-per-billion volume as carbon). Examination of individual species usually shows a strong resemblance to gasoline and its combustion products. However, biogenic hydrocarbons are undoubtedly present in low concentration relative to anthropogenic hydrocarbons, which are not specifically differentiated in these studies. Strong diurnal and seasonal variations in the distribution of urban/rural hydrocarbons are observed to be largely dictated by their reactivity and prevailing meteorology.

Rural NMHC mixing ratios are typically ranged from 20 to 100 ppbC and of principal anthropogenic origin, although a larger contribution from biogenic sources is often present. Isoprene and α-pinene are two principal biogenic hydrocarbons[41,42,43]. These biogenic hydrocarbons are highly reactive and have atmospheric lifetimes of minutes to hours. The isoprene abundance is affected by temperature, insolation and related to plant photosynthesis and photorespiration. Terpenes can have a large storage in plants and leak to the atmosphere at rates independent of light. The emission is dependent on leaf

diffusivity and on terpene temperature, volatility, and solubility[44,45]. Few long-term studies of NMHC in rural or forested areas have been performed. Highest concentrations of biogenic hydrocarbons were usually found in summer[46]. It is expected that biogenic emissions would be at their maximum under conditions that represent high temperatures, high humidity, and high insolation.

Few NMHC measurements have been made in the troposphere over the western Pacific region. The available measurements in the Pacific region were collected during shipboard studies[47,48]. Recently, air-borne measurements by PEM-West projects have been conducted during September/October in 1991 and February/March in 1994, which is a comprehensive measurement of a wide range of atmospheric trace gases in the western Pacific region. However, the data collected in these two air-borne missions were "snap-shot" measurements of limited time span and dictated by the meteorology at the time of measurement.

The advantage of air monitoring by the ground station is that it produces sufficient data for statistical analysis and sufficient time coverage to see seasonal trend and even interannual trend in the future and this point is exactly the limitation of aircraft expedition. The uniqueness of this project is on the data set that has such a high frequency in data collection of 15 months at low levels. Our data set is the most comprehensive one for the study of the pollution impact to the western Pacific region.

2. *The Hong Kong Polytechnic University Atmospheric Research Laboratory*

2.1. The Establishment of the Station

The Hong Kong Polytechnic University Air Monitoring Station/Atmospheric Research Laboratory was established in February 1993 with the collaboration of NASA. The establishment of this Laboratory is aimed at the systematic investigation and long-term monitoring of the distribution of trace gas species and their atmospheric composition changes in relation to the growing anthropogenic activities on the Asian Pacific Rim.

2.2. Measurement Site Description

Hong Kong is located on the coast of South China. Cape D'Aguilar (22.2°N, 114.3°E, 60 meters above sea level) is located at the southeast tip of Hong Kong Island (Figure 2.1). Selection of the location of the Laboratory was based on the intention that the trace species measured should reflect regional spatial scale atmospheric transport and conversion processes and have minimal influence by local sources and sinks.

There are several major metropolitan centers which must be considered in the study of regional air quality of Hong Kong. Immediately north of Hong Kong is Shenzhen (population of about 4 million). It is 30 km from Victoria Harbour. Zhuhai and Macau are located 70 km west on the opposite side of the Pearl River Estuary. Guangzhou is located 120 km northwest of Hong Kong. Xiamen is about 500 km northeast and Taiwan is about 700 km east of Hong Kong.

The Station is built on the top of a cliff facing the South China Sea. The cliff faces east and has an almost vertical drop to the sea. There is a small hill behind the station (312 m elevation). The prevailing wind direction measured at the Station is easterly. The Station has a view of the sea greater than 180 degrees from the northeast to the southwest. Over 60% of the time, the local wind is from the sea and the station is upwind of Victoria Harbor.

Concerning urban influence, the Station is about 13 km from the Victoria Harbour. The main industrial areas in Hong Kong are all located on the north to northwest side of the station. The two large industrial towns, Kwai Chung and Tsuen Wan, are 20 km northwest. There are two large thermal power plants in Hong Kong. They both consume mainly low sulfur coal (< 1% sulfur). Both power plants are located to the west side of the Station. Hong Kong also has heavy sea and air traffic. Ocean liners enter and leave Hong Kong by the Lamma channel which is 8 km to the south of the Station. The whole Hong Kong Island

is under flight paths. In 1996, there were a total of 158,797 aircraft and 40,808 ocean vessel arrivals. Concerning vehicle traffic, at the end of 1996 Hong Kong had about 466,068 licensed vehicles on the 1717 km of roads, or about 270 vehicles per kilometer. Available information showed that in 1994, over 90% of the VOC emissions came from vehicle exhaust, with minor contributions from power plants and aircraft.

Concerning the local environment, there is a small village with about 20 families located 1 km to the northwest. The village has some small industrial and agricultural undertakings. There is a telecommunication submarine cable station 50 m to the south of the Station. The operation of the cable station is wholly electric and very few pollutants are emitted except for its diesel emergency power generator. There is a Marine Science Laboratory located beside the sea. It is 300 m south of the Station. The trail (about 4 km) leading to the Station is a restricted road with low traffic volume.

Figure 2.1 : Map of Hong Kong and Location of Cape D'Aguilar

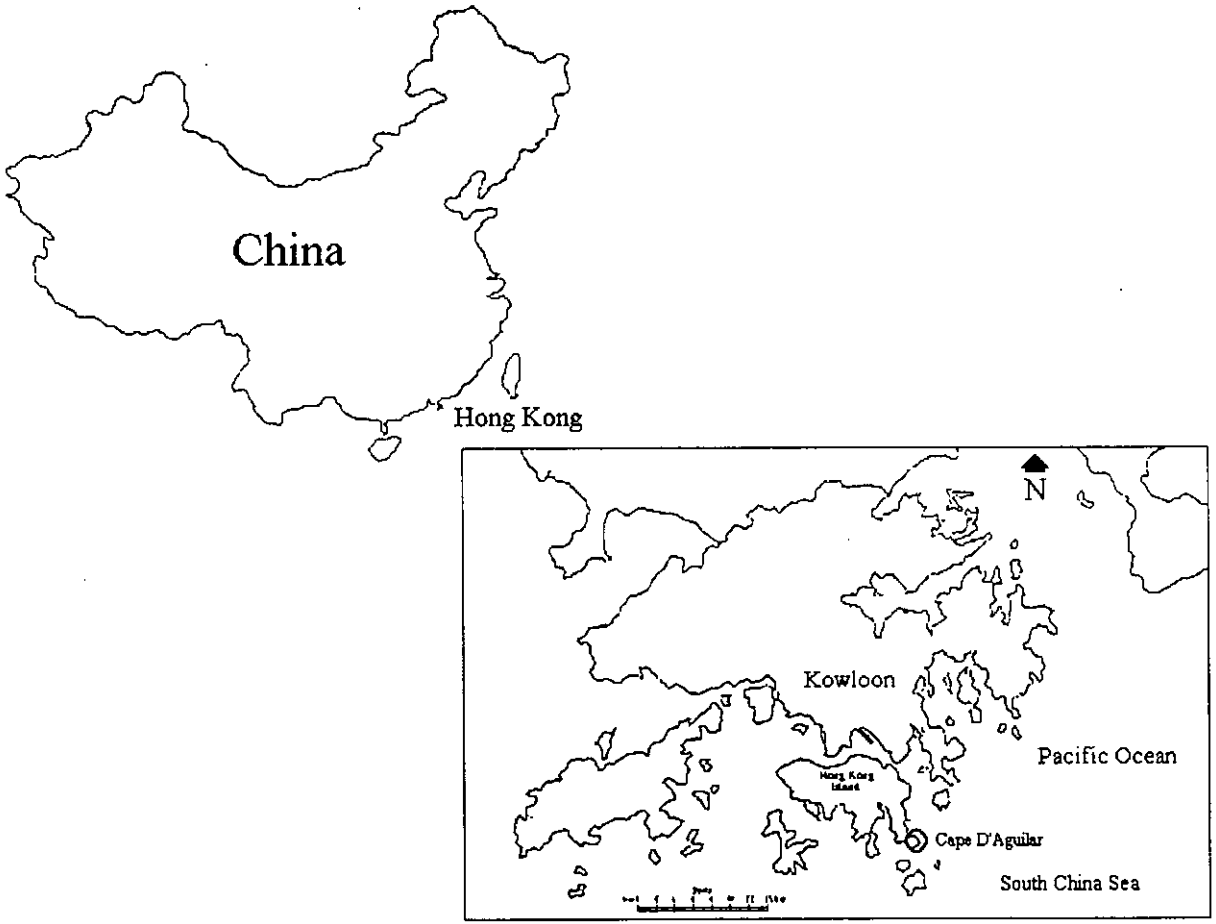

2.2.1. Asian Monsoon System

At the longitudes of the major continents the low-level tropical wind field exhibits a strong seasonal dependence, with a tendency toward onshore (sea to land) flow during summer and offshore flow during winter. The seasonal reversal is particularly pronounced over southeast Asia and adjacent regions of the Indian Ocean where the prevailing winds blow from the southeast during summer and northeast during winter. These seasonal wind regimes are known as monsoons[49].

Hong Kong, located at the western Pacific Rim, is under the influence of the Asian monsoon system. Dominant continental outflow conditions were experienced in winter whereas oceanic inflow was commonly observed in summer time. On a regional scale, Hong Kong offers an opportunity to study the composition of winter continental outflow air masses before they are discharged into the ocean and the cleanliness of summer time marine air masses prior to contamination by metropolitan sources.

2.2.2. Air Mass Movement and Transport by Back Trajectory Analysis

One of the factors that contributes to the fluctuations in hydrocarbon concentrations is that air parcels have passed through different locations which are different in hydrocarbon emissions. To trace the history of an air parcel,

backward trajectories from a receptor are commonly used to identify air pollution source regions. Air parcel trajectories have been extensively used over the past decade to study atmospheric transport because they are relatively simple to compute. Most computational methods use observed or model analyzed winds to compute the horizontal advection component and usually one of three assumptions to compute the vertical component of the trajectory motion. These three assumptions are that the trajectory remains on a surface of constant pressure (isobaric), the trajectory follows a surface of constant potential temperature (isentropic), or the trajectory moves with the vertical velocity winds fields (kinematic) generated by a disagnostic or prognostic meteorological model. There are many recent examples in the literature of all three approaches.

Isentropic trajectories account for adiabatic vertical motions that air parcels may experience enroute to their destinations. However, transport is perhaps more difficult to model in the planetary boundary layer (PBL) than in the upper troposphere or stratosphere due to significant amounts of moisture and the diabatic factors driving the growth and dissipation of the PBL itself. One underlying assumption is that the three-dimensional velocity fields generated by a meteorological forecast model contain all the adiabatic as well as diabatic components to the vertical motion. Many of the citations using dry isentropic approaches frequently are preceded by qualifying statements regarding the exclusion of situations that have large diabatic components: convective boundary

layers, cloud coverage, and areas of precipitation. These factors should not be a problem for application to upper tropospheric and stratospheric transport.

In the near-surface layer an air parcel cannot always be traced isentropically because the isentropic surface on which it is travelling may either intersect the ground or be ill-defined in an unstable boundary layer as mentioned above. The CMDL transport model, therefore, calculates trajectories on isentropic surfaces until the specified surface descends to within 100 m of the ground. At this point, the model switches to a layer-averaged mode, where an air parcel is advected by winds averaged through the layer 100-600 m above the surface topography. These heights were chosen to diminish the effects of surface friction and to represent winds in the lower boundary layer.

Isentropic back trajectories for Hong Kong were computed by NOAA-CMDL[50]. The CMDL Isentropic Transport Model was first used in a study of flow patterns for Barrow Observatory, Alaska[50]. Input to the trajectory model is in the form of 2.5-degree latitude-longitude gridded meteorological parameters and topography furnished by the European Centre for Medium Range Weather Forecasts (ECMWF). Most of the techniques employed in this model, such as the transformation from isobaric to isentropic coordinates, horizontal interpolation procedures, and the predictor-correction method for advection, derive from the earlier isobaric[51] and isentropic[52] trajectory models. All trajectory models are subject to uncertainty arising from interpolation of sparse meteorological data,

assumptions regarding vertical transport, observational errors, sub-grid-scale phenomenon, turbulence, convection, evaporation, and condensation. Five recent studies estimated average horizontal trajectory errors to be 140-290 km in 24 hrs. These uncertainties are also detailed in Merrill et al. (1985) and Harris (1992) and references therein.

Ten-day back trajectories arriving at 1 km above sea level were computed twice every day at 00:00 and 12:00 UTC. The 1 km height was chosen such to lesson the impact of the local complicated topography and yield the trajectories produced by the model be reasonably representative of the large-scale circulation. As such, the calculated trajectories can be used to suggest potential source regions. However, this does not imply that a particular air parcel sampled at the trajectory destination followed this path. Individual trajectory can have an error up to 200 km. Subsequent trajectory analysis are based upon ensemble averaging.

3. *Aims and Objectives of Study*

The aim of this research is to measure the NMHC levels at the Hong Kong Polytechnic University Air Monitoring Station/Atmospheric Research Laboratory at Cape D'Aguilar for a one-year period. Together with monitoring data collected on CO, NO, O_3 and SO_2, and alongside with meteorological data on surface wind direction/speed, UV radiation, temperature and relative humidity, the data set would provide the most comprehensive baseline information on air pollution and air quality at Hong Kong.

The specific objectives of this project are:

1. to develop/build two dedicated air sampling-gas chromatographic system for measuring atmospheric methane and NMHCs, respectively;
2. to validate a measurement protocol for atmospheric NMHCs in the Hong Kong environment;
3. to collect a yearly NMHC data set for Hong Kong; and
4. to conduct an overview interpretation of the one-year data set, with emphasis on the regional transport of air masses and its effect on NMHC levels in Hong Kong.

SECTION II: EXPERIMENTAL

4. *Air Sampling Techniques*

Methane measurements were conducted from April 1996 to October 1997 and NMHC measurements were conducted from October 1995 to March 1997. During the period of study, air samples were collected at the Hong Kong Polytechnic University Air Monitoring Station/Atmospheric Research Laboratory located at Cape D'Aguilar, Hong Kong, and assayed for methane and NMHCs. The sampling and analysis protocol are described as follows.

4.1. Sampling Line and Canisters

Samples were collected through a stainless steel tubing (4 mm I.D.) and a metal bellows pump (Parker Hannifin Corp., Sharon, Mass. MB-21E). The sampling line was mounted on a scaffolding adjacent to the laboratory container which housed the air monitoring analytical instrumentation. The sample inlet was 8.5 m above the ground surface.

Sample canisters were provided by National Center for Atmospheric Research (NCAR), Boulder, Colorado. These canisters are made of electropolished stainless steel, with inlet and outlet stainless steel bellows valves. The outside valve has a tube extending within the canister approximately ¾ the length of the can. The center valve is welded directly to an opening at the top of

the canister. The valves are fitted with high vacuum seal hardware (CAJON® ULTRA TORR) for connection to sampling and analytical equipment. The seal of these vacuum fittings is made on a nickel gasket, which is placed between the two halves of the vacuum fittings at the union, and operated by squeezing the fittings together firmly with long wrenches.

The canister cleaning procedure was based on the protocol used by NCAR[53]. They were pre-cleaned for sampling by evacuation and flushing with zero air for 3 times, then heated at 100°C with evacuation for 24 hours. The canisters were then filled with zero air to test for cleanliness before sample collection.

4.2. Ambient Air Sampling Procedure

The air sampling steps included sample line flush, followed by canister flush and canister pressurization. At the start of sample collection, the stainless steel metal bellows pump was turned on to purge the pump and the sampling line with air for 15 minutes. The canister was coupled while the pump was running. With inlet and outlet valves opened, the canister was purged with ambient air for 45 minutes. After purging, the downstream canister valve was closed. Sample air was pressurized into the canister for 5 minutes to approximately 30 psi, after which the inlet valve was closed and the canister removed from the inlet sampling line.

No provisions were made to remove O_3 from the directly sampled air inlet system. Passage of the airstream through the stainless steel sample line and bellows pump removes most of the O_3. Previous studies by Zimmerman and Greenberg using the same canisters have shown that O_3 is generally destroyed relatively quickly within stainless steel vessels[53]. This will pose less of a problem when whole air sample is collected in canisters. No attempt was made to prevent ambient water vapor or aerosol from being collected in the canister. This is because water apparently occupied active (polar) wall sites more efficiently than NMHCs, and so humidity in canister reduces NMHC adsorptive losses[54].

To check for validity of the sampling procedure, zero air was used instead of ambient air in control sampling experiment. Zero air was generated by an oil-less compressor (GAST) and a zero air generator (Whatman, Model: 76-807-220, total hydrocarbons: <0.1ppm). No significant NMHC peaks were observed in the zero air samples collected in the stainless steel canisters. Thus the sampling procedure was proved to be effective in collecting representative sample air without being affected by canister contamination and its previous history.

4.3. Sampling Schedule

Canister samples were collected three times daily at typically 1200, 1430, and 1700 local time. Sample collection started on 15th October, 1995 and all measurements continued through 20th March, 1997.

5. *Custom-Built Analytical Systems for Measurement of Methane and NMHCs*

Two dedicated air sampling and GC analytical systems, one for methane and the other for NMHCs, were custom-built for quantitative measurements in this study. The material of construction was ultra-clean 316 stainless steel tubing, connectors and unions, and NUPRO® bellow needle valves (SS-4BK) supplied by Crawford Fitting Co., Willonghby, Ohio, USA. The details of the two analytical systems are described below.

5.1. Analytical System for Methane

The general flow pattern in the methane analytical system was sample transfer from the canister to the sample loop, then from the sample loop to the chromatographic column and detector (Figure 5.2). The system was made up of a 6ft x 1/8" O.D. Unibeads A packed gas chromatographic column enclosed in a temperature-controlled Hewlett Packard 5890 Series II Plus Gas Chromatograph (GC), and detection by a Flame Ionization Detector (FID). This system was interfaced and controlled via a HP GC ChemStation software (resident on an AST, Bravo LC 4/33 computer) for data acquisition, storage, and reduction. Chromatographic retention times were recorded automatically, while baseline assignment for the methane peak was conducted manually for each chromatogram recorded.

Figure 5.2 : Analytical System for Measurement of Methane

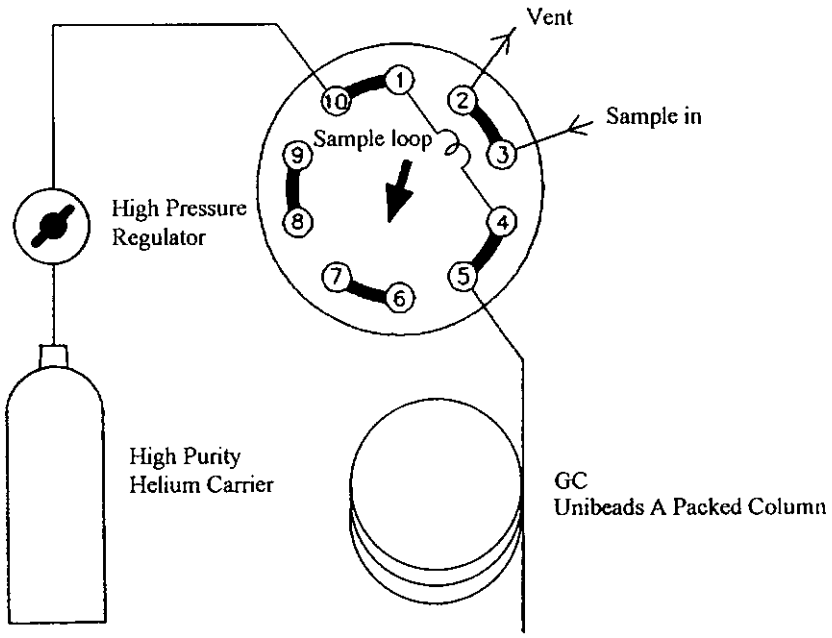

The Valco 10-port switching valve is the one piece of equipment central to the loading and injection of an ambient air sample onto the GC column. A 1-mL sample loop (Alltech-Applied Science, USA) is connected to positions 1 and 4 of the switching valve. To position 5 is attached an Unibeads A packed column, and to position 10 is attached the cylinder containing high-purity He carrier gas. In-line charcoal and molecular sieve 5A gas purifiers (Alltech-Applied Science, USA) are installed in the carrier gas stream to remove moisture and organics.

5.2. *Analytical System for Nonmethane Hydrocarbons*

The analysis of each air sample must follow a specific operational procedure, and must be timed very carefully to enhance the analytical precision for such a large number of air samples. NMHCs in air were analyzed utilizing the air sampling and GC analytical system as shown in Figure 5.3. It comprised of a Hewlett-Packard Porous Layer Open Tabular (PLOT) Aluminum Oxide (Al_2O_3) chromatographic column enclosed in a temperature-controlled Hewlett-Packard Model 5890 Series II Plus GC with FID detection. The GC control software (Hewlett-Packard HP3365 GC ChemStation) was used for data acquisition, storage, and chromatographic processing.

The air sampling vacuum line consisted of a 2.2-liter storage tank (Aldrich Chemical Company, Inc., Sure/Pac™ Cylinder) permanently fixed to a vacuum

line having an internal volume of 50 ml (i.e. the volume of the entire vacuum line is 2250 ml) (Refer to Note).

Sample pressure measurements were made manometrically. An Edwards capacitance manometer (Barocel Type 600, 0-100 mbar, accuracy ±0.15% FS) with an Edwards digital readout (Model 1570) was used to monitor accurately the subambient pressure changes. The sample volume was then measured by application of the ideal gas law using the following equation:

$$Volume\ of\ air\ sample = \frac{\Delta\ Pressure}{Atmospheric\ Pressure} \times \text{System Volume (2250 ml)}$$

The sampling valves for introduction of air samples are depicted in Figure 5.4(a) and in greater detail in Figure 5.4(b).

Note: The volume of the sampling vacuum line, including that of storage tank, was determined from air expansion experiments using dilution bottles of accurately calibrated volume. The air expansion relationship $P_1V_1 = P_2V_2$ was assumed in the volume calculation. The system volume of 2250 ml at 25°C was assumed throughout this study to calculate the equivalent volume and amount of air sample introduced at standard temperature and pressure (STP) conditions. Since only the pressure readings of the air sample and calibrated methane and NMHC working standards were involved in the actual calculation of sample concentrations (see Section 7.3.1), the value and accuracy of the system volume at 2250 ml did not affect the accuracy of our quantitative

Figure 5.3 : Analytical System for Measurement of NMHC

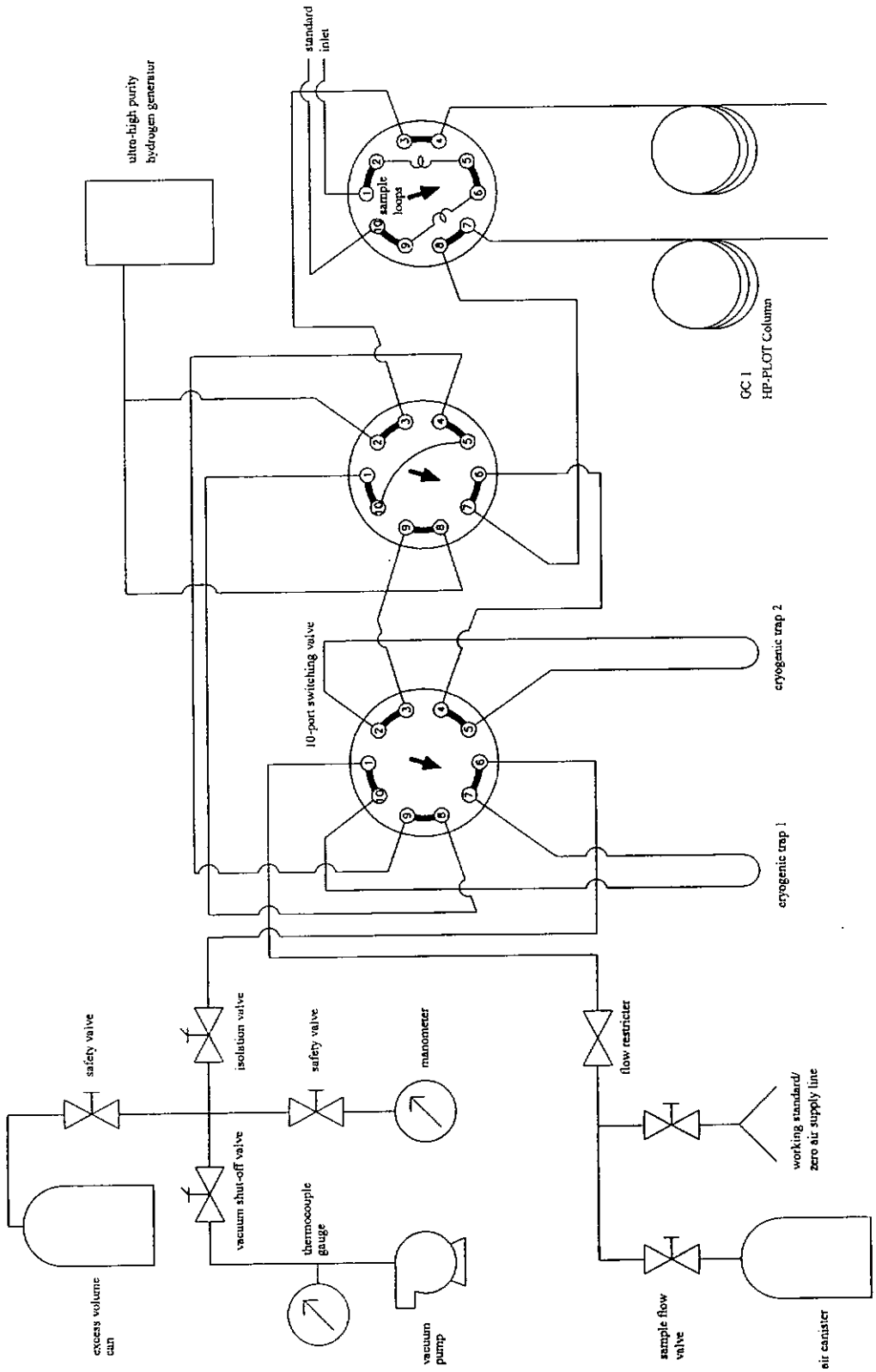

Figure 5.4 : The two 10-port switching valves, (a) Overview, and (b) Sample Flow Scheme

(a) Overview

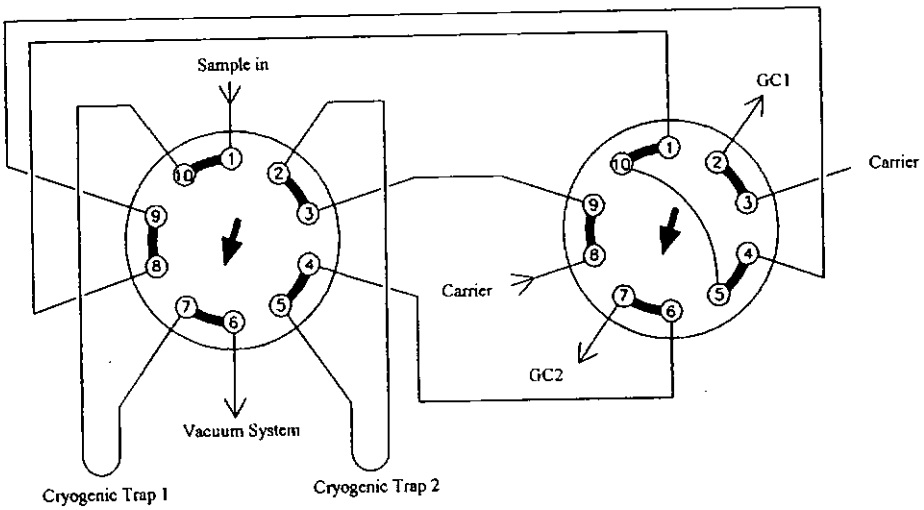

(b) Sample Flow Scheme

Step 1 : Switching valve **A** (INJECT), Switching valve **B** (INJECT)

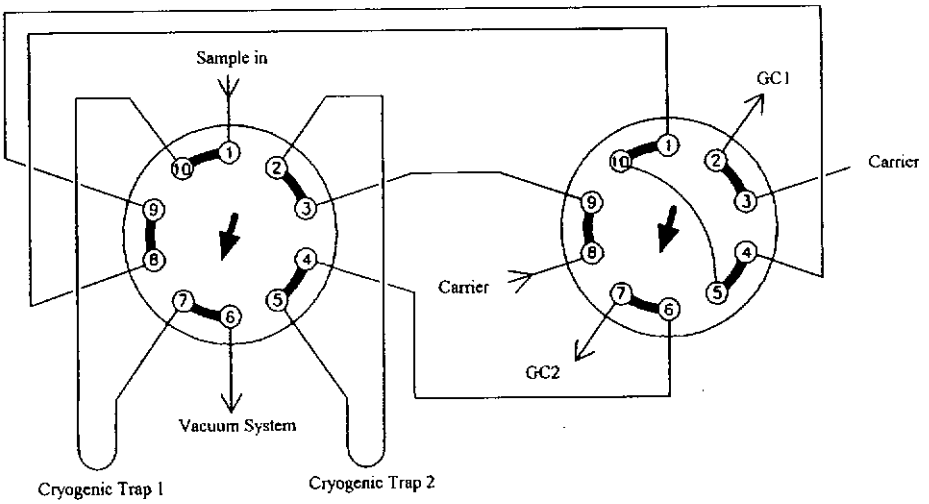

Step 2 : Switching valve **A** (LOAD), Switching valve **B** (INJECT)

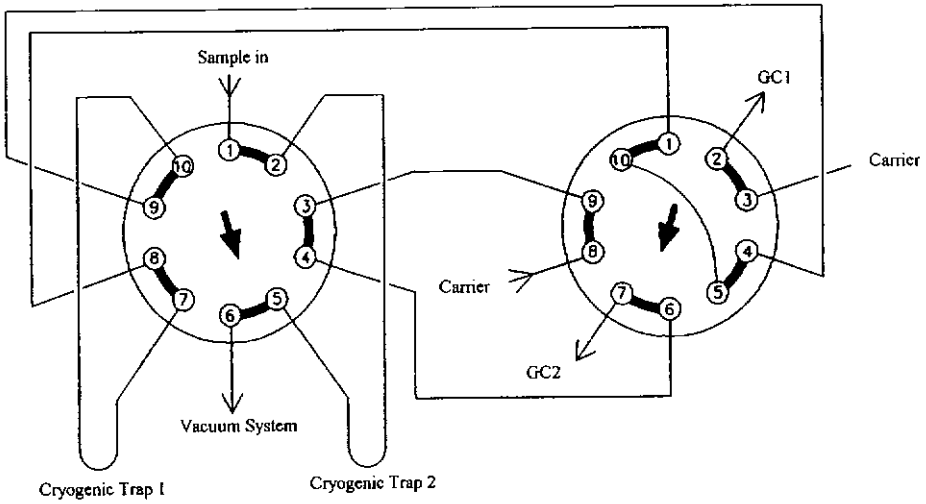

Step 3 : Switching valve **A** (INJECT), Switching valve **B** (INJECT)

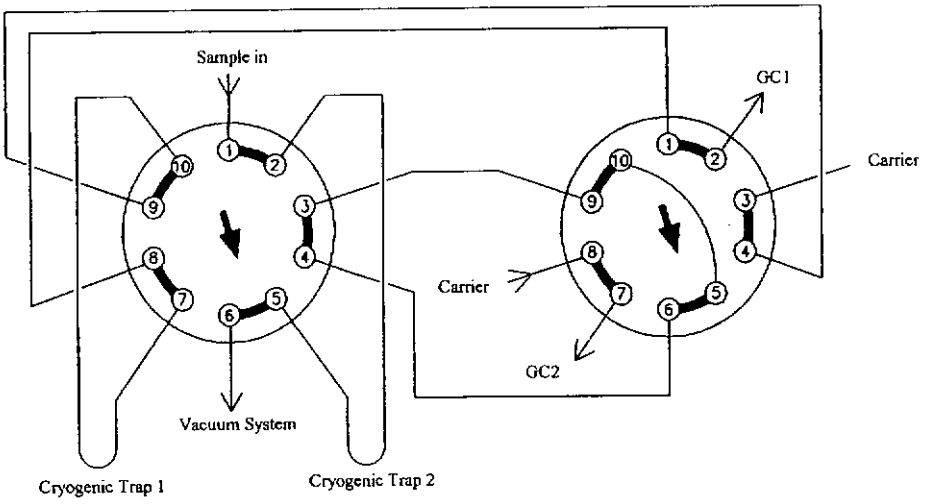

Figure 5.4(a) depicts the two switching valves and the corresponding connections to the vacuum line, cryogenic trap, and GC system. Position 1 of the switching valve A was connected to the air canister. To position 6 was attached the vacuum system and the storage tank, which was evacuated by an Edwards E2-M2 rotary vacuum pump. Between the vacuum pump and the sampling reservoir/lines, there was a foreline moisture trap containing molecular sieve to prevent backflow of any volatile trace gases which may have originated from the rotary pump. A stainless steel trap was used for cryogenic collection which was cooled to liquid nitrogen temperatures during analysis. Air samples were pre-concentrated before injection in this 24"x1/8" O.D. stainless steel loop filled with 80/100 mesh glass-bead. To position 2 of switching valve B was attached the Hewlett-Packard PLOT Al_2O_3 chromatographic column. The GC column was connected to the sampling system by zero volume union (Valco) to reduce dead volume in the system. Ultra-high purity H_2 carrier gas stream, supplied by a hydrogen generator (Packard, Model 9200, purity of H_2: 99.995%), was introduced into the GC column via position 3 of the 10-port switching valve B.

Two switching valves were used in the design of the air sampling/introduction system. The two-stage switching of the injection valves, as shown in sample flow scheme in Figure 5.4(b), allowed continuous flow of H_2 carrier gas through the column to the FID detector while at the same time allowed the isolation of the trap for desorption and re-volatilization of the air

sample. This design feature enabled very good reproducibility of the system performance and chromatographic retention times because the air sample was injected as a plug of vapor without the need of re-cryofocusing in the GC column. The precision of GC analysis will be discussed in detail in subsequent sections.

6. *Quantitative Chemical Analysis of Methane & NMHCs*

The experimental procedures used in the analysis of methane and NMHC were described below. The two GC columns used were:

1. Methane analysis - 6ft x 1/8" OD SS Unibeads A Packed Column, 35°C isothermal; and
2. NMHCs analysis - 50m x 0.53mm ID, 15 μm, HP-PLOT Al_2O_3 column, 35°C-5min, 20°C/min to 130°C, 10°C/min to 190°C, 190°C-60min.

6.1. Analytical Procedure-Methane

For the analysis of methane, the sample canister containing the compressed air sample (~ 2 atmospheres) was attached to position 3 of the 10-port switching valve. The switching valve was set at "INJECT" position and the air sample was introduced by opening the canister valve. The outlet tube of the sample flow path was immersed in water for checking the flow rate. The sample flow rate was adjusted at approximately 1 bubble per second for 10 seconds. The canister valve was then shut off and the air in the sample loop was allowed to equilibrate for 2 seconds. The switching valve was actuated to the "LOAD" position and the GC "START" button was activated simultaneously. This

would initiate the GC temperature program and the data acquisition process. The experimental parameters were:

GC Column	Unibeads A Packed Column
GC Column Temperature	35°C isothermal
FID Detector Temperature:	250°C
He Carrier Gas	25 ml/min
H_2 for FID	27 ml/min
Compressed Air for FID	330 ml/min

Every time when methane analysis was conducted, the response of the GC/FID system was calibrated against National Institute of Standards and Technology (NIST) reference standard (NIST-SRM 1660a, 3.90±0.04 ppmV methane and 0.970±0.010 ppmV propane) which was introduced in the same manner as the air sample. The methane concentration in the air sample was calculated by direct comparison with that of the reference standard.

$$[CH_4]_{sample} = \frac{A_{sample}}{A_{reference}} \times [CH_4]_{reference}$$

where A_{sample} = GC peak area of air sample

$A_{reference}$ = GC peak area of NIST-SRM 1660a methane standard

$[CH_4]_{reference}$ = 3.90±0.04 ppmV, = methane concentration in NIST-SRM 1660a reference standard

6.2. *Analytical Procedure - Nonmethane Hydrocarbons*

To analyze an air sample, the air canister was connected to the air sampling analytical system through the sample flow valve connection (CAJON® ULTRA TORR) in Figure 5.3. The sample flow valve was fully opened to evacuate the air between the canister and the sampling vacuum line. After evacuation, the sample flow valve was closed and the canister valve opened to prepare for the cryogenic pre-concentration step. The cryogenic trap was immersed in liquid nitrogen and allowed to equilibrate at -190°C. The sample flow valve was opened again to allow the sample air to be transferred from the canister, through the cryogenic trap, and to the storage tank as shown in Step 1 in Figure 5.4(b). About 100 mbar of air sample was introduced for each analysis, and the sample introduction time (hence sample flow rate through the trap) was controlled to about 20 minutes, resulting in an approximate sample flow rate of 10 ml/min. This flow rate was optimized in a series of trapping efficiency experiment discussed in Section 7.1. After the condensable vapor from the 100-mbar air sample was trapped in the sample loop, the sample flow valve was closed. The pressure of the air sample introduced was accurately measured by an Edwards membrane manometer.

The switching valve A was actuated to "LOAD" position (Step 2 in Figure 5.4(b)). In this position, the vacuum sampling line and the cryogenic trap were isolated. Hydrogen carrier gas continued to flow to the GC because the

two switching valves were designed to isolate the cryogenic trap but allowing a continuous carrier gas flow. Liquid nitrogen was then removed from the loop (cryogenic trap) and replaced with a dewar of hot water (about 90°C). After approximately one minute, the temperature in the loop (cryogenic trap) had equilibrated, and the trace species contained within revolatilized to the vapor phase. The switching valve B was then actuated to the "LOAD" position to redirect the H_2 carrier gas to flush the previously trapped contents of the pre-concentration loop to the GC column (Step 3 in Figure 5.4(b)). At the same time, the "START" switch on the GC was activated, which also electronically activated by the computerized GC data system to begin the chromatographic run. The GC column temperature program was: 35°C for 5 minutes, then ramped to 130°C at 20°C/minute, then to 190°C at 10°C/minute, and finally held for 60 minutes at 190°C before being terminated. The last 60 minutes of the temperature program was to flush out slow-moving, high boiling components out of the GC column in preparation for the next GC run.

During GC analyses, ultra-high purity nitrogen at 23 ml/min was added to the effluent of the capillary columns before the FID detector as makeup gas to sharpen the peaks and to increase the sensitivity of the FID[55].

Initial temp. (°C)	Final temp. (°C)	Hold Time (minutes)	Temp. Ramp Rate (°C/minute)
35	35	5	--
35	130	--	20
130	190	--	10
190	190	60	--

Detector Temperature:	250°C
H_2 Carrier Gas	7 ml/min
H_2 for FID	27 ml/min
N_2 for Make-up Gas	23 ml/min
Zero Air	330 ml/min

For qualitative analysis, identity of NMHC peaks was obtained by comparing the GC retention times with that of known NMHC standards. The standards (Scott Specialty Gases Co.) used include

1. Can Mix Standard 1: Ethane, Propane, n-Butane, n-Pentane, n-Hexane (~ 16.5 ppmV)
2. Can Mix Standard 2: i-Butane, 2,2-Dimethylpropane, 2-Methylbutane, 2,2-Dimethylbutane, 3-Methylpentane, 2-Methylpentane (~ 15.0 ppmV)
3. Can Mix Standard 3: Ethylene, Propylene, Acetylene, 1-Butene, 1-Pentene, 1-Hexene (~ 16.5 ppmV)

The concentrations of these NMHC standards had a stated accuracy of ±10% and they were diluted 200 to 1000 times by injecting 1-5 ml of the standards (using air-tight gas syringes) into 500 ml or 1 liter dilution bottles which had been flushed and filled with zero air to atmospheric pressure. The

diluted standards (~ 50 ppbV) were analyzed in the same manner as the air samples, and the retention times of the respective NMHCs noted. The retention times were very reproducible, usually varying by no more than 0.02 minutes. The retention times of GC peaks eluting out of the PLOT capillary column was found to vary slightly, depending on the amount of H_2O and CO_2 introduced to the column.

Whenever in doubt, the identity of specific NMHC peaks in air samples was confirmed by the standard addition method. In the standard addition method, NMHCs in an ambient air sample was collected on the pre-concentration loop in the normal fashion, and then a small amount of one or more of the NMHC standards were added. If the added NMHC standards co-eluted with the sample peak, then the identity of the sample peak was confirmed. The identified NMHCs and their respective retention times are shown in Table 6.3.

Quantitation of NMHCs was made with respect to our laboratory prepared working standard of propane in air (46.9 ppbV), assuming that the FID had the same response factor per carbon atom for all the C_2-C_6 hydrocarbons as to propane. The quantitation procedure is outlined in the following section.

Table 6.3 : GC Retention Times of NMHCs

Compound Name	Retention Time (min.)
Ethane	2.91
Ethylene	3.72
Propane	5.37
Propylene	8.40
i-Butane	9.24
n-Butane	9.56
Acetylene	10.12
1-Butene	11.28
2,2-Dimethylpropane	11.77
2-Methylbutane	12.26
n-Pentane	12.53
1-Pentene	13.98
2,2-Dimethylbutane	14.82
3-Methylpentane	15.08
2-Methylpentane	15.14
n-Hexane	15.40
1-Hexene	16.69

6.3. *Quantitative Calibration*

6.3.1. Preparation of Working Standards for Measurements of NMHCs

The propane working standard was prepared by serial dilution of the standard from NIST SRM 1660a containing 3.90±0.04 ppmV methane and 0.970±0.010 ppmV propane.

A canister was cleaned by flushing with zero air and evacuated overnight. The canister, the zero air supply line, and the NIST SRM 1660a standard were connected to the sample vacuum system; vacuum/pressure within the vacuum system was measured with an Edwards Model EPS10 total pressure transducer (0-1000 mbar, accuracy ±1.0% FS). The SRM methane/propane standard was introduced accurately to about 50 mbar and zero air was then introduced and made up to a final pressure of 1000 mbar. The dilution factor was approximately 1/20 based on the accurately measured pressure readings.

The concentration of this working standard was checked by two independent methods. The first method involved static dilution of the SRM standard. The concentration of the working standard was found from the pressure readings:

$$0.970\ ppmV\ \text{Propane} \times \frac{49 \pm 1\ \text{mbar}}{999 \pm 1\ \text{mbar}} = 47.6 \pm 0.9\ ppbV\ \text{Propane}$$

Secondly, the SRM 1660a standard and the diluted working standard were introduced to the GC system via the 2-ml sample loop and the GC peak areas for the two standards were compared:

$$0.970\ ppmV\ \text{Propane} \times \frac{961.4\ \text{area count per injection}\ (n = 9, SD = 3.8)}{20{,}356\ \text{area count per injection}\ (n = 4, SD = 30)}$$

$$= 45.8\ ppbV\ \text{Propane}$$

Since the errors in the pressure readings were small (±1% FS), the systematic relative error in the calculated concentration was only ±2%. Provided enough time was allowed for equilibrium mixing of the SRM standard and zero air, this static method of dilution was expected to yield accurate concentration of the working standard.

For the second method, only small loss or error would be introduced because the sample-loop injection was operationally relatively simple and the primary and secondary working standards were introduced in the same way. The error in GC peak area integration could be minimized by repeated analysis (n=9 in this calibration method).

The concentration of the working standard was taken to be the average of the values obtained from this static pressure reading, and the sample loop injection calibration method. This concentration value (46.9 ppbV propane) was used for subsequent interlaboratory comparison and proved to be accurate for quantitative calibration (Section 6.4).

6.4. Analytical Protocol

A quality control protocol was established to ensure the reproducibility of retention times and FID detector response during the measurement period for NMHCs. This was conducted by checking the performance of the sampling and GC system using the NIST SRM 1660a standard and our 46.9 ppbV working standard prepared by serial dilution of the NIST SRM 1660a propane standard. The frequency of system checking and calibration was once every 9 sample analyzed, with the introduction of the working standard in the same manner as the air sample. System maintenance, including baking of GC column and FID detector cleanup, would be conducted when there was a ±0.5 minute shift in GC retention times or a ±10% change in detector response. During the period of study, the FID response factor was very reproducible and remained at 3.30 ± 0.16 ($n=88$, mean ± SD) area count per ppbC per mL.

SECTION III: RESULTS & DISCUSSION

7. *Accuracy and Validation of the Analytical Protocol*

7.1. Trapping Efficiency as a Function of Trapping Time

Since the NMHCs were cryogenically trapped prior to GC analysis, the trapping efficiency was tested with trapping time ranging from 13 minutes to 47 minutes. The measured concentrations of selected NMHCs for the same amount of NMHC standard introduced were tabulated in Table 7.4, showing that there was no significant deviation in the measured NMHC concentrations due to variation in trapping time. Typical trapping time used in our analysis was in the range of 20 to 25 minutes.

7.2. Effect of Sampling Volume on Analytical Accuracy

The volume of air sample trapped for analysis in the summer (about 300 ml at STP) was greater than that in the winter (about 200 ml at STP) because lower NMHC levels were observed in the summer months. More water and carbon dioxide would be trapped alongside with the NMHCs in the cryogenic trap as the volume of the sampled air was increased. Increased amounts of trapped water and carbon dioxide might affect the efficiency of NMHC desorption and GC separation. The effect of sample volume increase on analytical accuracy was tested by comparing the quantitative results measured

with two different volumes of the same air sample (Table 7.5). Very close agreement in quantitative results were obtained for 204 ml and 334 ml air samples, indicating that the analytical accuracy of the sampling and GC system was not affected by variations in the volumes of air sample analyzed.

7.3. Linear Working Range of Flame Ionization Detector (FID)

Since ppbV to pptV levels of NMHCs in the collected air samples are to be analyzed, the linearity of the flame ionization detector (FID) in the concentration range of the actual samples has to be established. This was done by measuring the FID output signal (as GC peak area counts) as a function of the amount (in volume x concentration units, i.e., ppbC x ml at STP) of propane working standards introduced into the GC measuring system.

This first step was to prepare working standards of lower concentrations by the method of serial dilution. The procedure was similar to that used for the preparation of the 46.9 ppbV propane working standard. Two working standards containing 2.3 ppbV and 120 pptV, respectively, of propane in zero air were prepared.

In control blank runs, the zero air was found to contain 20 pptV propane. The contribution of this residual amounts of propane in zero air to GC/FID signal output had to be corrected (subtracted), especially when the low

concentration 120 pptV working standard was used in the measurement of FID response factor. The signal output of the FID as a function of amount of propane injected is shown in Figure 7.5. A very good linear plot (r^2 = 1.000) was obtained, indicating that for the NMHC concentration range involved in this work, the FID output signal was directly proportional to the amount of propane or NMHC present in the air sample.

7.3.1. Proportionality of FID Output to Carbon Numbers in the NMHC

For the quantitation of NMHCs in air samples, one approach is to assume that, experimentally, the FID output signal is directly proportional to the number of carbon atoms in the NMHC molecule. The unit, parts-per-billion by volume as carbon (ppbC), is defined as:

$$ppbv \text{ x no. of C atoms per NMHC molecule} = ppbC$$

Table 7.4 : Test of Trapping Efficiency as a Function of Trapping Times

Trapping Time (min)	*13.5*	*27.5*	*47.1*		
	Concentration (ppbV)			SD	RSD (%)
Ethane	0.60	0.58	0.58	0.01	2.3%
Ethylene	1.67	1.67	1.71	0.02	1.2%
Propane	1.11	1.12	1.12	0.00_5	0.5%
Propylene	0.38	0.39	0.40	0.01	3.4%
i-Butane	0.85	0.86	0.86	0.00_3	0.4%
n-Butane	1.81	1.81	1.82	0.00_7	0.4%
Acetylene	1.49	1.50	1.51	0.01	0.7%

Table 7.5 : Effect of sample volume difference in measured NMHC concentrations

Vol. of Air Sample (ml at STP)	*334*	*204*		
	Concentration (ppbV)		Mean	Dev. from Mean (%)
Ethane	0.29	0.30	0.29	1.15
Ethylene	0.22	0.26	0.24	7.39
Propane	0.23	0.23	0.23	1.76
Propylene	0.12	0.14	0.13	8.34
i-Butane	0.28	0.30	0.29	3.20
n-Butane	0.32	0.35	0.34	4.86
Acetylene	0.12	0.14	0.13	6.90

Figure 7.5: FID Linearity Range using SRM Propane as Standard

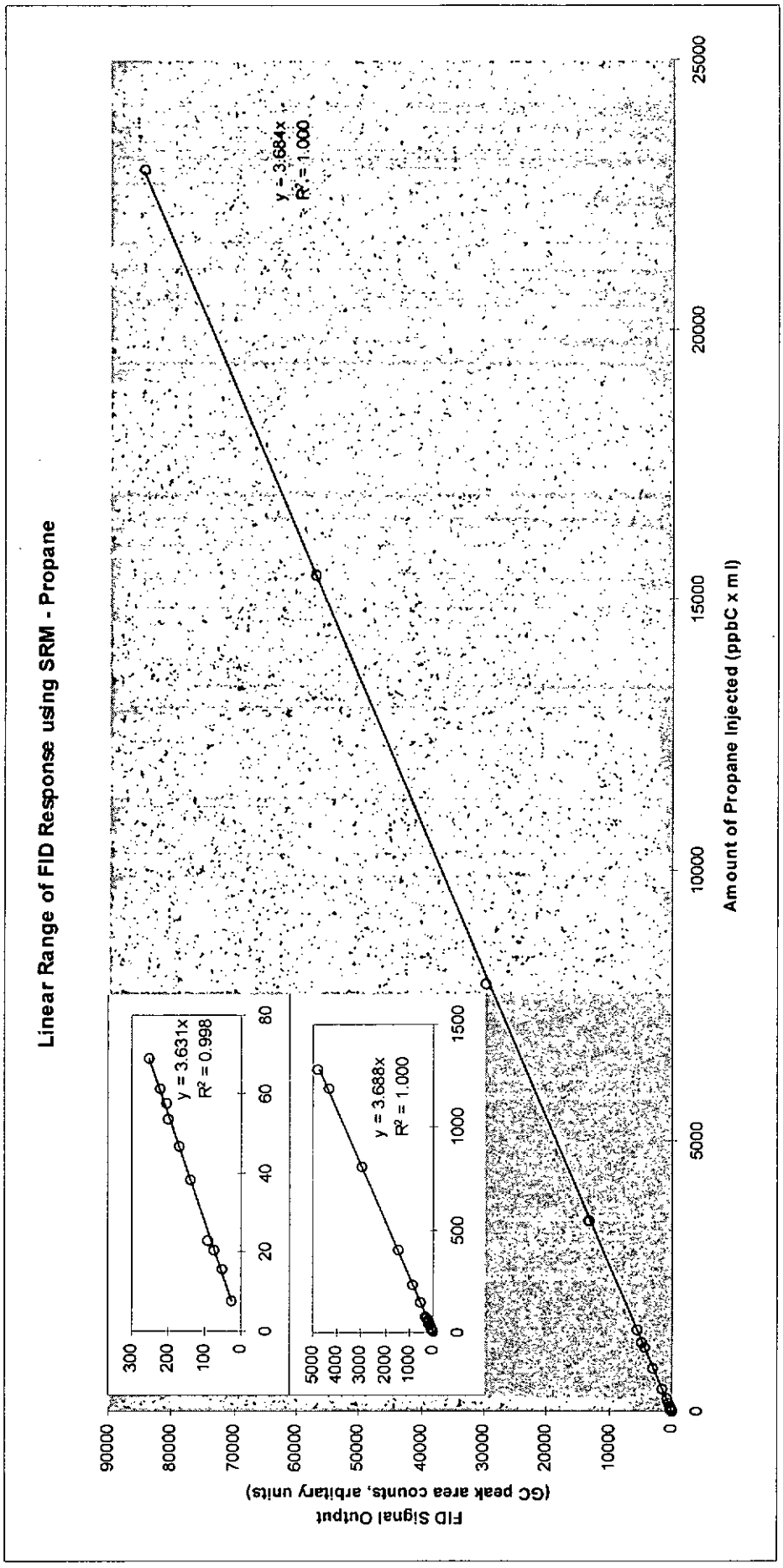

In other words, the FID response factor, expressed as GC peak area counts per ppbC per ml (at STP), should be the same for all the NMHC species measured. The NMHCs in the air samples were then quantified with respect to the FID response factor obtained by using the propane concentration (0.970±0.010 ppmV) in the NIST SRM 1660a standard as reference. In addition, the response factor obtained by using the Scott Specialty Gases 2,2-dimethylbutane (neohexane) secondary reference standard (201 ppbV, ±5%) was compared to the NIST propane SRM 1660a.

The FID response factors measured by using diluted secondary working standards derived from NIST SRM 1660a is shown in Table 7.6, indicating that the FID response factor (volume by volume as carbon) is nearly constant in the NMHC concentration range measured in this project. The average FID response factor, 3.65 area counts per ppbC per ml (STP), was used throughout this project to calculate the concentration of the individual NMHC species in the air sample. The average FID response factor measured with the 2,2-dimethylbutane secondary standard (Scott Specialty Gases, stated accuracy ±5%) was 3.74 area counts per ppbC per ml (n=10, SD=0.05). This average FID response factor was in good agreement (<±5%) with the value obtained using the NIST SRM 1660 a reference standard.

The FID response factors from other Scott Specialty Gases NMHC standards (stated accuracy ±10%) are also tabulated in Table 7.7. The measured

FID response factors were also in good agreement (<±10%) with the average value obtained using the NIST SRM 1660a reference standard, and the small differences could be attributed to possible quoted errors in the concentration of the NMHC secondary standards.

Thus, our results showed that under the GC/FID experimental conditions adopted in this project, the GC/FID response factor can be assumed to be the same for C_2 - C_6 NMHCs measured. Judging from the relative standard deviation shown in Table 7.7, the error introduced by this assumption is ±5% measured with respect to the NIST 1660a propane reference standard.

The concentration of individual NMHC was calculated by

$$C_{sample}\ (ppbC) = \frac{A_{sample}}{R.F.} \qquad \text{[Equation 12]}$$

where C_{sample} = concentration of sample NMHC in units of parts-per-billion-volume per carbon

A_{sample} = GC peak area of NMHC species

$R.F.$ = GC/FID response factor (in units of GC peak area per ppbC per ml (STP))

The NMHC concentrations in ppbC (or pptV) units are easily converted back to ppbV (or pptV) units according to [Equation 12].

In this thesis, total NMHC concentration is expressed in ppbC units as it is easily computed from the summation of C_2-C_6 GC peak areas and divided by the GC response factor. For individual NMHCs, measured concentrations are expressed in units of pptV (1 in 10^{-12}, volume by volume).

7.3.2. Co-elution of Chlorofluorocarbons (CFCs) with NMHCs in GC Separation Using PLOT column

The occurrence of co-elution of CFCs with NMHCs in the GC separation using Al_2O_3 PLOT column (Chrompak, Raitron, NJ) has been reported[56,57], and this would affect the accuracy of the measured concentrations of the NMHCs. The GC chromatograms of NMHC in an air sample, with and without CFC standards added, are shown in Figure 7.6 (a) and (b) respectively. Our results showed that no overlap of CFC peaks with our reported NMHCs. This is probably due to differences in the retention behavior of the Al_2O_3 PLOT GC columns used in our NMHC analysis, which was purchased from Hewlett-Packard Supplies (Hewlett-Packard, HP-PLOT Al_2O_3 "S" Deactivated column).

Table 7.6 : FID Response Factors Measured Using NIST Propane SRM 1660a Reference Standard

Concentration of Propane Working Standard (ppbv)	Amount (ppbC x ml at STP)	FID Response Factor (area count/ppbC x ml)
0.12	7.49	3.40
0.12	15.6	3.42
0.12	20.4	3.56
0.12	22.9	3.92
0.12	38.5	3.62
0.12	46.9	3.63
0.12	53.7	3.70
0.12	57.6	3.53
0.12	61.3	3.61
0.12	68.9	3.67
0.12	75.7	3.97
2.3	1.49	3.49
2.3	2.29	3.69
2.3	4.03	3.62
2.3	8.08	3.59
2.3	1.19×10^4	3.61
2.3	1.52×10^4	3.62
46.9	1.28×10^4	3.75
46.9	3.53×10^4	3.77
46.9	7.92×10^4	3.74
46.9	1.55×10^4	3.68
46.9	2.30×10^4	3.68
46.9	2.90×10^4	3.68
Average FID Response Factor	*3.65*	
SD (n=24)	*0.13*	
RSD(%)	*3.7%*	

Table 7.7 : FID Response Factors Measured Using NMHC Secondary Standards from Scott Specialty Gases[a]

	Secondary Standard	Concentration (ppmv)	FID Response Factor (area count/ppbC x ml)[b]
Alkanes	Ethane	16.5	3.43
	Propane	16.5	3.39
	n-Butane	16.5	3.38
	n-Pentane	15.5	3.54
	n-Hexane	15.8	3.71
Alkenes	Ethylene	15.0	3.62
	Propylene	15.0	3.52
	1-Butene	14.9	3.46
	1-Pentene	14.8	3.40
	1-Hexene	15.0	3.55
C4 isomers	i-Butane	15.2	3.39
	n-Butane	15.1	3.41
	trans-2-Butene	14.8	3.61
	1-Butene	14.9	3.51
	isobutylene	15.2	3.40
	cis-2-Butene	14.9	3.54
	1,3-Butadiene	15.1	3.26
Alkyne	Acetylene	15.0	3.47
		Overall Average	*3.48*
		SD (n=18)	*0.11*
		RSD(%)	*3.14*

[a] The secondary NMHC standards were introduced into the GC/FID system via a 2-ml (nominal) sample loop.

[b] Average of triplicate injections (n=3).

7.4. Inter-Laboratory Comparison on Analytical Accuracy

The overall analytical accuracy of our sampling and GC systems, and our adopted analytical protocol for NMHCs, were tested and validated against two accurately calibrated NMHC standards and one standard air sample provided by Dr. D.R. Blake, Department of Chemistry, University of California, Irvine (UCI), CA, USA. The identity and concentrations of NMHCs in the calibrated standard and air samples were determined in our laboratory, and sent to UCI for confirmation and validation.

Figure 7.6: Typical Chromatograms for Determination of CFC Co-elution (a) without CFC added, (b) with CFC added

(a)

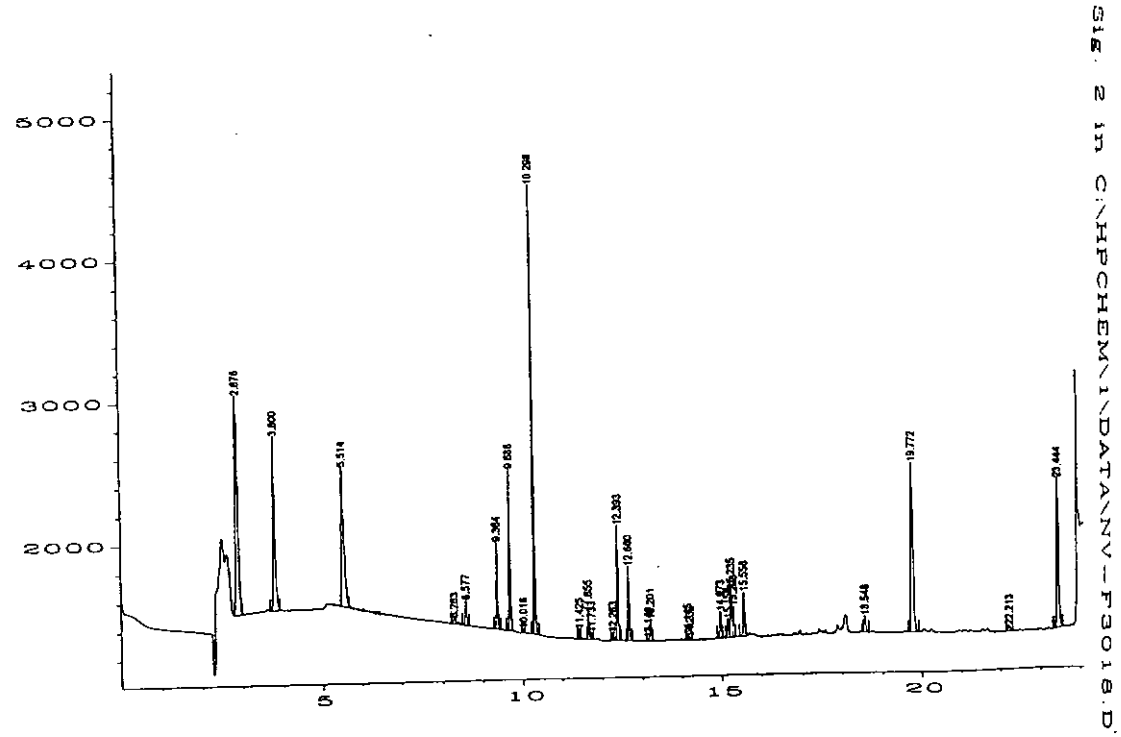

(b)

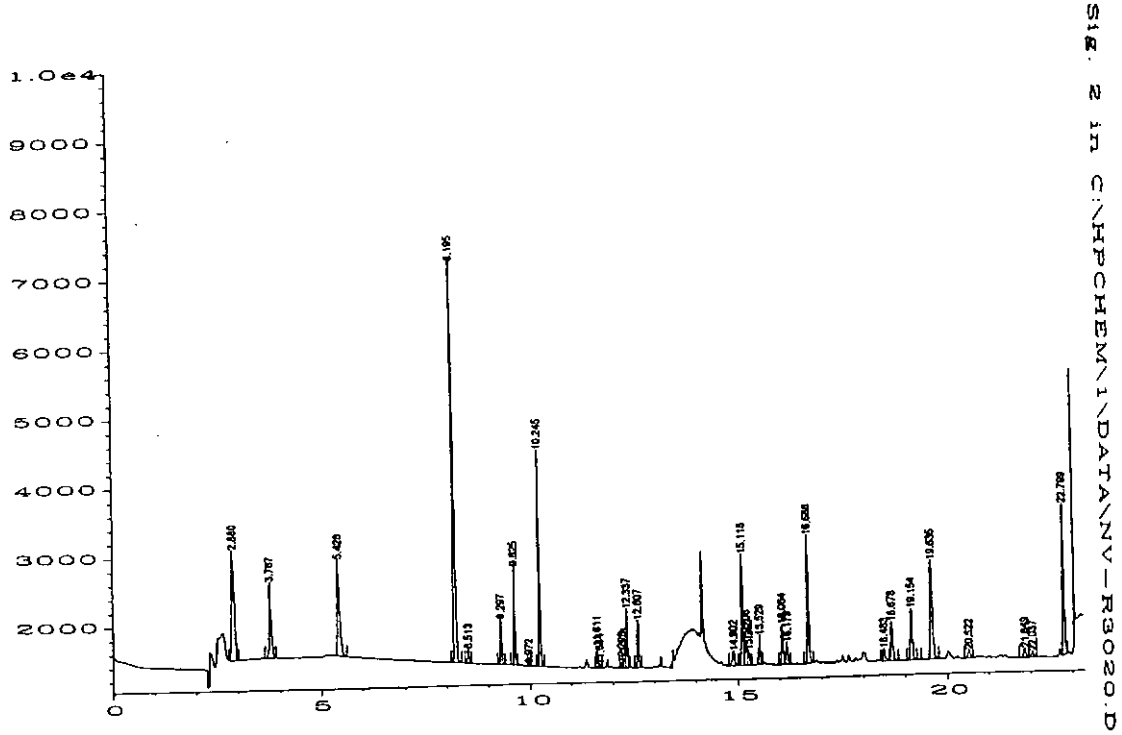

Aside from analysis using the HP-PLOT/Al_2O_3 GC column, separate analysis using two packed GC columns were carried out to provide confirmation on the quantitative results for C_2-C_4 NMHCs. The experimental conditions e.g. carrier gas flow rates, FID response factors for analysis using packed GC columns were very different from that of using the HP-PLOT/Al_2O_3 columns, and agreement between data sets obtained by using different GC columns is generally regarded as experimental proof on the quality and accuracy of the analytical protocol adopted. In our case, very good agreement, with average percentage deviation of $< 2\%$, was obtained on C_2-C_4 NMHC results measured using the PLOT, phenyl isocyanate/Porasil C (80/100 mesh) and Unibeads A (60/80 mesh) columns.

The results of inter-laboratory comparison on the two NMHC standard samples provided by UCI laboratory are shown in Table 7.8. For C_2 to C_6 hydrocarbons, our results showed relative deviations ranging from -7% to 13%, but mostly in the -3.0 to +4.0% range. An underestimation was observed in 1-hexene with a relative deviation of 21%, but 1-hexene was not found in our air samples.

Table 7.8 : Results for the Intercomparison Experiment (a) standard #3802 and (b) standard #3227

(a) standard #3802

NMHC Species	Our Results (ppbV)[a]	Calibrated Values from Dr. Don Blake Laboratory (ppbV)	% Deviation
Ethane	21.5	21.41	-0.42
Ethylene	20.8	20.47	-1.61
Propane	21.6	21.41	-0.89
Propylene	20.1	19.55	-2.81
I-Butane	16.8	16.47	-2.00
n-Butane	21.3	21.41	0.51
1-Butene	19.6	20.44	4.11
2,2-dimethylpropane	17.1	16.80	-1.79
2-methylbutane	16.7	16.70	0.00
n-Pentane	20.7	21.41	3.32
1-Pentene	19.1	20.44	6.56
2,2-dimethylbutane	16.4	16.70	1.80
3-methylpentane	16.1	16.80	4.17
2-methylpentane	16.2	16.80	3.57
n-hexane	18.7	21.41	12.66
1-hexene	16.3	20.44	20.25

[a] Average results from n=7 independent GC analysis

(b)standard #3227

NMHC Species	Our Results (ppbV)[b]	Calibrated Values from Dr. Don Blake Laboratory (ppbV)	% Deviation
Ethane	11.89	11.83	-0.51
Ethylene	7.48	7.37	-1.49
Propane	11.87	11.83	-0.34
Propylene	7.26	7.05	-2.98
I-Butane	1.06	0.99	-7.07
n-Butane	11.75	11.83	0.68
1-Butene	7.04	7.37	4.48
2,2-dimethylpropane	1.05	1.01	-3.96
2-methylbutane	1.05	1.01	-3.96
n-Pentane	11.45	11.83	3.21
1-Pentene	6.79	7.37	7.87
2,2-dimethylbutane	1.05	1.01	-3.96
3-methylpentane	1.00	1.01	0.99
2-methylpentane	1.00	1.01	0.99
n-hexane	10.34	11.83	12.60
1-hexene	5.81	7.37	21.17

[b] Average results from n=8 independent GC analysis

Table 7.9 : Inter-laboratory Comparison of Quantitative Results on NMHC Analysis of an Ambient Air Sample Collected at the HK Air Monitoring Station

NMHC Species	Our Results (pptV)	UCI results(pptV)	% Deviation from UCI results
Ethane	2608	2610	-0.1
Ethylene	276	249	10.8
Propane	1109	1185	-6.4
Propylene	44	51	-13.7
i-Butane	208	205	1.5
n-Butane	315	312	0.1
Acetylene	1443	1133	27.4
1-Butene	13	36	63.9
2,2-dimethylpropane	37	(a)	N/A
2-methylbutane	149	(a)	N/A
n-Pentane	81	76	6.6
2,2-dimethylbutane	30	(a)	N/A
3-methylpentane	63	(a)	N/A
2-methylpentane	32	(a)	N/A
n-hexane	42	43	2.3

(a) not measured

A second inter-laboratory comparison on quantitative results was carried out on an ambient air sample collected at the HK PolyU Atmospheric Research Laboratory at Cape D'Aguilar on 4th March, 1997. This air sample was analyzed by our laboratory and then taken back to the UCI laboratory for analysis and the comparison results were tabulated in Table 7.9.

The agreement between the two laboratories on NMHC quantitative results was very satisfactory; the percentage deviation ranges from -13.7% to +10.8% for 8 NMHC species measured. The percentage deviations were expected to be greater this time because of the much lower concentrations (pptV) of NMHCs measured in the ambient air sample than in the previous NMHC standards (ppbV).

Much higher percentage deviations were observed for acetylene (+27.4%) and 1-butene (+63.8%). The causes for the observed differences are unknown, but differential sample loss during transport and storage of the air sample, as well as during the sampling and analytical steps, are possible sources of error.

On the whole, our inter-laboratory comparison results (percentage deviation $<\pm 15\%$) on NMHC analysis are very satisfactory to be within internationally accepted standards. This shows that our NMHC data set are of good quality in terms of accuracy and precision.

7.5. Integrity Studies

7.5.1. Sample Storage Stability and Canister Integrity

Successful storage of trace NMHCs in air samples depends on the nature of inner surfaces of the containment canister and the cleaning processes used on these surfaces[58].

Since the time delay between sample collection and analysis was in the range of 2 hours to 2 days, laboratory tests on NMHC stability during sample storage were conducted. Two canisters of air samples were analyzed within different period from the air sampling time. One canister was analyzed within one day after sample filling, then weekly for the next 4 weeks. Another canister of air sample was assayed within 30 minutes after sample collection, and the analysis was repeated at 3½ hours, 1 day, and 2 days period from the time of sampling. The results of the sample stability and storage experiments are shown in Table 7.10. All the measured concentrations were shown to lie within a relative standard deviation of 10% over the period of storage and analysis. No significant deviations in any of the concentrations of the measured NMHCs were observed except a slightly greater variation of propylene concentrations. This may be due to greater errors in peak area integration as the propylene concentration was lower than other NMHCs in the air sample. No direct information is available about possible alternations in trace gas concentrations occurring in the canisters during the 30 minutes between collection and analysis, but the consistency of the results suggests that any such concentration variations

are negligible. These studies confirm that the sample canisters used in our project could maintain sample integrity for at least several weeks.

7.6. Other measurements

7.6.1. Surface O_3 and CO

Surface O_3 and CO measurements were conducted by other members of the research groups in the Atmospheric Research Laboratory.

The sampling lines for the gas analyzers were Teflon lines (1/4" OD) housed in a weatherproof metal box. This box was fitted on the top of a tower in which contained the Teflon solenoid valves and filters for flow controls and spiking of standards during calibration. These sampling lines were approximately 7 m long which are roughly at the same height as the sample inlet for NMHC analysis.

Table 7.10 : Qualitative Results of the Sample Stability and Canister Storage Experiment

(a) (1 day to 28 days)

Days	1	3	7	14	22	28	Mean	SD (n=6)	RSD (%)
Ethane	1.59	1.58	1.54	1.63	1.55	1.58	1.58	0.03	1.98
Ethylene	0.37	0.33	0.31	0.35	0.34	0.36	0.34	0.02	6.69
Propane	0.61	0.62	0.62	0.59	0.57	0.62	0.60	0.02	3.89
Propylene	0.11	0.08	0.09	0.10	0.10	0.12	0.10	0.01	12.69
n-Butane	0.21	0.20	0.20	0.22	0.21	0.22	0.21	0.01	4.78
Acetylene	0.94	0.94	0.96	0.96	0.99	0.99	0.96	0.02	2.50

Note: All concentrations in ppbV

(b) (0.5 hour to 2 days)

Time	0.5 hour	3.5 hours	1 day	2 days	Mean	SD (n=5)	RSD (%)
Ethane	1.71	1.62	1.62	1.50	1.61	0.09	5.28
Ethylene	2.17	2.12	2.11	2.03	2.11	0.06	2.85
Propane	3.62	3.62	3.57	3.47	3.57	0.07	2.01
Propylene	0.30	0.28	0.30	0.28	0.29	0.01	3.67
n-Butane	3.73	3.71	3.64	3.52	3.65	0.09	2.55
Acetylene	4.64	4.55	4.41	4.35	4.49	0.13	2.92

Note: All concentrations in ppbV

Ozone measurements were obtained with a commercial UV photometric analyzer (Thermo Environmental Instruments Inc., Franklin, MA, Model 49). This instrument uses absorption of 254 nm radiation and it has a dual cell design. It automatically corrects for pressure and temperature fluctuations in the absorption cell. Artifact checks were performed once a day by automatically injecting charcoal scrubbed zero air (Thermo Environment Instruments Inc., Model 111 & 146) through the sampling line. CO measurements were obtained with a gas filter correlation, non-dispersive infrared absorption instrument (Thermo Environment Instrument Inc., Model 48). This instrument automatically corrects for pressure and temperature fluctuations in the absorption cells. A zero trap, 50 cm^3 of 0.5% Pd on alumina (Type E221 PID catalyst, Degussa Corp., Plainfield, NJ) maintained at 250°C was installed on a bypass loop immediately upstream of the CO analyzer. The calibration was routinely accomplished by the standard addition method. Calibration was conducted every four hours because the constant baseline determination was essential for this instrument. The change of sensitivity was less than 3% over one year of observation.

7.6.2. Meteorological Measurements

Several types of meteorological data and analyses were used for interpretation of the sample profiles. Ten-day spanned, three-dimensional isentropic back-trajectories at 1000 m elevation were calculated and provided by

the Climate Monitoring and Diagnostic Laboratory, National Oceanic and Atmospheric Administration, Boulder, CO, USA, every day at 0h and 12h UT.

Wind speed and direction, air temperature, dew point, rainfall were derived from continuous measurements at the Hong Kong Observatory site located at Waglan Island. These meteorological parameters were merged with the NMHC data for data analysis and interpretation.

7.7. Accuracy and Precision Measurement

The precision of the air sample measurements was estimated from repeated analyses of the same air sample. The precision of individual C_2-C_6 hydrocarbon mixing ratios varied by better than $\pm 2\%$, depending on their respective concentrations (SEM, $n=8$). As individual hydrocarbon mixing ratios approached detection limits, errors were larger. Some chromatographic peaks, especially those near the detection limits, were integrated manually. This increased the uncertainty of those determinations. The detection limit for a 200 mL sample was estimated from the repeated integration of the smallest chromatographic peaks, and was approximately 10 parts-per-trillion by volume as carbon (pptvC) for propane.

8. *NMHCs and Methane Measured at Cape D'Aguilar, Hong Kong*

8.1. Description and General Features of the Data Set

8.1.1. Methane Measurements

Methane measurements were conducted typically on alternate days from the period 12 April 1996 to 21 October 1997 and a total of 194 samples were analyzed. The variation of the methane mixing ratios (concentration) during the study period is shown in Figure 8.7. Its average concentration over the study period was 1870±174 ppbV (n=194, mean ± SD). No significant seasonal variation was found as compared to C_2-C_6 NMHC species. This is due to the long lifetime of methane and it is evenly distributed and well mixed in the atmosphere.

Occasionally, daily methane concentrations exceeding 2,000 ppbV were measured. The elevated methane concentrations on 25-27 July 1996 and 21 October 1997 were associated with episode days due to localized stagnant meteorological conditions. It was possible that local emissions of methane from landfill sites in Hong Kong were transported to the Station, leading to the temporal high level of methane recorded.

8.1.2. Nonmethane Hydrocarbon Measurements

Atmospheric concentrations of 14 C_2-C_6 NMHCs including ethane, propane, isobutane, n-butane, isopentane (2-methylbutane), n-pentane, 2,2-dimethylbutane, 2-methylbutane, 3-methylbutane, n-hexane, ethylene, propylene, 1-butene, and acetylene were measured for the period between October 1995 and March 1997. A typical gas chromatogram (C_2-C_6) of an air sample collected at Cape D'Aguilar is given in Figure 8.8. About 27-30 NMHCs were generally found in the C_2-C_6 range. C_2-C_6 NMHCs are much more reactive and has a much larger temporal and spatial variability compared to methane. Therefore C_2-C_6 NMHCs are more important in studying the regional-scale atmospheric photochemistry and transport.

A total of 552 ambient air samples were analyzed during study period. The total NMHC concentration was obtained by summing the concentrations of the 14 individual species expressed on a per carbon basis (ppbC). The total NMHC data set is graphically presented in Figure 8.9. Isolated episode days or periods associated with high levels of total NMHC are observed and scattered throughout the period of study, indicating that the level of NMHC pollutants is strongly affected and dependent on local meteorological conditions. For example, many episode days associated with incidents of typhoons were observed during the July and August months of 1996.

Figure 8.7: Variation of the Methane concentration during the period Apr'96 to Oct'97

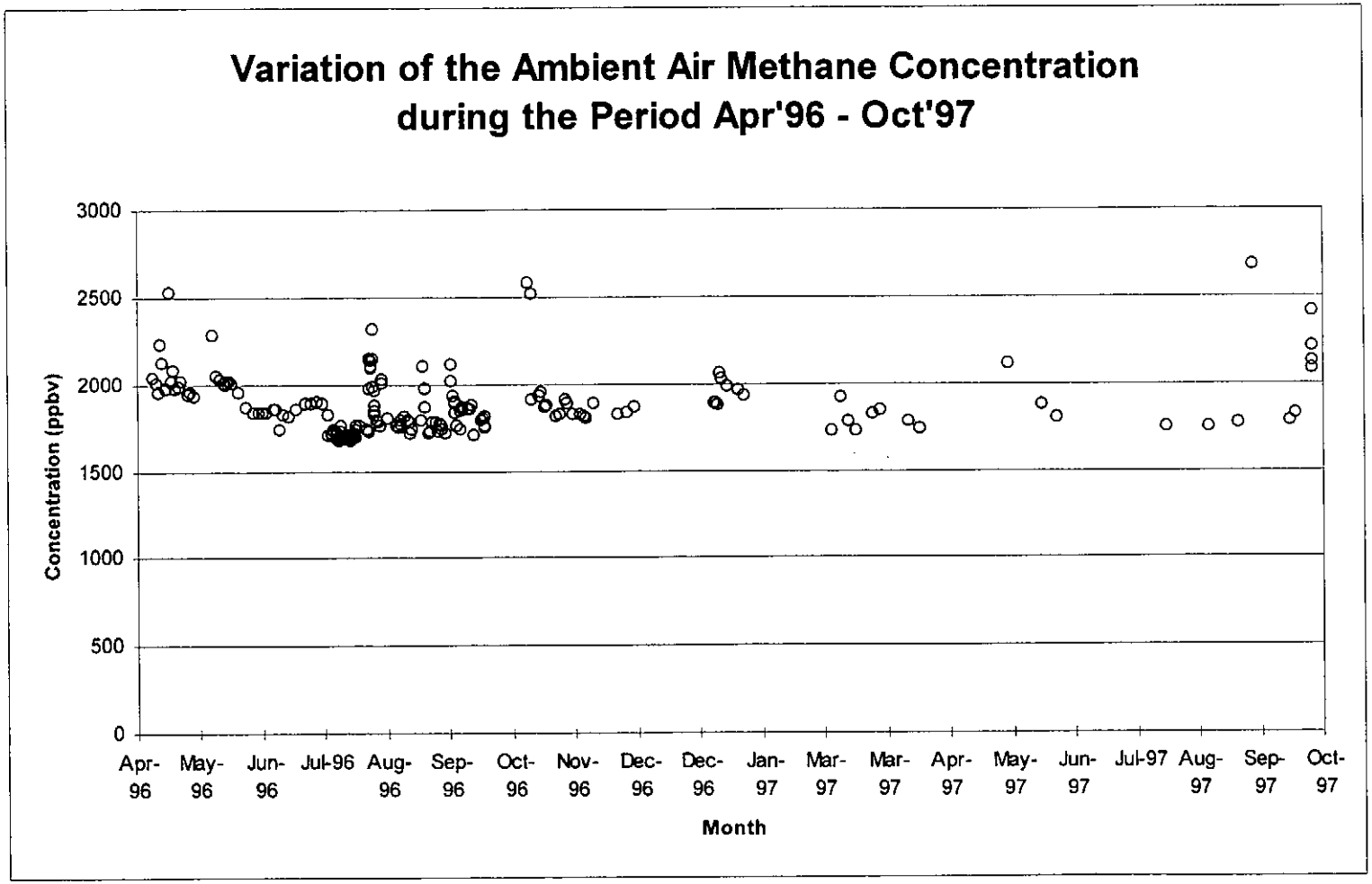

Figure 8.8 : An example chromatogram from the HP-PLOT column used in the determination of C_2-C_6 NMHCs in Air Samples

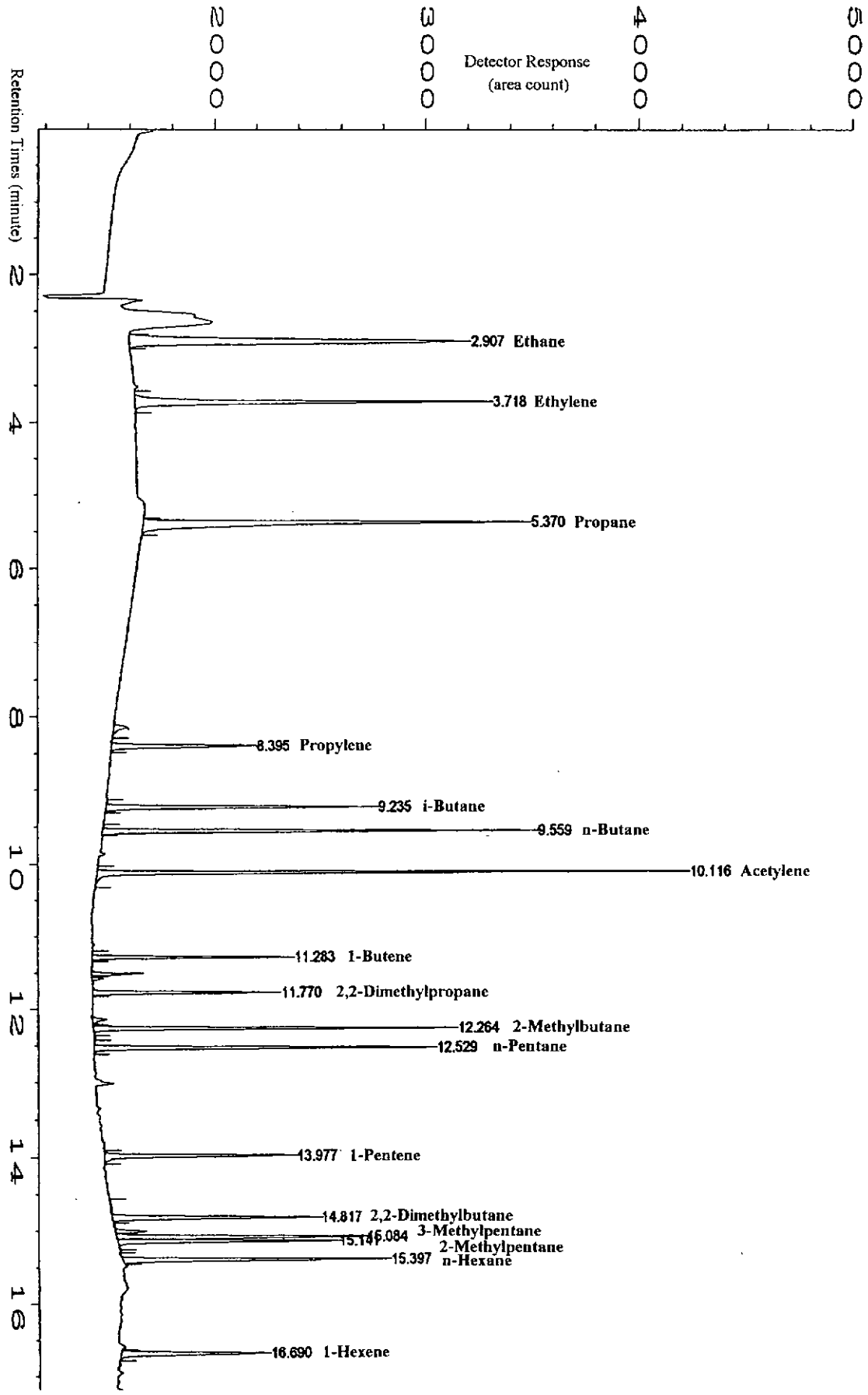

8.1.3. Monthly & Seasonal Variations of NMHC Concentrations

The monthly averages of total NMHCs and individual NMHC species are tabulated in Table 8.11. To minimize the effect of episode days on the monthly statistics, monthly averages of individual C_2-C_6 NMHCs with top 5% cut-off of the data points are also calculated and presented in Table 8.12. Irrespective of the different method of statistical treatment, distinct trends of seasonal variation are observed for total NMHC, and major components like ethane, propane, ethylene, and acetylene.

Variations of monthly averages of total NMHC together with selected NMHCs, including alkanes (ethane & propane), alkenes (ethylene & propylene), and alkyne (acetylene) are graphically presented in Figure 8.10(a) to (d), respectively. A general increasing trend was observed starting from October, which peaked in January, then decreased slowly and reached a very low level in June, July and August. The NMHCs then increased gradually from September.

Figure 8.9 : Variation of Total NMHC for the Period Oct'95-Mar'97

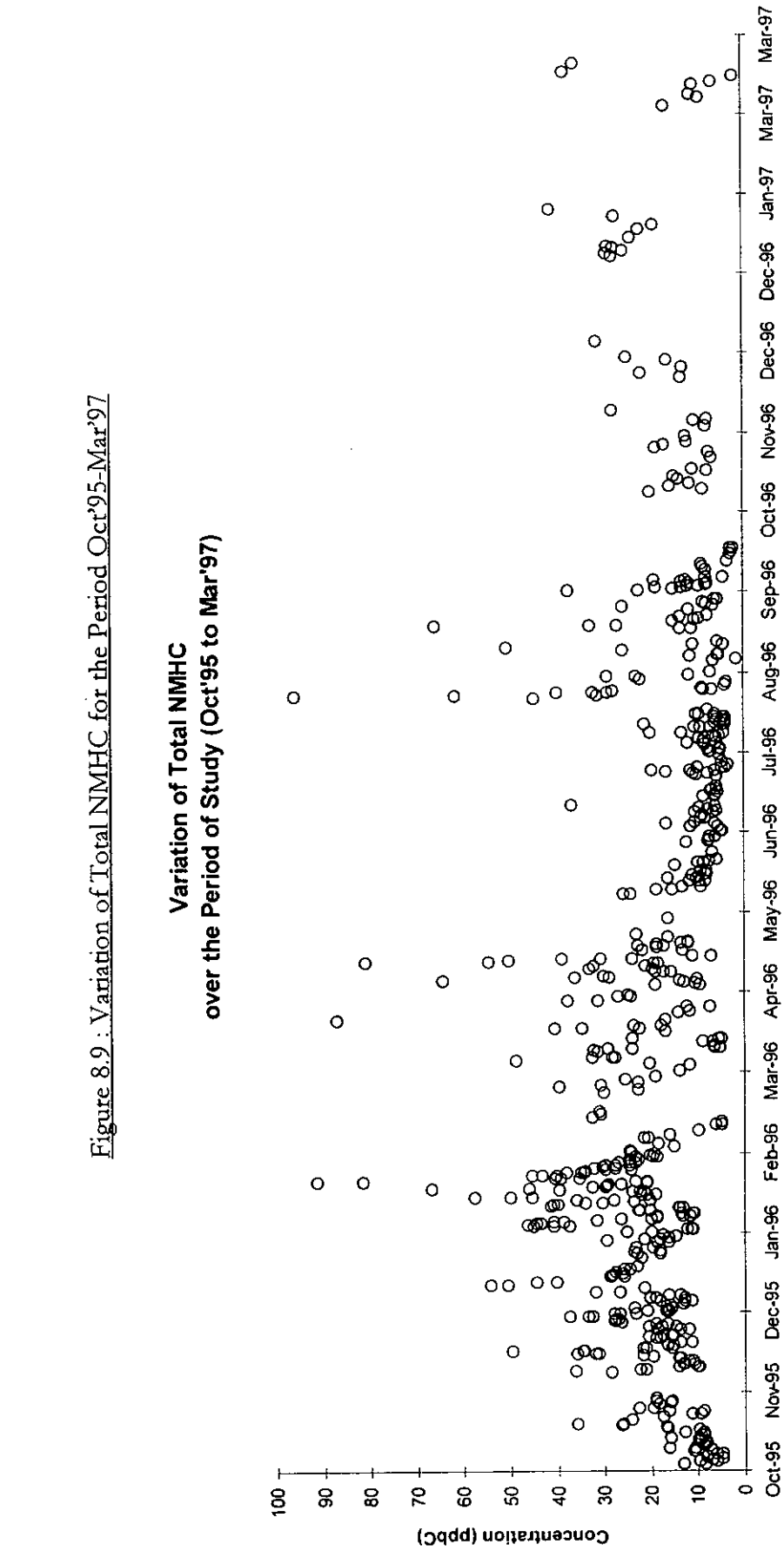

Table 8.11 : Monthly Averages of Total NMHC and Individual NMHCs (No data filtering)

Month	No.of Measuring Days	n=no. of data points	Total NMHC	Ethane	Ethylene	Propane	Propylene	iso-Butane	n-Butane	Acetylene	1-Butene	2-methylbutane	n-Pentane	2,2-dimethylbutane	3-methylpentane	2-methylpentane	n-Hexane
Oct-95	21	36	12.33	1479	575	566	125	123	224	1288	64	109	83	35	48	29	60
Nov-95	18	48	19.48	2276	1016	893	134	204	381	2155	62	181	135	44	62	38	82
Dec-95	26	56	23.90	2698	1267	1091	132	267	485	2760	50	221	160	51	81	53	93
Jan-96	30	87	29.85	3119	1588	1423	137	353	643	3315	36	326	236	73	111	65	119
Feb-96	18	31	22.13	2627	1141	1120	131	254	467	2408	40	224	160	36	55	31	58
Mar-96	20	35	22.02	2122	813	1081	144	460	791	1626	48	265	209	52	80	50	95
Apr-96	19	44	24.40	2356	934	1075	149	417	859	2003	47	323	282	76	87	56	101
May-96	14	28	11.88	1296	404	482	140	209	342	686	56	193	186	33	41	25	53
Jun-96	22	42	11.72	441	286	458	133	552	725	147	47	298	167	20	26	17	38
Jul-96	23	53	40.16	497	477	446	107	248	393	528	32	295	181	505	55	231	4384
Aug-96	20	29	16.05	599	374	707	108	339	803	458	42	484	304	61	110	70	103
Sep-96	13	24	19.40	675	242	565	61	827	1913	591	24	269	228	42	51	32	53
Oct-96	14	16	12.93	1645	546	683	66	161	249	1339	16	150	93	30	29	18	41
Nov-96	9	9	15.86	1729	656	785	113	186	312	1508	25	189	121	50	83	46	112
Jan-97	10	10	27.24	2912	1317	1481	157	346	572	2434	38	323	204	78	140	75	130
Mar-97	8	8	16.18	1912	813	749	124	183	287	1328	36	178	103	118	102	46	72

Note: Total NMHC concentration in ppbC; individual NMHC concentration in pptV

Table 8.12 : Monthly Averages of Total NMHC and Individual NMHCs (Top 5 % cut-off)

Month	No.of Measuring Days	n=no. of data points	Total NMHC	Ethane	Ethylene	Propane	Propylene	iso-Butane	n-Butane	Acetylene	1-Butene	2-methyl butane	n-Pentane	2,2-dimethylbutane	3-methylpentane	2-methylpentane	n-Hexane
Oct-95	21	34	11.52	1387	516	527	123	115	213	1181	63	102	79	34	46	28	58
Nov-95	18	45	18.07	2184	922	847	125	187	348	2002	61	162	119	35	56	34	66
Dec-95	26	53	22.43	2617	1100	1049	118	255	462	2580	48	203	148	47	77	47	86
Jan-96	30	81	27.20	3025	1399	1326	109	310	565	3097	31	279	205	59	93	54	97
Feb-96	18	29	21.17	2606	1072	1061	119	237	432	2354	37	208	148	32	49	28	53
Mar-96	20	32	18.57	2062	706	988	133	273	463	1494	47	231	185	43	71	44	86
Apr-96	19	40	20.58	2281	791	939	133	315	521	1758	44	276	256	63	73	47	87
May-96	14	26	10.87	1229	342	456	137	203	320	578	56	175	163	25	36	22	47
Jun-96	22	38	7.42	387	277	352	127	216	206	141	45	244	150	19	22	15	35
Jul-96	23	50	10.92	452	455	400	106	232	364	465	31	281	172	50	46	37	186
Aug-96	20	26	12.15	590	282	647	98	244	614	343	32	314	229	43	62	39	59
Sep-96	13	22	9.81	660	223	420	58	222	393	529	22	236	193	41	44	28	46
Oct-96	14	15	12.46	1631	509	672	62	154	235	1313	15	143	87	24	27	17	29
Nov-96	7	7	12.89	1625	514	711	93	148	227	1323	25	129	80	19	42	22	69
Jan-97	8	8	25.25	2896	1245	1388	144	308	494	2408	36	276	166	64	112	59	98
Mar-97	7	7	13.05	1619	570	576	110	137	214	1040	34	143	76	123	92	40	62

Note: Total NMHC concentration in ppbC; individual NMHC concentration in pptV

Figure 8.10 : Variation of monthly mean concentration of (a) alkanes (ethane & propane), (b) alkenes (ethylene & propylene), and (c) alkyne (acetylene)

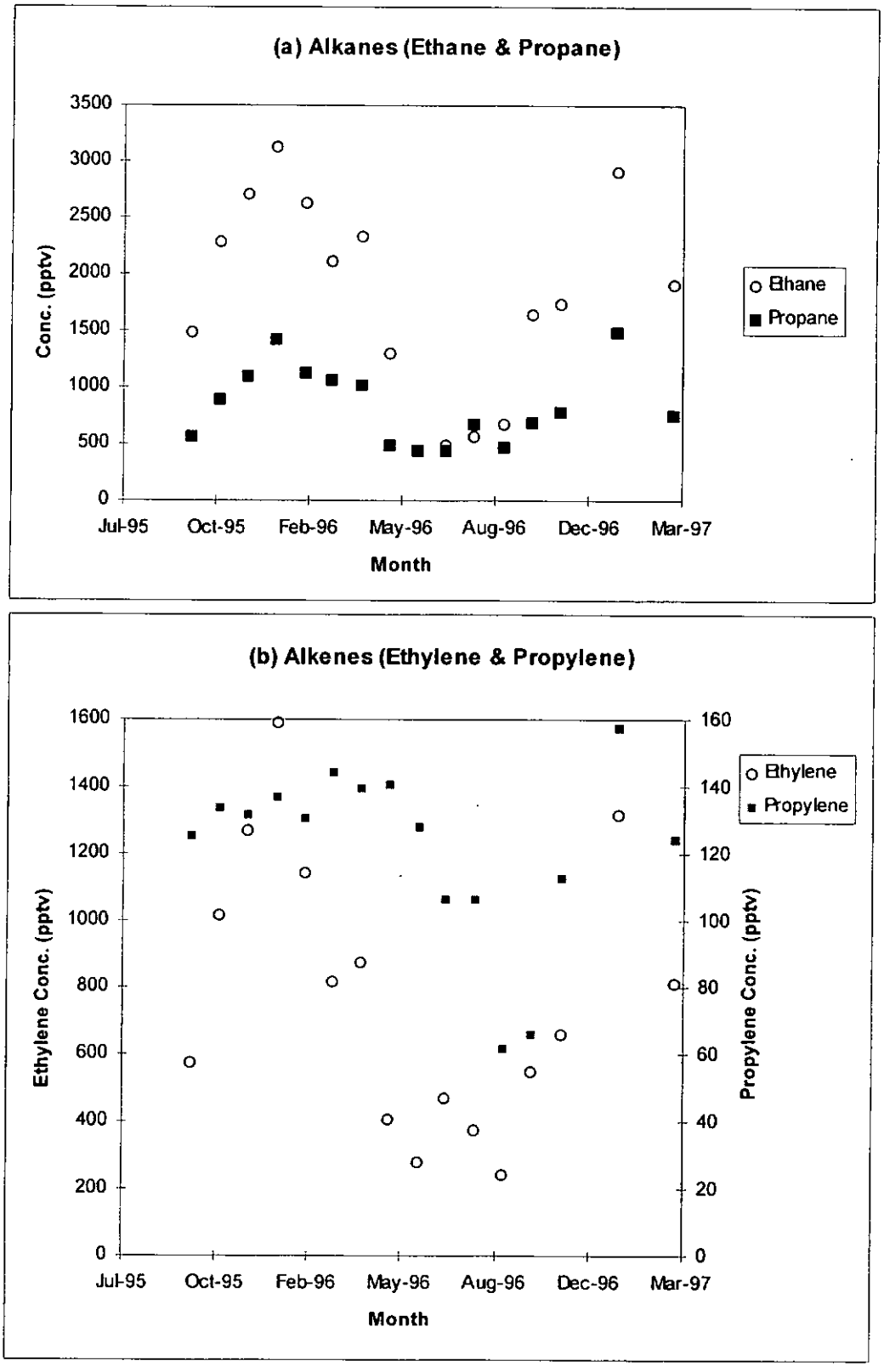

Figure 8.10 (cont'd)

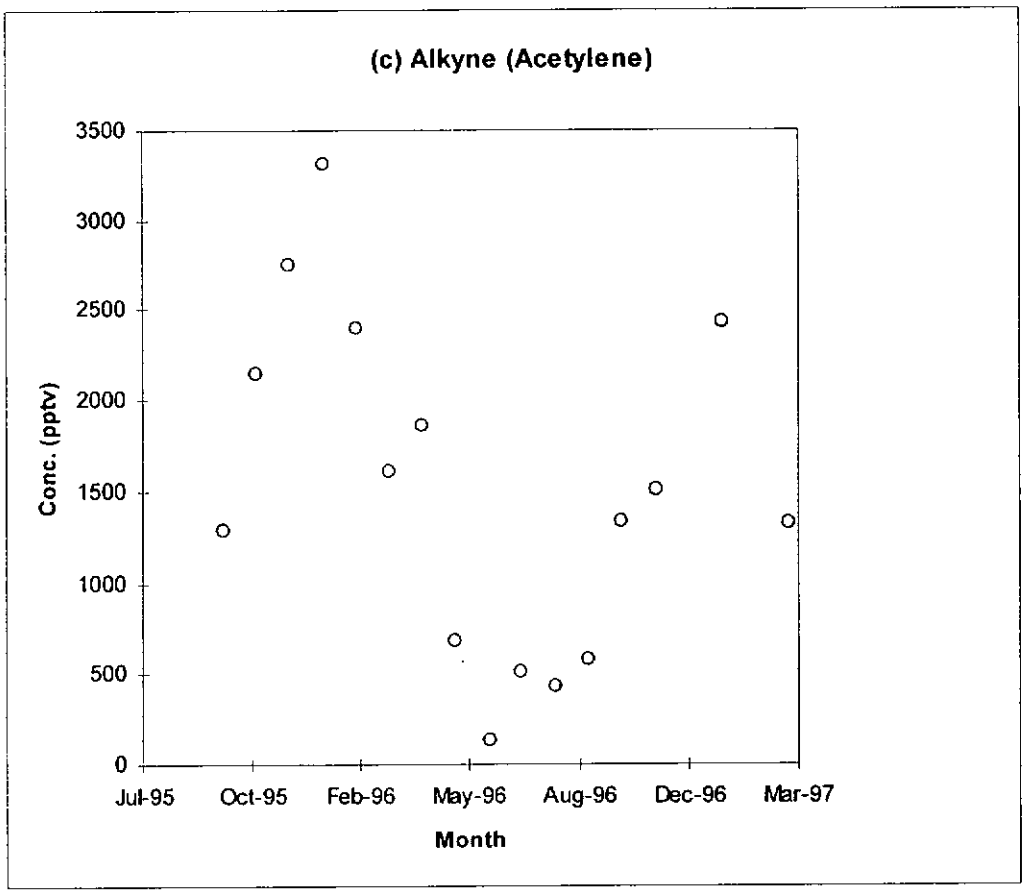

However, the seasonal variation of propylene (Figure 8.10 (c)) was relatively less as compared to other NMHCs , which showed a more steady concentration over the period of study except during August and September. Since the winter period in Hong Kong is from December to February whereas summer is from June to August, the observed variations in NMHC concentrations show that the NMHC levels have a seasonal dependence, with high concentrations during winter and low concentrations during summer.

Similar winter (January/February) maxima and summer minima (July/August) in NMHC concentrations were observed for a number of background monitoring stations in the northern hemisphere[39,59,60]. The elevated levels of NMHC observed in winter could be attributed partly to enhanced emissions from fuel consumption and biomass burning in the winter for domestic heating, or the decreasing OH concentrations and hence slow-down in the rate of photochemical degradation of NMHCs. Furthermore, NMHCs were reported to have a significant hemispheric gradient, with high concentrations in the Northern Hemisphere and decrease towards the Equator in the Pacific[61,62]. Therefore continental outflow from the north will enhance surface NMHC levels in the winter. The low NMHC levels observed in the summer months was due to the transport of relatively clean oceanic air masses from the Pacific Ocean.

Apart from the variations in absolute concentrations, there were monthly variations in the chemical compositions of NMHCs, in terms of relative distributions of alkanes, alkenes, and alkynes as shown in Table 8.13. Alkanes were the major constituents among the three classes of hydrocarbons over the period of study, reaching a maximum of 86% of the total NMHC during the summer months. However, the percentage of alkanes dropped to about 65% in the winter whereas that of alkenes increased from 7% in the summer to about 12% in the winter. Higher NMHC concentrations as well as increased shares of reactive hydrocarbons (alkenes) were observed in the winter, whereas the long-lived alkanes dominated the oceanic air masses in the summer.

The alkyne percentage contribution also increased from below 10% in the summer to about 23% in the winter. The percentage of alkyne (acetylene) increases indicated that contributions due to anthropogenic sources, namely vehicle emissions and biomass burning became more dominant in the winter months.

8.2. Seasonal Variation of NMHC

The climate of Hong Kong is influenced by the Asian monsoon system[63]. It has a marked seasonal change with prevailing winds blowing from southeast during the summer, and blowing from northeast during the winter. Hence, the

seasonal variations of NMHCs were correlated with surface wind directions and speed.

8.2.1. Influences of Local Meteorology - Surface Wind Directions and Speed

Influences of surface wind direction on NMHC concentrations are best illustrated by the wind rose of total NMHC shown in Figure 8.11. Total NMHC concentrations were elevated in the 0^{o} to 100^{o} surface wind direction, whereas relatively lower concentrations were found in the 120^{o} to 260^{o} wind direction.

This was in agreement with the observation that typical surface wind directions during the winter months were northerly to northeasterly winds. The range of wind angles indicated that the measured NMHCs originated mostly from regions north of Hong Kong, from the mainland of the Asian continent.

In contrast, summer NMHC concentrations were much lower than that in the winter. In the summer months, surface winds were mainly southerly and southwesterly, which were in the opposite direction to the winter surface winds. Thus, the origin of the air masses reaching Hong Kong in the summer months were coming from the South China sea and the South Pacific.

Table 8.13 : Monthly Average Percentage Contributions in Alkanes, Alkenes, & Alkynes

Month	Percentage of Alkane	Percentage of Alkene	Percentage of Alkyne
Oct'95	66%	14%	21%
Nov'95	64%	14%	22%
Dec'95	65%	12%	23%
Jan'96	65%	12%	23%
Feb'96	65%	13%	22%
Mar'96	73%	11%	16%
Apr'96	73%	10%	17%
May'96	77%	12%	11%
Jun'96	81%	15%	4%
Jul'96	79%	12%	9%
Aug'96	86%	8%	6%
Sep'96	83%	7%	11%
Oct'96	69%	10%	21%
Nov'96	69%	11%	21%
Jan'97	69%	12%	19%
Mar'97	72%	12%	16%

* percentages on a per-carbon (ppbC) basis

Figure 8.11 : Variation of Total NMHC Concentrations in Relation to Surface Wind Directions

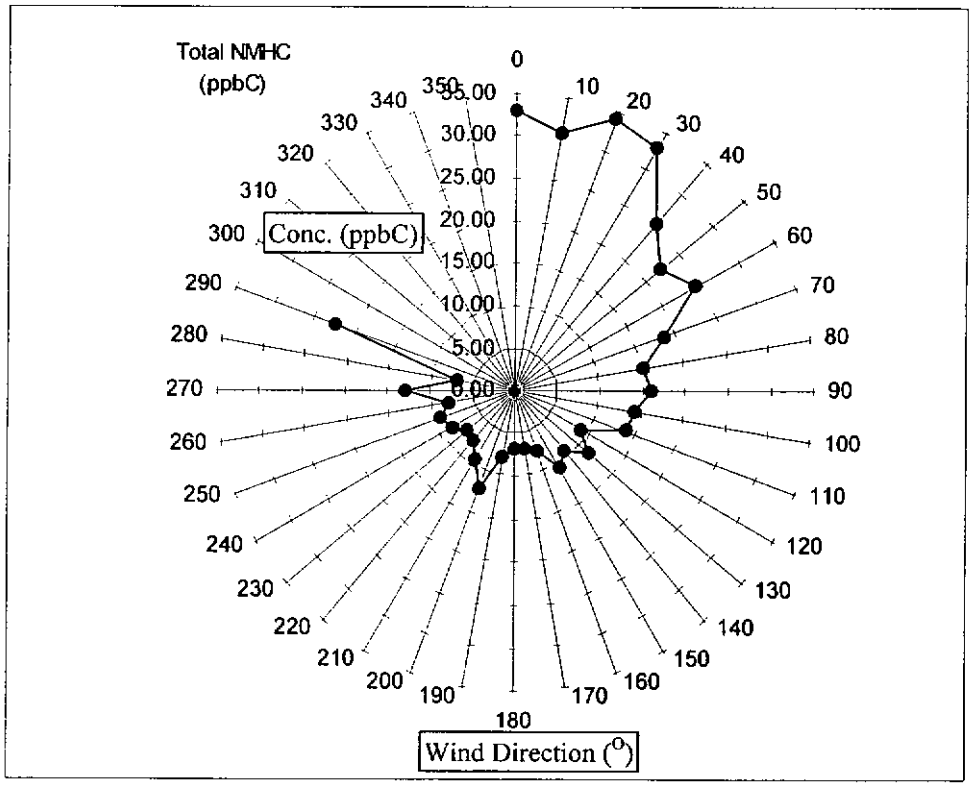

The dependence of total NMHC concentrations on surface wind speed in the winter and summer is shown in Figure 8.12. No clear trend of correlation between total NMHC concentrations and wind speed was observed in the winter (Figure 8.12(a)). The same could be said for the data set in the summer (Figure 8.12(b)), although scattered data points associated with high NMHC concentrations were found at low wind speeds (<2 m/s). Thus surface wind directions have a greater effect on the measured NMHC concentrations than wind speeds. This is expected because wind direction is related to the different origins and emission sources of air masses reaching Hong Kong.

8.2.2. Classification of Air Masses by Back Trajectories

NMHCs are trans-boundary pollutants and the concentrations of the NMHCs observed are related to the origins of different air masses reaching Hong Kong. To help estimate the possible origin of the observed NMHCs and to study the chemical and physical processes affecting NMHCs during the transport to the measurement site, backward air trajectories are used to classify the observed air masses into several categories.

Figure 8.12 : Variation of Total NMHC concentrations in relation to Surface Wind Speed during (a) Winter (Dec'95 to Feb'96), and (b) Summer (Jun'96 to Aug'96)

(a) Winter

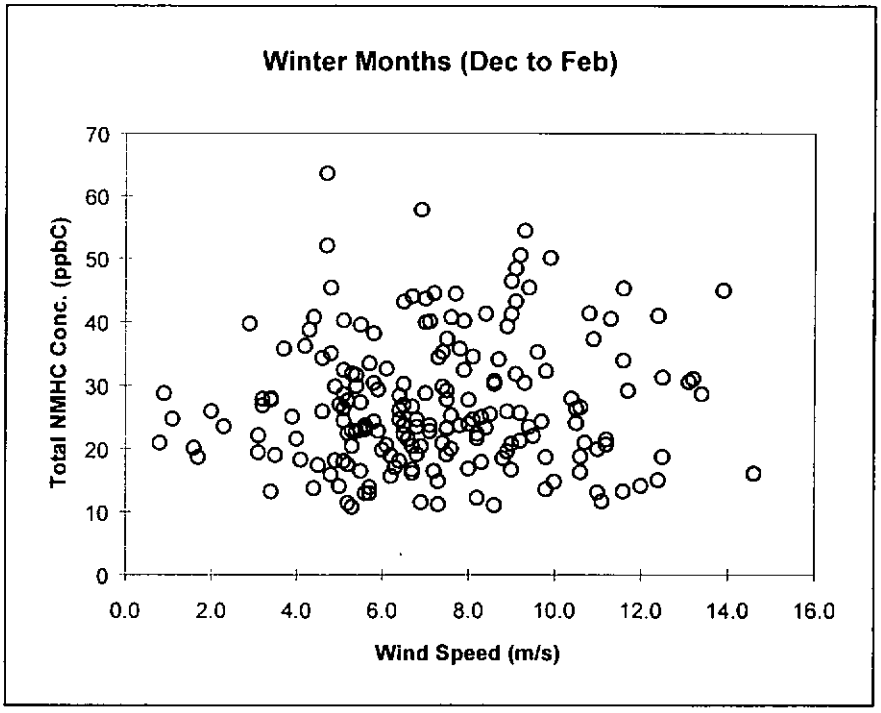

(b) Summer

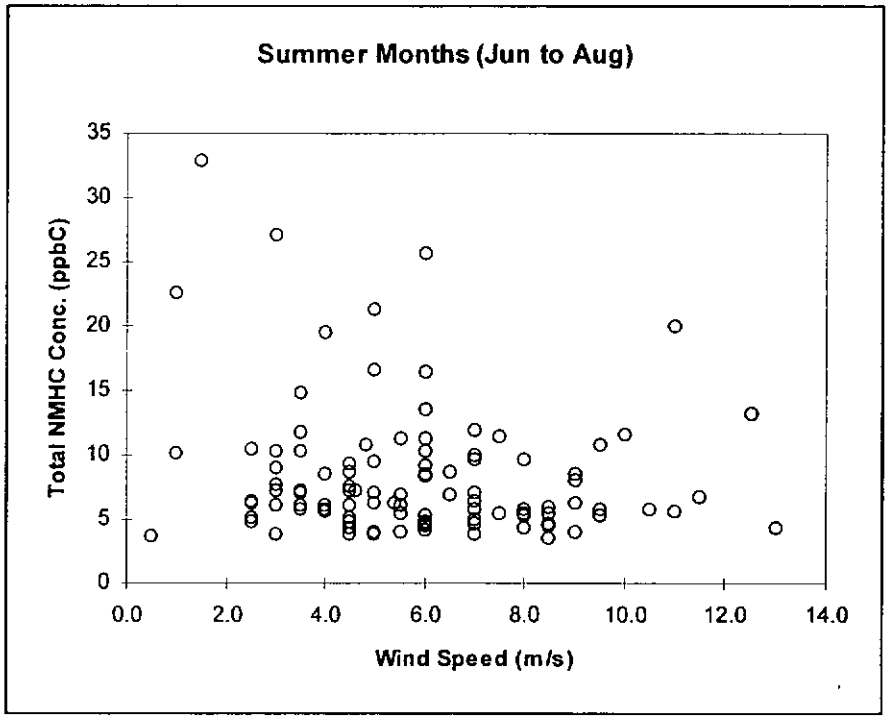

Based on back trajectory analysis, the air masses arriving at the Hong Kong Air Monitoring Station could be broadly classified into the following three types:

1. Asian continental outflow air masses (Figure 8.13(a) to (c))
2. South Pacific oceanic inflow air masses (Figure 8.14(a) to (d))
3. Local circulation air masses (Figure 8.15)

The back trajectory for each day was designated as either continental, marine, or local circulation if more than 80% of the trajectory path followed one of these major types along the geographical locations and the trajectories at 00:00 and 12:00 UTC followed the same paths. Otherwise, the trajectory of the day was regarded as unclassified.

The frequency of occurrence of different trajectory types over the period of study is shown in Table 8.14. Air masses of continental origin predominate in the autumn and winter, while air masses of marine origin became more frequent in the summer months, arriving at Hong Kong more than 80% of the time in June, July, and August'96.

The local circulation type air masses were mostly found in the winter months. This group of trajectories had no defined path and meandered close to Hong Kong.

Figure 8.13 : Typical Back Trajectory of Continental Type Air Masses

(a) "Purely Continental" Sub-type air masses (coded as PC)

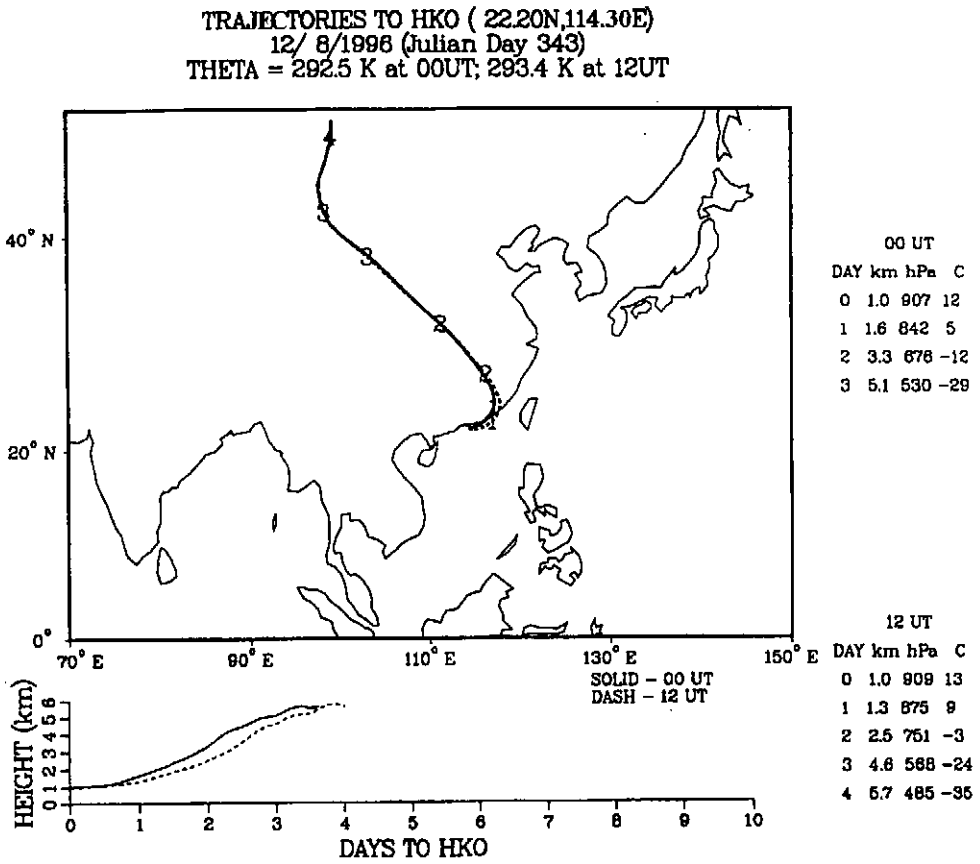

(b) "Continental plus marine" Sub-type air masses (coded as C+M)

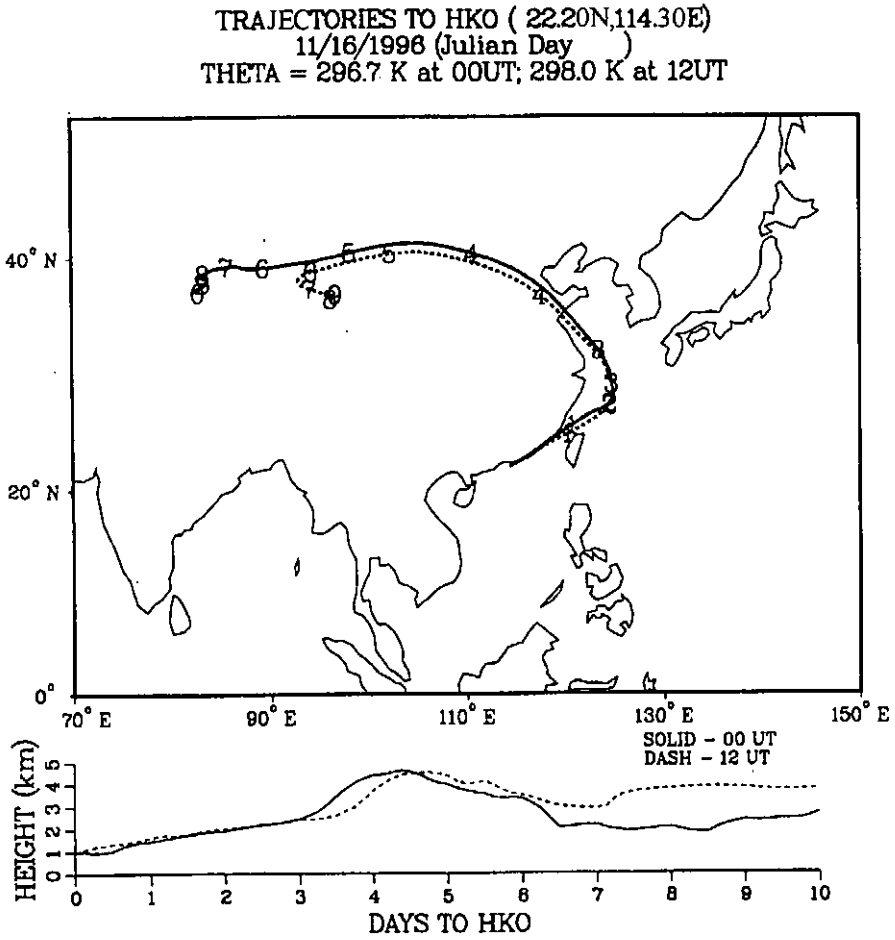

00 UT

DAY	km	hPa	C
0	1.0	907	16
1	1.5	863	11
2	1.9	813	6
3	2.4	757	1
4	4.4	590	-18
5	4.0	624	-14
6	3.3	676	-7
7	2.2	783	1
8	2.1	795	3
9	2.4	768	2
10	2.7	739	-2

12 UT

DAY	km	hPa	C
0	1.0	909	17
1	1.6	845	11
2	2.0	804	7
3	2.4	763	3
4	3.7	644	-10
5	4.4	594	-16
6	3.5	664	-7
7	2.9	715	-1
8	3.8	647	-7
9	3.8	644	-8
10	3.8	644	-4

(c) "Coastal China" Sub-type air masses (coded as CC)

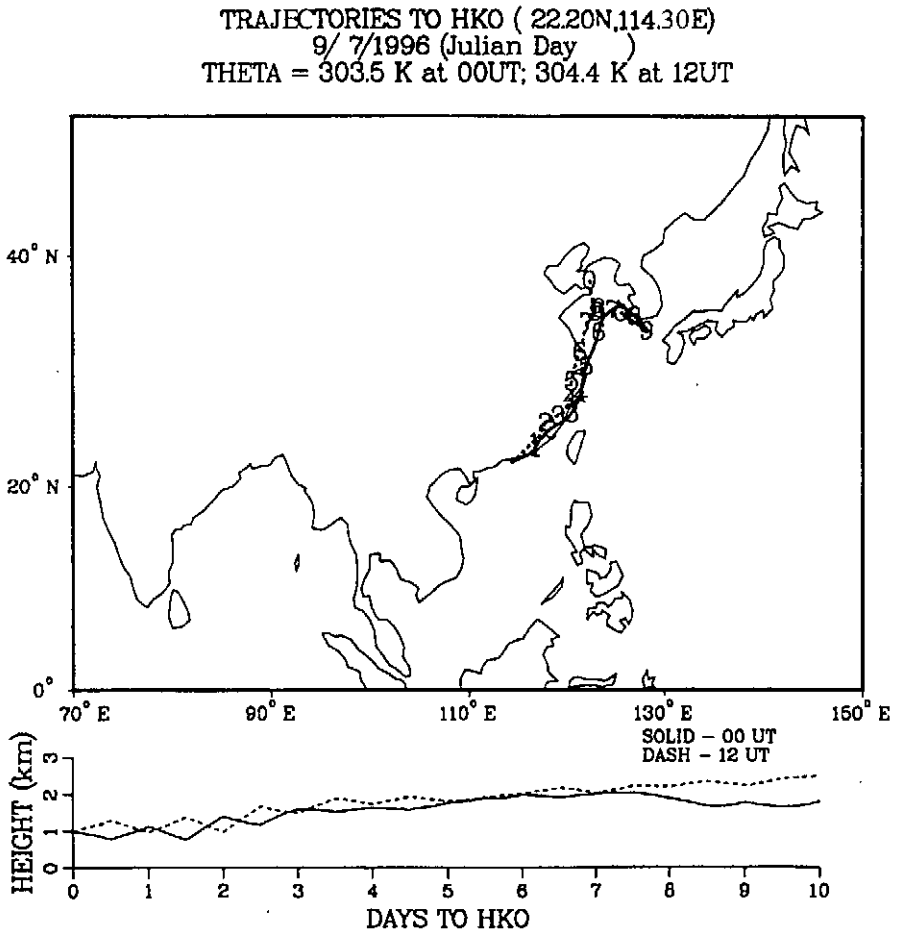

00 UT

DAY	km	hPa	C
0	1.0	899	21
1	1.1	887	20
2	1.4	860	18
3	1.6	841	16
4	1.7	836	15
5	1.8	824	14
6	2.0	803	12
7	2.0	800	12
8	1.9	811	13
9	1.8	818	13
10	1.8	814	13

12 UT

DAY	km	hPa	C
0	1.0	898	22
1	1.0	904	23
2	1.0	902	22
3	1.5	852	18
4	1.8	826	15
5	1.8	819	14
6	2.0	800	12
7	2.0	799	12
8	2.2	781	10
9	2.2	776	10
10	2.5	751	7

Figure 8.14 : Typical Back Trajectory of Marine Type Air Masses

(a) "Marine-Eastern" Sub-type air masses (coded as ME)

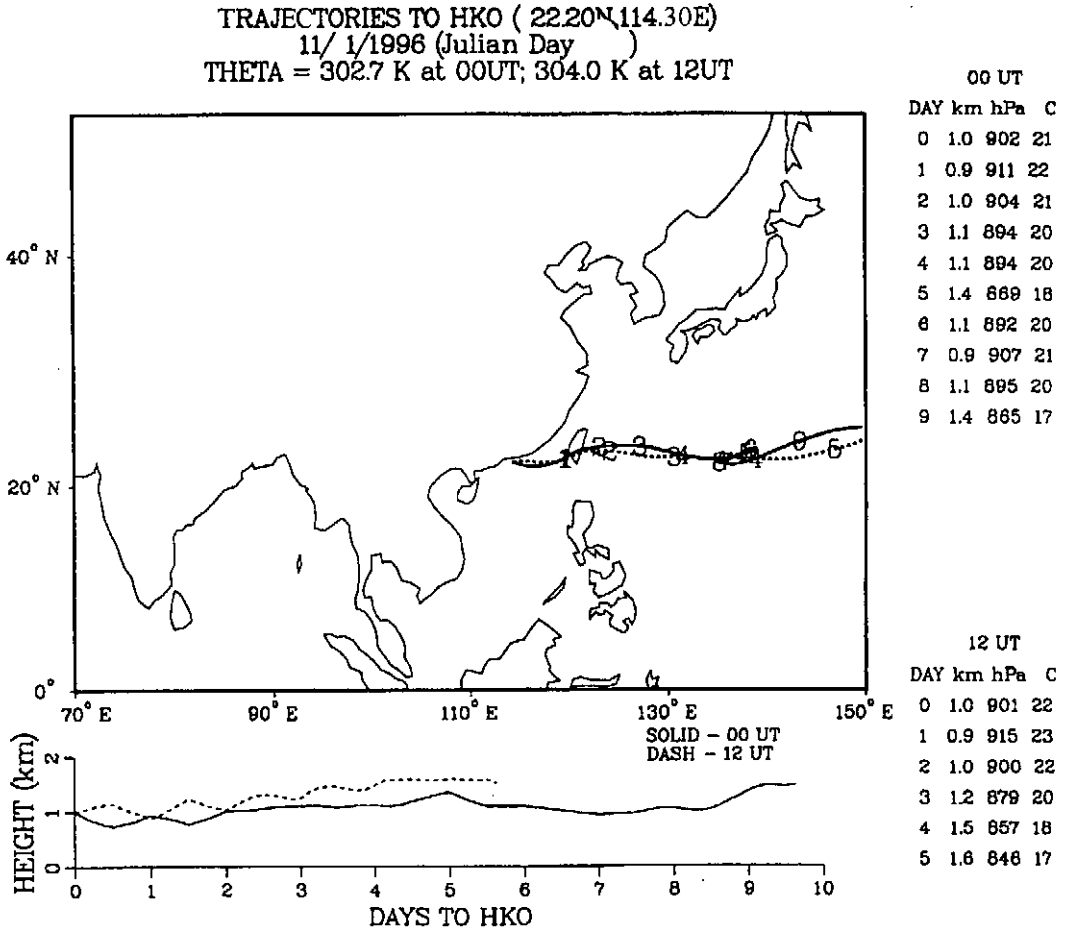

(b) "Marine-Southeast" Sub-type air masses (coded as MSE)

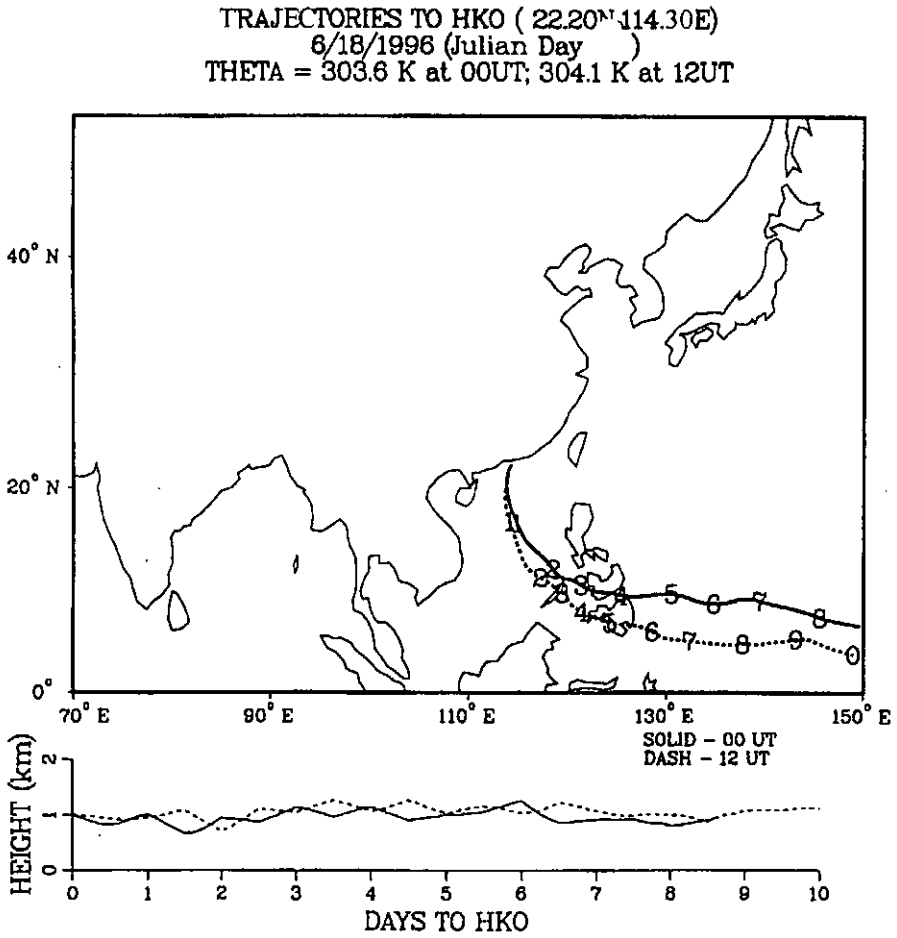

00 UT

DAY	km	hPa	C
0	1.0	900	21
1	1.0	899	21
2	0.9	905	22
3	1.1	884	20
4	1.1	883	20
5	1.0	898	21
6	1.3	872	19
7	0.9	908	22
8	0.8	919	23

12 UT

DAY	km	hPa	C
0	1.0	899	22
1	0.9	906	22
2	0.7	930	25
3	1.0	895	21
4	1.1	892	21
5	1.0	897	22
6	1.0	895	21
7	1.1	892	21
8	1.0	899	22
9	1.1	891	21
10	1.1	887	21

(c) "Marine-Circulation" Sub-type air masses (coded as Mcir)

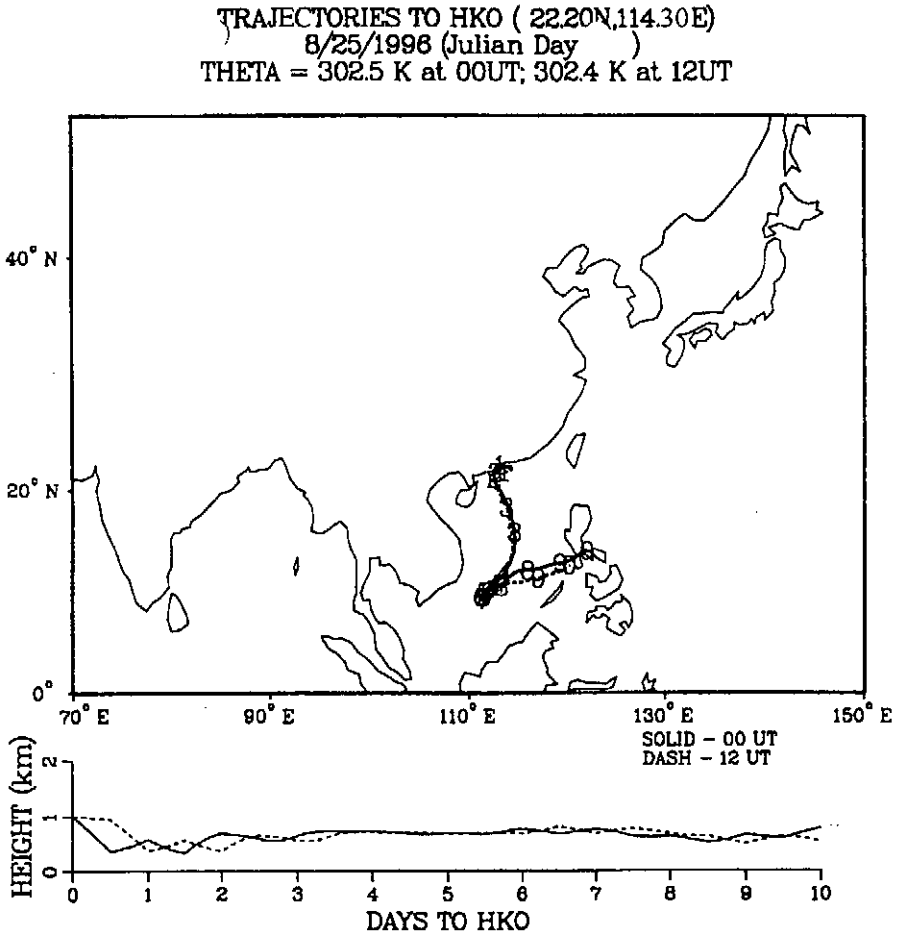

00 UT

DAY	km	hPa	C
0	1.0	900	20
1	0.6	946	25
2	0.7	934	23
3	0.6	938	24
4	0.7	927	23
5	0.7	932	23
6	0.8	923	22
7	0.8	923	23
8	0.6	939	24
9	0.7	937	24
10	0.8	924	23

12 UT

DAY	km	hPa	C
0	1.0	900	20
1	0.4	967	25
2	0.4	968	26
3	0.6	948	25
4	0.7	931	23
5	0.7	933	23
6	0.7	933	23
7	0.7	932	23
8	0.7	933	23
9	0.5	954	25
10	0.5	951	25

(d) "Marine-Southwest" Sub-type air masses (coded as MSW)

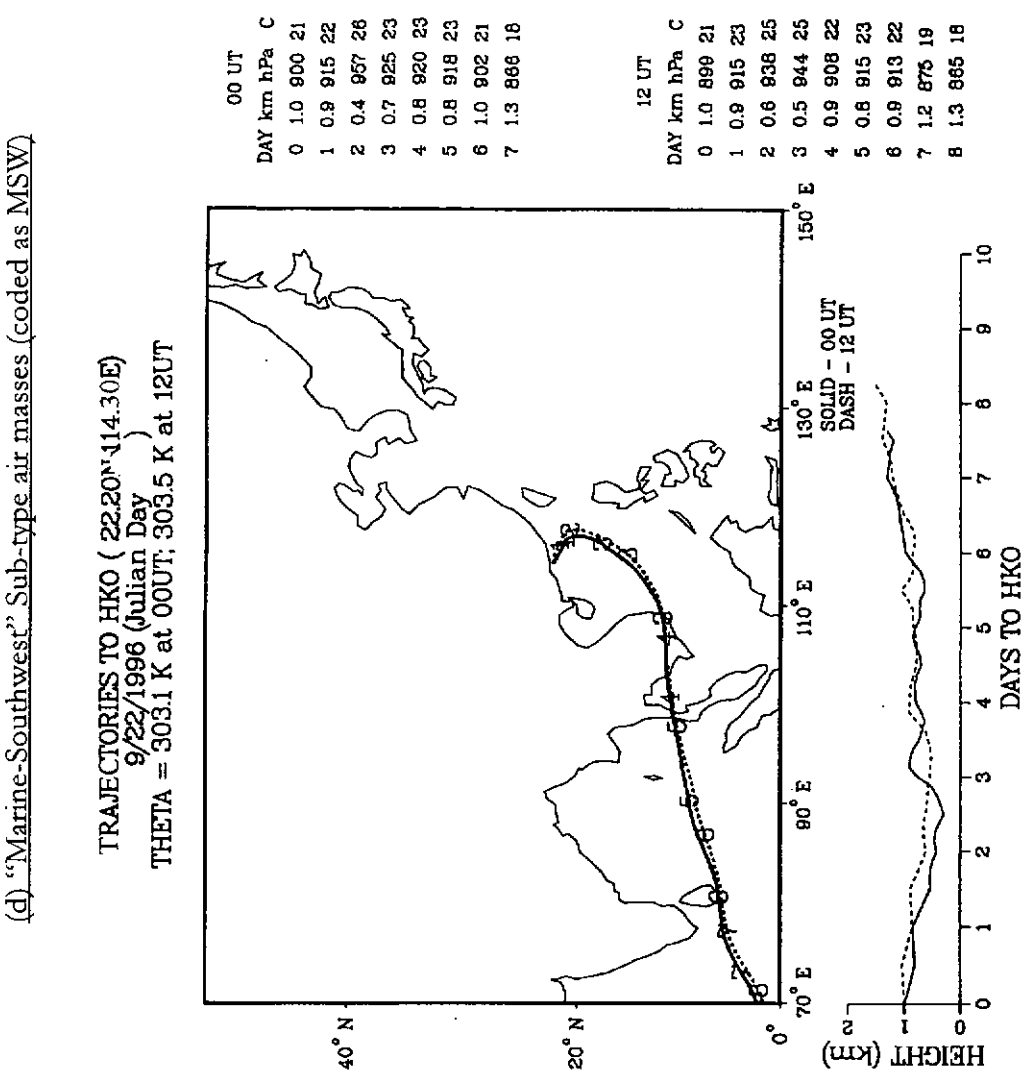

Figure 8.15 : Typical Back Trajectory of Local Circulation Type Air Masses

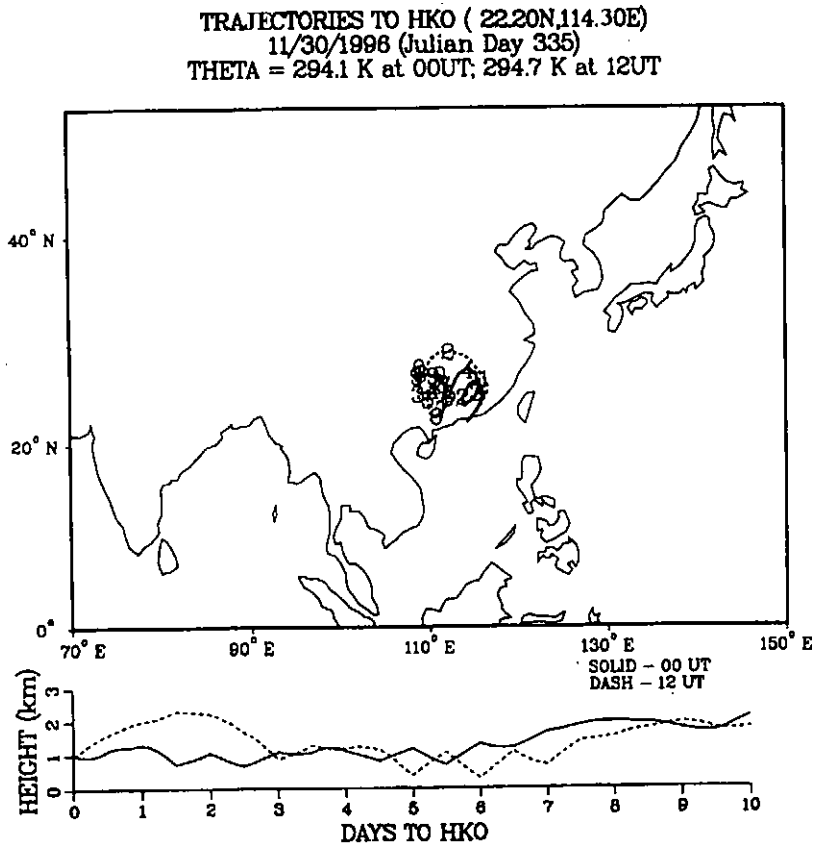

00 UT

DAY	km	hPa	C
0	1.0	906	13
1	1.3	878	10
2	1.0	900	12
3	1.1	900	12
4	1.1	896	12
5	1.2	888	11
6	1.3	875	10
7	1.7	838	6
8	2.0	808	3
9	1.8	829	6
10	2.1	797	2

12 UT

DAY	km	hPa	C
0	1.0	912	14
1	2.0	803	4
2	2.2	779	1
3	0.9	919	15
4	1.2	890	12
5	0.4	972	16
6	0.3	983	16
7	0.7	943	14
8	1.5	853	8
9	1.9	811	4
10	1.8	830	6

Table 8.14 : Frequency of Each Major Types of Air Masses reaching Hong Kong

Month	Continental	Marine	Local Circulation	Unclassified
Jan-96	16%	0%	71%	13%
Feb-96	24%	0%	52%	24%
Mar-96	29%	32%	13%	26%
Apr-96	-	-	-	-
May-96	19%	32%	26%	23%
Jun-96	0%	87%	0%	13%
Jul-96	0%	87%	0%	13%
Aug-96	0%	81%	0%	19%
Sep-96	40%	43%	3%	13%
Oct-96	71%	10%	6%	13%
Nov-96	23%	17%	33%	27%
Dec-96	65%	0%	26%	10%

* frequency expressed as % of days in the month

8.2.2.1. Asian Continental Air Masses

Based on the trajectory analysis, the Asian continental air masses which affected the NMHC levels measured at Hong Kong could be further divided into three back trajectory sub-types:

(a) Purely Continental air masses (coded as PC): the air masses originated from the Asian continent, and moved southward to Hong Kong without reaching out to the ocean (Figure 8.13a);

(b) Continental plus marine air masses (coded as C+M): the air masses flowed out of northern China, drifted over Taiwan and/or the East China sea before turning southwest to reach Hong Kong (Figure 8.13b); and

(c) Coastal China air masses (coded as CC): the air masses originated from and moved along the East China coastal regions to Hong Kong (Figure 8.13c).

The average concentrations of total NMHC and individual NMHCs associated with these three sub-types of continental air masses are shown in Table 8.15, while the percentage distributions of alkanes, alkenes and alkynes in these sub-type air masses are shown in Table 8.16.

The "Purely Continental" sub-type air masses were the most frequently occurring ones in the winter months. The average concentrations of the total

NMHC and individual NMHCs associated with this type of air masses were highest among the continental sub-types (Table 8.15); 24% of measured NMHCs were acetylene (Table 8.16), which is also the highest alkyne content among the continental sub-type air masses.

Hydrocarbon emission sources were mostly located on the continental mainland. Under continental outflow conditions, large quantities of NMHCs were transported from the source regions to our measurement site. Since acetylene was the only alkyne measured, and vehicle emission and biomass burning were the major anthropogenic contributing sources, the high percentage of acetylene observed suggested that the "Purely Continental (PC)" air masses are possibly loaded with more vehicle emissions and biomass burning than the other sub-types of continental air masses.

Similar observations of these enhanced acetylene concentrations in continental China were also reported[64]. Aside from contribution due to automobile emissions, the elevated acetylene levels were attributed to emissions from biomass burning.

Table 8.15 : Average NMHC Concentrations associated with Different Continental Air Masses

Trajectory Types	Total NMHC	Ethane	Ethylene	Propane	Propylene	iso-Butane	n-Butane	Acetylene	1-Butene	2-methylbutane	n-Pentane	2,2-dimethylbutane	3-methylpentane	2-methylpentane	n-Hexane
PC (n=11)	22.37	2881	995	1113	98	245	443	2656	30	200	147	34	55	30	59
C+M (n=36)	14.50	1852	568	738	95	199	348	1238	31	166	135	28	41	25	51
CC (n=14)	7.72	841	238	350	56	142	245	484	19	145	117	27	26	17	21

Note: *1. n = number of data points*

2. Total NMHC concentrations are in units of ppbC; individual NMHC concentrations are in units of pptV

3. PC: Purely continental; C+M: Continental plus marine; CC: Coastal China

Table 8.16 : Percentage Distribution of Alkanes, Alkenes and Alkynes associated with Different Continental Air Masses

Trajectory Types	Alkane	Alkene	Alkyne
PC	66%	11%	24%
C+M	72%	11%	17%
CC	80%	9%	13%

Note: *1. percentages on a per-carbon (ppbC) basis*

2. PC: Purely continental; C+M: Continental plus marine; CC: Coastal China

The second sub-type of continental air masses, "Continental plus marine (C+M)", originated from continental Asia, out-flowing in the direction from northwest to southeast and travelling over the South China sea, travelling over the ocean and returning to the continent from east to west (Figure 8.13b). The average total NMHC concentration associated with this sub-type of air masses was found to be significantly reduced (about 35% in a relative sense as compared to "PC" type air masses, Table 8.15). This was in agreement with the trajectory estimation. The decrease in observed total NMHC levels might suggest that during the air mass movement over the East/South China Sea, continental air masses may be diluted by oceanic air which has a relativley lower concentrations of NMHCs. Ethane is the longest-lived species (τ = 78 days) among the C_2-C_6 NMHCs, and its concentration would be least affected by long range transport processes. Hence ethane shows lower percentage of reduction when compared with shorter lifetime species like ethylene (τ = 2 days) and acetylene (τ = 23 days). Ethylene and acetylene are derived mainly from vehicle emissions in urban areas (relative abundances at 98.9 and 100% respectively, as shown in Table 1.2, Section 1.2.2). Other land-based hydrocarbon emission sources yield very little ethylene and acetylene. The lifetime of ethylene is about 1/10 that of acetylene. If the measured ethylene and acetylene are derived from mainly from anthropogenic, land-based emission sources (i.e. vehicle emissions and biomass burning), then the observed percentage reduction for ethylene should be greater than the longer lived acetylene. However, our data showed that using the "Purely Continental (PC)" air masses as the reference, the percentage reduction

for ethylene (about 43%) is actually less than that of acetylene (about 53%) for the "Continental plus marine (C+M)" air masses. Acetylene was found in extremely low levels (~ pptV) in oceanic air, and no oceanic sources of acetylene has been reported or found[65]. On the contrary, marine sources of ethylene and propylene were recorded[1]. Thus, for this "Continental plus marine (C+M)" sub-type of air masses, photo-degradation of ethylene may be compensated by oceanic contributions, which might explain the relatively less percentage decrease for ethylene than that of acetylene.

Another interesting case is that of n-butane and isobutane, which have intermediate lifetimes of 8 and 9 days, respectively. Yet their percentage decreases (21% for n-butane and 19% for i-butane with reference to the "PC" sub-type air masses) were much less than that of acetylene and ethylene. This may suggest that besides continental land-based emissions, there are additional emission sources for n-butane/isobutane along the trajectory pathways of the "Continental plus marine (C+M)" sub-type air masses. N-butane and isobutane are major components of liquefied petroleum gases (LPG), and their leakage from offshore or coastal oilfields along the East/South China Sea is a possible source. Anther possible source is LPG leakage contributions from Taiwan, which are gathered by the "Continental plus marine (C+M)" air masses before they reached Hong Kong.

The third sub-type of continental air masses, "Coastal China (CC)", originated and traveled along the East China coast before they reached Hong Kong (Figure 8.13c). The measured NMHC levels associated with this sub-type of air masses were the lowest of the classified continental air masses: the average total NMHC level was only 35% (i.e. a 65% decrease) that of the "Purely Continental (PC)" sub-type air masses. The much reduced NMHC levels suggest that land-based anthropogenic emissions from the Asian continent were less sampled by these air masses. The anthropogenic emissions from offshore Taiwan were only marginally included or not included at all. Compared to the "Pure Continental (PC)" sub-type air masses, the percentage decrease in the average values of the major components NMHCs are: ethane (70%), ethylene (76%), acetylene (82%), n-butane (45%) and isobutane (43%). The pattern of percentage decrease is the same as that found for the "Continental plus marine (C+M)" sub-type air masses, so the effect of dilution by oceanic air, input from marine sources of ethylene, and offshore LPG leakage contribution to n-butane/isobutane are also applicable to this sub-type of air masses.

8.2.2.2. Maritime Air Masses

Back trajectory analysis showed that during the summer months, oceanic air masses frequently moved across the South or East Pacific Ocean before they reached Hong Kong. These oceanic air masses could be classified into four sub-types according to their direction of approach to Hong Kong., i.e. (a) Marine East (coded as ME), (b) Marine Circulation (coded as Mcir), (c) Marine Southeast

(coded as MSE), and (d) Marine Southwest (coded as MSW) (Figure 8.14(a) to (d)). The average total NMHC and individual NMHC levels of these four sub-types of maritime air masses were found to be very similar, and are summarized in Table 8.17. Since the marine sub-type air masses showed no significant difference in their NMHC compositions, they were regrouped into one single "Marine" air mass, and their NMHC characteristics were compared to that of the continental air masses.

There are few reports on the chemical characteristics of air masses derived from the South/East Pacific Ocean. Our results showed that the measured NMHC concentrations associated with the "Marine" air masses were comparable to that of "Coastal China" sub-type continental air masses, but with a much reduced acetylene content (Table 8.18). As shown in Table 8.19, the percentages of alkanes associated with "Marine" air masses and "Coastal China (CC)" air masses were similar at 80% and 81%, respectively. However, the percentage of alkyne or acetylene associated with "Marine" air masses was only 5% as compared to 13% for "Coastal China" sub-type air masses. The low acetylene content associated with "Marine" air masses is expected because there is no oceanic source of acetylene.

8.2.2.3. Local Circulation Air Masses

These air masses circulated over a relatively small area around Hong Kong before dispersion. A large amount of local and regional emissions were

gathered during the circulation period. The total NMHC level and relative percentage distribution of individual NMHCs were found to be highly variable, depending on the surface wind speed and directions. Because these air masses were not related to long-range transport of pollutants to Hong Kong, they were not analyzed in depth in the present work.

Table 8.17 : Average NMHC Concentrations associated with Different Marine Air Masses

Trajectory Types	Total NMHC	Ethane	Ethylene	Propane	Propylene	iso-Butane	n-Butane	Acetylene	1-Butene	2-methylbutane	n-Pentane	2,2-dimethylbutane	3-methylpentane	2-methylpentane	n-Hexane
ME (n=9)	7.89	392	269	512	99	194	213	272	39	207	144	38	22	14	35
Mcir (n=51)	7.17	329	266	309	89	186	316	128	31	219	134	24	31	19	32
MSE (n=18)	6.43	459	304	176	134	142	177	192	53	167	118	19	32	21	40
MSW (n=25)	6.90	504	247	321	95	155	193	219	32	212	136	15	19	13	27
Marine (n=103)	7.04	400	269	306	99	171	253	174	36	207	133	22	28	17	32

Note: *1. n = number of data points*

2. Total NMHC concentrations are in units of ppbC; individual NMHC concentrations are in units of pptV

3. ME: marine east; Mcir; marine circulation; MSE: marine southeast; MSW: marine southwest

Table 8.18 : Comparison of Marine air masses with Continental air masses

Trajectory Types	Total NMHC	Ethane	Ethylene	Propane	Propylene	iso-Butane	n-Butane	Acetylene	1-Butene	2-methylbutane	n-Pentane	2,2-dimethylbutane	3-methylpentane	2-methylpentane	n-Hexane
PC (n=11)	22.37	2881	995	1113	98	245	443	2656	30	200	147	34	55	30	59
C+M (n=36)	14.50	1852	568	738	95	199	348	1238	31	166	135	28	41	25	51
CC (n=14)	7.72	841	238	350	56	142	245	484	19	145	117	27	26	17	21
Marine (n=103)	7.04	400	269	306	99	171	253	174	36	207	133	22	28	17	32

Note: *1. n = number of data points*

2. Total NMHC concentrations are in units of pppbC; individual NMHC concentrations are in units of pptV

3. PC: Purely continental; C+M: Continental plus marine; CC: Coastal China

Table 8.19 : Percentage Distribution of Alkanes, Alkenes and Alkynes associated with Continental and Marine Air Masses

Trajectory Types	Alkane	Alkene	Alkyne
PC	66%	11%	24%
C+M	72%	11%	17%
CC	80%	9%	13%
Marine	81%	14%	5%

Note: *1. percentages on a per-carbon (ppbC) basis*

2. PC: Purely continental; C+M: Continental plus marine; CC: Coastal China

8.3. Correlation Analysis & Identification of Emission Sources

Since NMHCs are specific to sources of emission and have a wide range of lifetimes, regression analysis can be performed to estimate their possible contributors and range from the observatory site. Regression analysis on measured NMHCs was conducted independently for the winter and summer season since air masses of different geographical origins were measured.

8.3.1. Correlation Analysis & Sources of Emission in the Winter

Previous investigations of pollution impact on Asian Pacific Rim have characterized the release of hydrocarbons from natural gas and the incomplete combustion processes[66]. The well-known signature compounds from fossil fuel combustion, such as ethylene and acetylene[1], were the dominant NMHCs in our data set during the winter period. As shown in Figure 8.16, the correlation of acetylene with total NMHC was excellent for the winter data set (Dec'95 to Feb'96) with a correlation coefficient r^2 of 0.89. Very good correlations were also found between acetylene and ethane, and acetylene and ethylene having correlation coefficients (r^2) of 0.89 and 0.80, respectively (Figure 8.17). These correlations clearly indicate that during winter, air masses loaded with vehicle exhaust emission and biomass burning were sampled in the Hong Kong atmosphere.

Alkane hydrocarbons (propane, isobutane, and n-butane) from liquefied petroleum gas (LPG) might be another possible emission source because of its common use for domestic cooking and heating in many cities[25]. As discussed in section 7.2.2.1, butanes showed relatively less concentration changes as compared to other NMHCs associated with Asian continental air masses in the winter. The correlations of n-butane and isobutane with propane were excellent in our winter data set (Dec'95 to Feb'96), with slopes 0.466 (correlation coefficient r^2=0.84) and 0.255 (r^2=0.88), respectively (Figure 8.18(a) & (b)). Similar correlation values were reported for LPG leakage at Mexico City[25]. This suggested that these alkanes in the air masses sampled in the Hong Kong atmosphere during winter might be contributed from LPG source.

Propane (winter) also correlated well with acetylene and 2-methylbutane (isopentane), with r^2 =0.66 and r^2 =0.75, respectively (Figure 8.19 (a) & (b)). Acetylene is solely derived from auto exhaust[65,67] and isopentane is a well-known gasoline combustion and evaporation product. In contrast, propane is not expected from auto exhaust[1]. These good correlations suggest the co-existence of NMHC emissions from vehicle exhaust and LPG leakage in the air masses sampled in the Hong Kong atmosphere or from different geographical sources/regions along the path of movement of the continental air masses. These good correlations might also be associated with mixing of NMHCs from several emission sources in the air masses sampled in Hong Kong.

8.3.2. Correlation Analysis & Sources of Emission in the Summer

During the summer season, concentrations of NMHCs were found to be lower than that in the winter. The oceanic inflow during summer affected NMHC levels over the western Pacific. Relatively clean air, with ethane concentrations between 220 and 761 pptV, coincided with low ozone levels observed (5-23 ppbV).

The NMHCs associated with these clean air masses were analyzed by correlation analysis. The correlation of acetylene with total NMHC was poor ($r^2=0.10$) (Figure 8.20). Correlation of the LPG signature species, propane, with total NMHC resulted in a low r^2 value of 0.48 (Figure 8.21). The regression between isobutane and n-butane was poor ($r^2=0.32$), indicating that LPG emissions were not influencing the NMHC levels observed in summer. No correlation was found between other NMHC tracer species of anthropogenic origin. This might suggest that in the summer, relatively aged air masses or air masses of natural emissions were sampled in Hong Kong, resulting in the low level of NMHC pollution observed. This is in agreement with the conclusion drawn from the PEM-West experiments[68], which also showed that southern hemispheric air could be brought to Asian coastal regions in the summer.

Figure 8.16 : Correlation between Total NMHC and Acetylene in the Winter Season (Dec'95 to Feb'96)

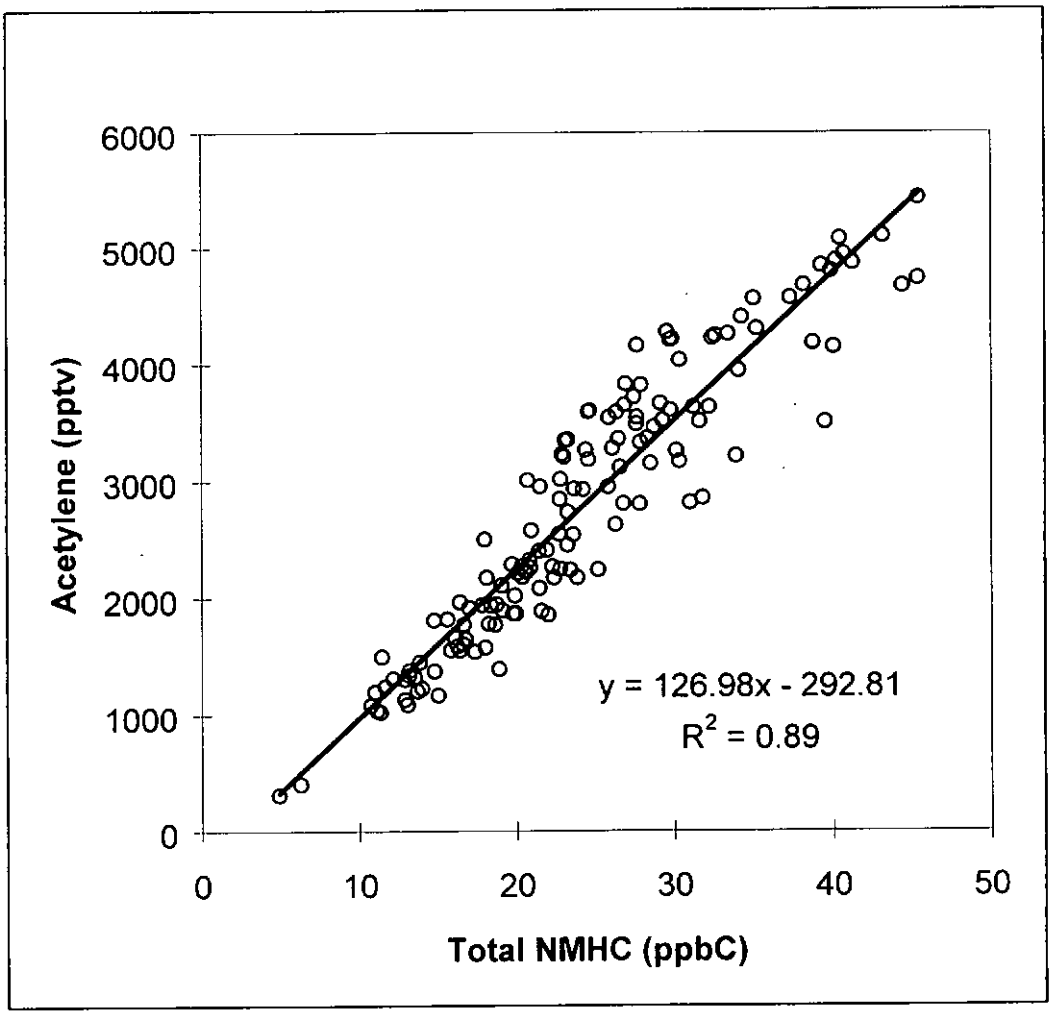

Figure 8.17 : Correlation between (a) Acetylene & Ethane, and (b) Acetylene & Ethylene in the Winter Season (Dec'95 to Feb'96)

(a)

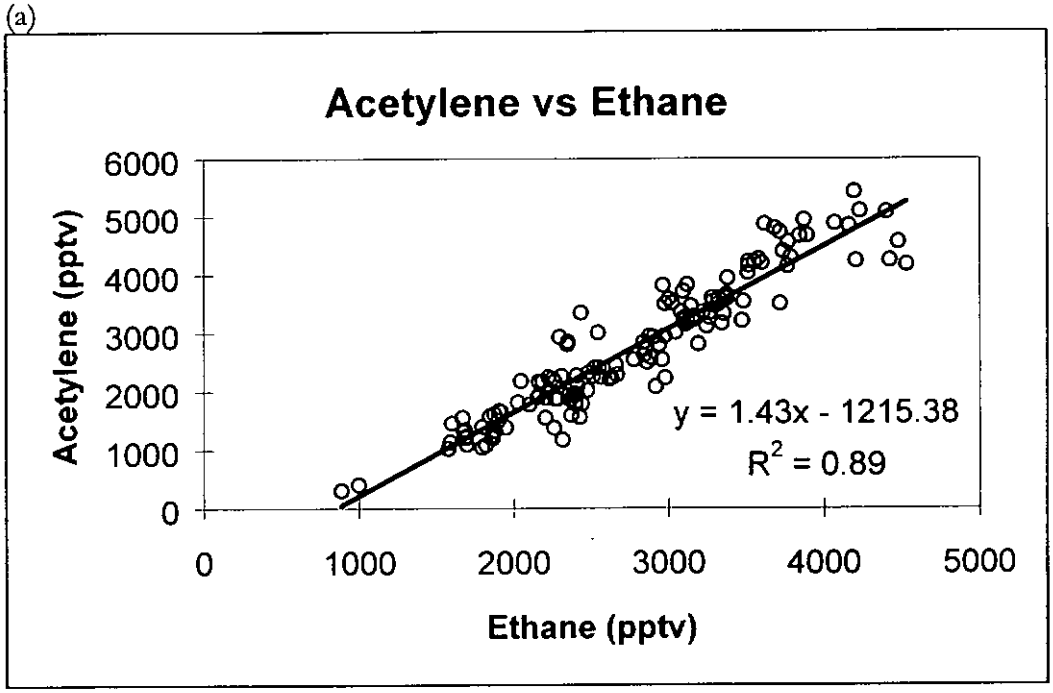

(b)

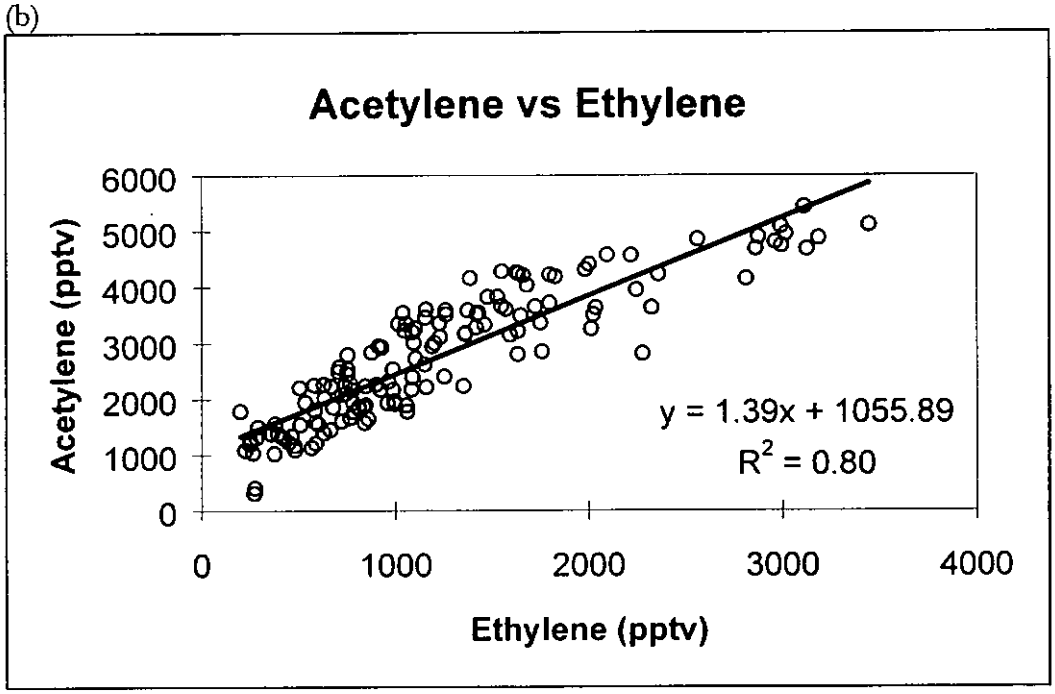

Figure 8.18 : Correlation of Propane with (a) n-Butane and (b) Isobutane in the Winter Season (Dec'95 to Feb'96)

(a)

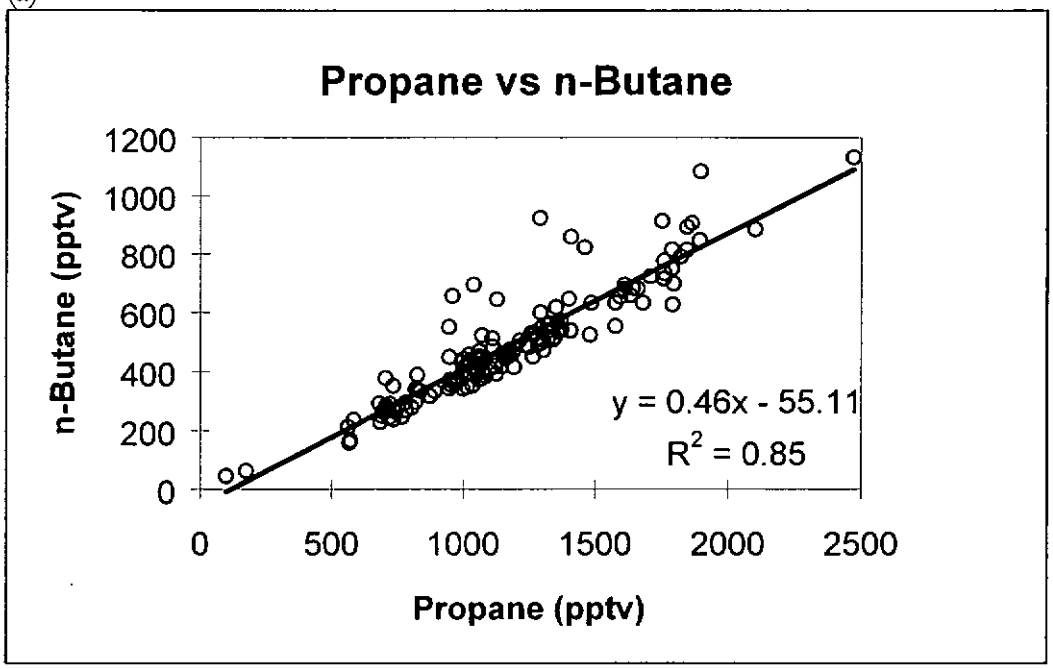

(b)

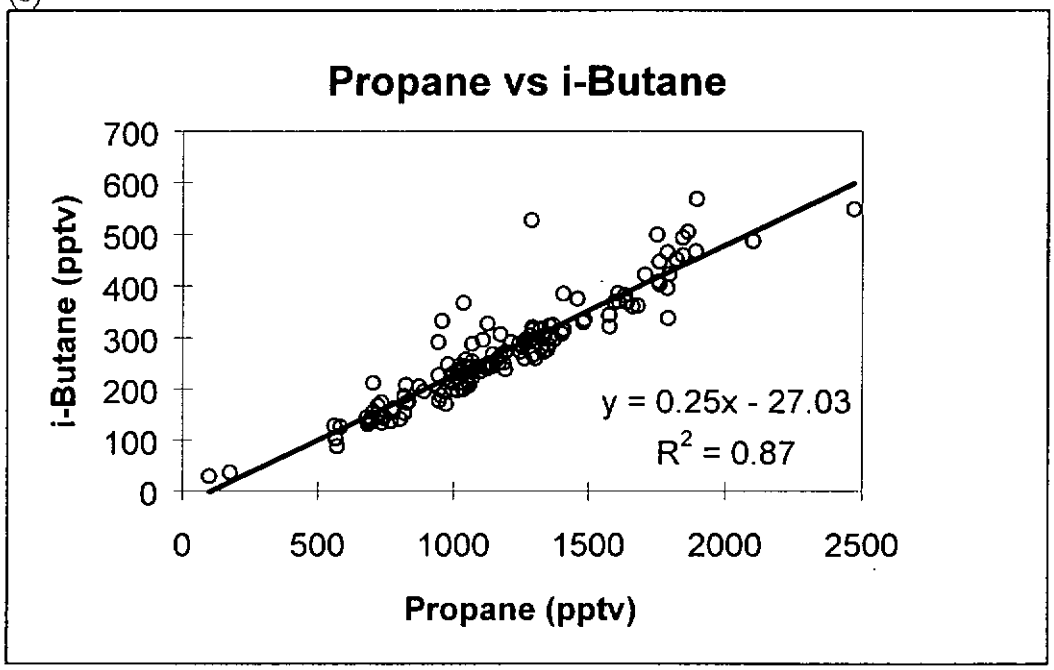

Figure 8.19 : Correlation of Propane with (a) Acetylene and (b) 2-Methylbutane (Isopentane) in the Winter Season (Dec'95 to Feb'96)

(a)

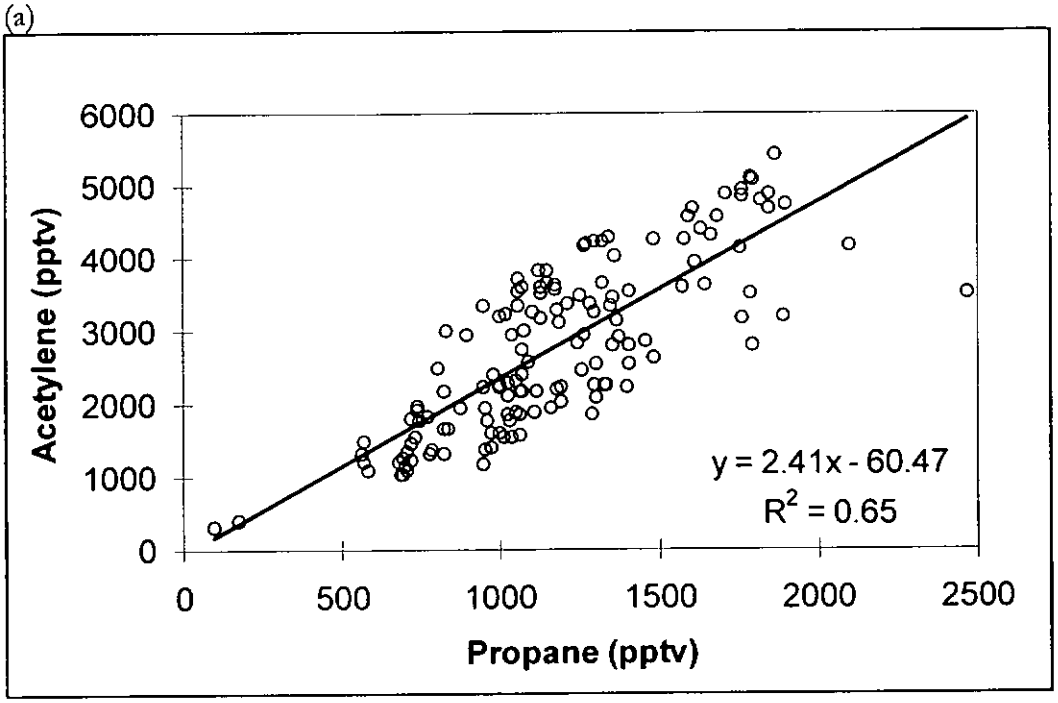

(b)

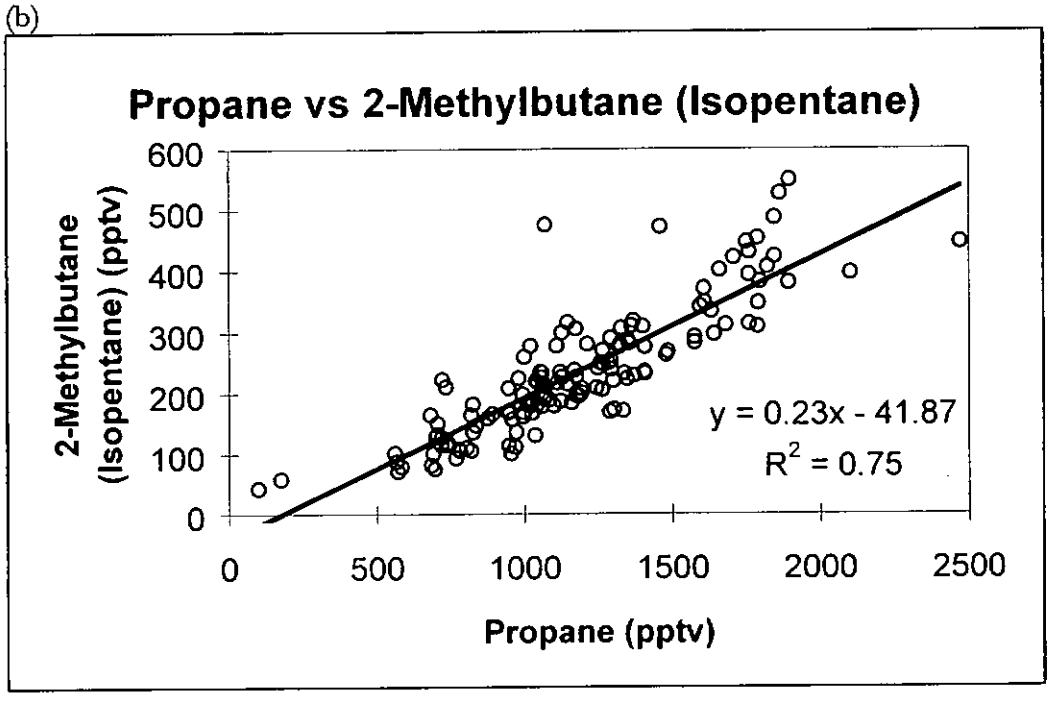

Figure 8.20 : Correlation Analysis (Summer) between Total NMHC and Acetylene

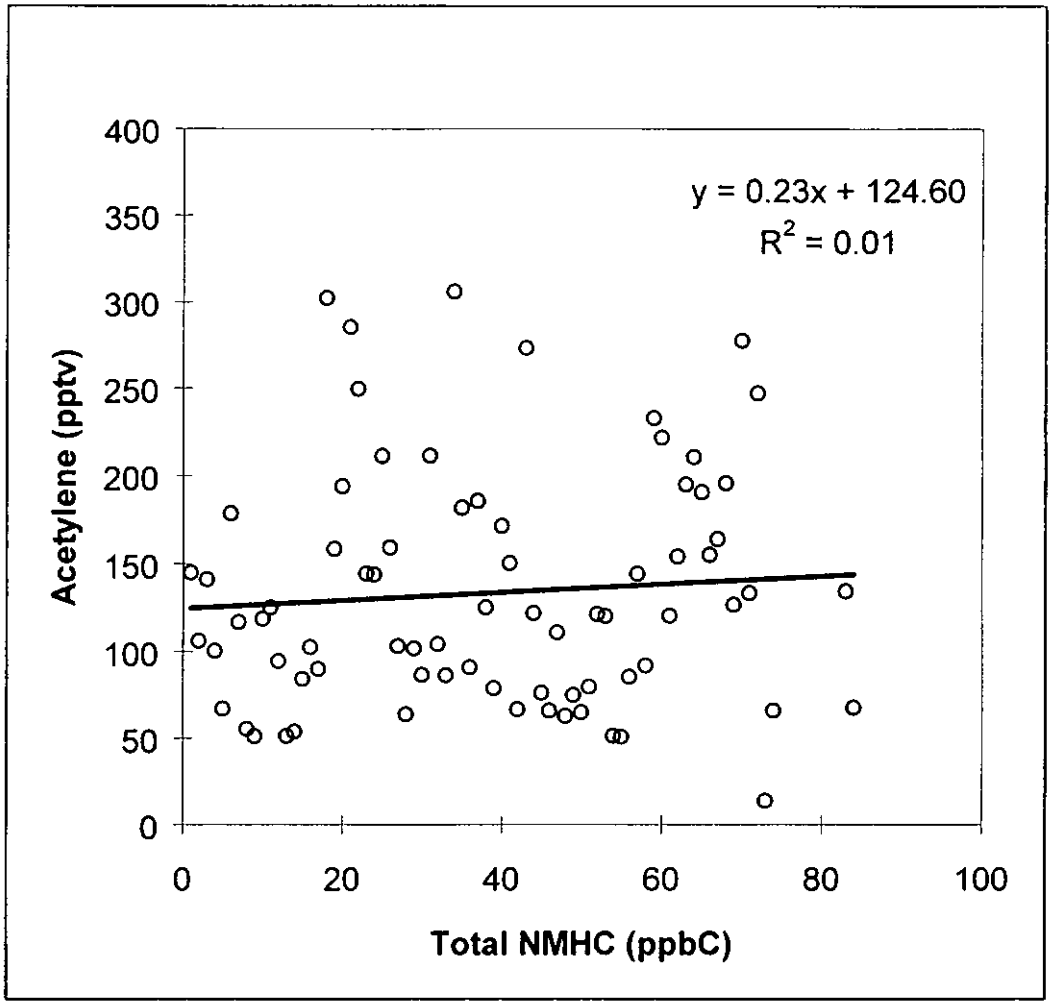

Figure 8.21 : Correlation Analysis (Summer) between Total NMHC and Propane

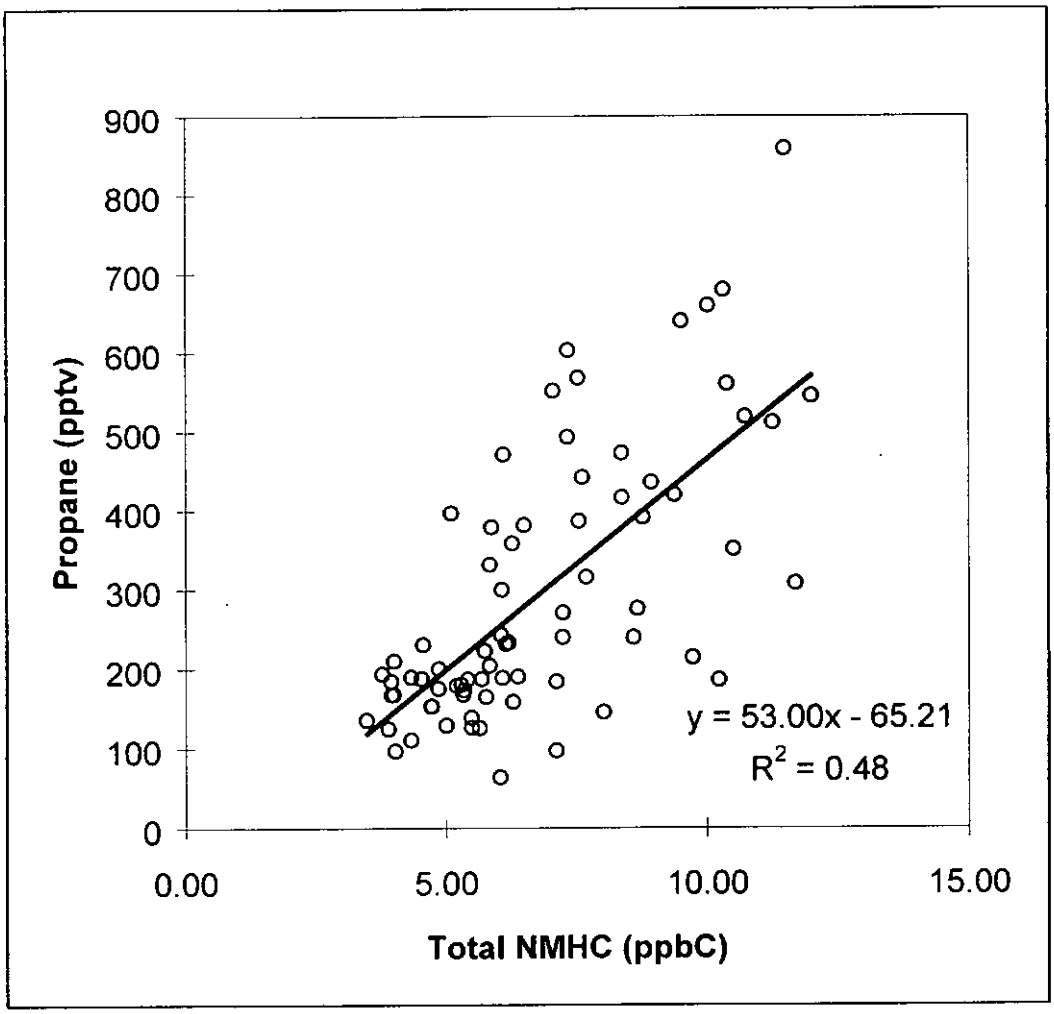

9. *Case Studies on Episode Days*

Influences on the variability of the NMHC concentrations and interrelationships between individual NMHCs were studied as a function of different origin, influences of local sources, and local meteorology. Two cases of episode days, one in the winter and one in the summer, were selected for more in depth analysis to demonstrate (i) the characteristic NMHCs of localized stagnant meteorological conditions and (ii) the cold front days when strong continental outflow conditions were experienced in Hong Kong.

9.1. Local Episode Days

An episode was observed on 25-26 July 1996, during which drastically elevated NMHC concentrations were monitored. The variations of the NMHC levels would be compared with the surface meteorological parameters and the CO and O_3 concentrations with reference to the typical values observed during the episodic event, in an aim to study the possible impact of urban emissions due to the local transport pattern of air pollutants and the relationships among the pollutants during the episode.

Total NMHC levels changed from an average of below 10 ppbC 10 days before the episode to above 90 ppbC on July 25. CO observations showed a similar trend of increase in concentrations, from an average of about 100 ppbV to

about 600 ppbV during the episode (Figure 9.22). Individual NMHCs showed a significant enhancement in concentrations (range from 2 to 60 folds as shown in Figure 9.23). The enhancement was particularly pronounced for the C_6 hydrocarbons (Figure 9.23b). This might be due to the contribution of solvents, gasoline evaporation, and car exhaust from the urban center of Hong Kong, which are the mostly likely contributing source of these C_6 hydrocarbons in urban emissions (Table 1.2). The level of n-hexane was first observed in the afternoon of July 24 before the arrival of the episode day. This could be due to transitional changes in surface air circulation which brought C_6 hydrocarbons from local Hong Kong urban sources to the monitoring station.

Lack of emission profiles for different sources in Hong Kong and from China is a main difficulty which limits a more comprehensive explanation of the data set. In addition to the C_6 hydrocarbons, acetylene and ethylene showed the greatest increase in concentrations at 13.4 and 8.1 folds. As these two NMHCs were derived almost solely from vehicle exhaust, their predominance was a definitive evidence that pollutants, mostly vehicle exhaust emitted in nearby urban centers such as Hong Kong or cities/towns around the Pearl Estuary, were brought to the monitoring station during the episode. This was supported by the meteorological observations that easterly winds (wind angle : 60-80^{o}) were prevailing on 20 July and 24 July, but the winds turned northwesterly (wind angle : 290^{o}) on the episodic period (25 & 26 July) as shown in Figure 9.24. This change in wind directions was one of the typical conditions observed in the

episodic situations in Hong Kong[69], with the possibility to swap the pollutants emitted over the urban regions during easterly wind to the west and transport of these pollutants to the monitoring site due to the reversal of wind direction to northwesterly.

Ethylene showed less enhancement than acetylene. This was a possible cause of higher reactivity of ethylene (τ = 2 days) which would have a faster photochemical degradation rate, and this was similar in explaining the difference in concentration increases in n-pentane and propylene. Isobutane and n-butane would probably show changes in concentrations because of the possible contribution from LPG leakage as discussed in previous sections. The similarity in source contributions as well as atmospheric lifetimes should indicate similar enhancement in concentrations. However, the magnitude of increase in n-butane concentration was much greater (n-Butane: 7.7 times; isobutane: 4.8 times). This was probably the differential contributions of butanes from vehicle exhaust to the atmosphere (n-butane: 24%; isobutane: 16%). Propane was not from vehicle exhaust and so the magnitude of increase in concentration was much smaller (3.8 times), but this increase could be due to the LPG leakage contribution. However, we could not exclude the possibility of transport of natural gas emissions from different parts of continental Asia. This was because ethane showed about a 2-time enhancement, which might contribute from natural gas emissions or from the insignificant proportion from vehicle exhaust.

Ozone levels observed in our monitoring site dropped rapidly on the morning of 25 July (9:00) from about 27 ppbV to less than 2 ppbV (Figure 9.22b) due to the titration effect of fresh pollutants[69]. Then O_3 started to increase and peaked in the afternoon on 25 July with a concentration of 76 ppbV. The increasing O_3 concentration along with a preferential reduction in reactive NMHCs in the afternoon was most probably due to active photochemical O_3 production in the afternoon. In conclusion, from the enhancement and change in the relative distribution of the individual NMHCs during the episodic days in relation to their reactivity allows the identification of the local influences, which are mainly vehicle emissions and leakage of domestic LPG.

Figure 9.22 : Variation of (a) Total NMHC and (b) CO & O_3 during the Local Episode Period

(a)

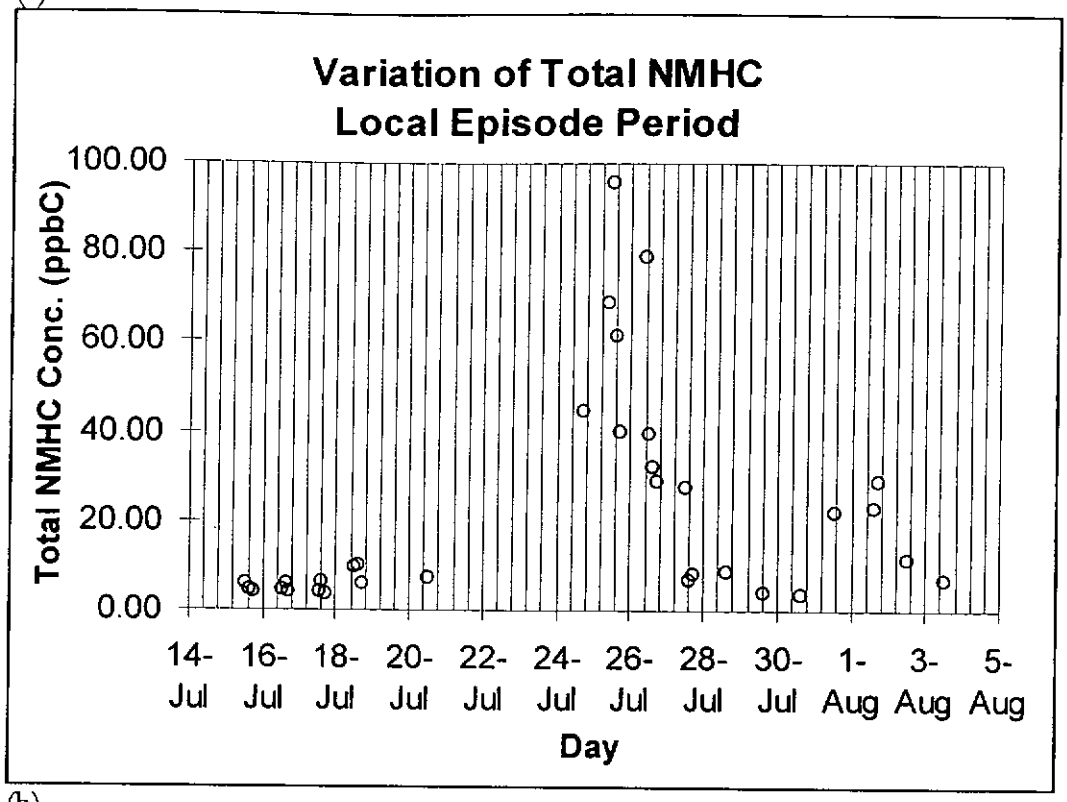

(b)

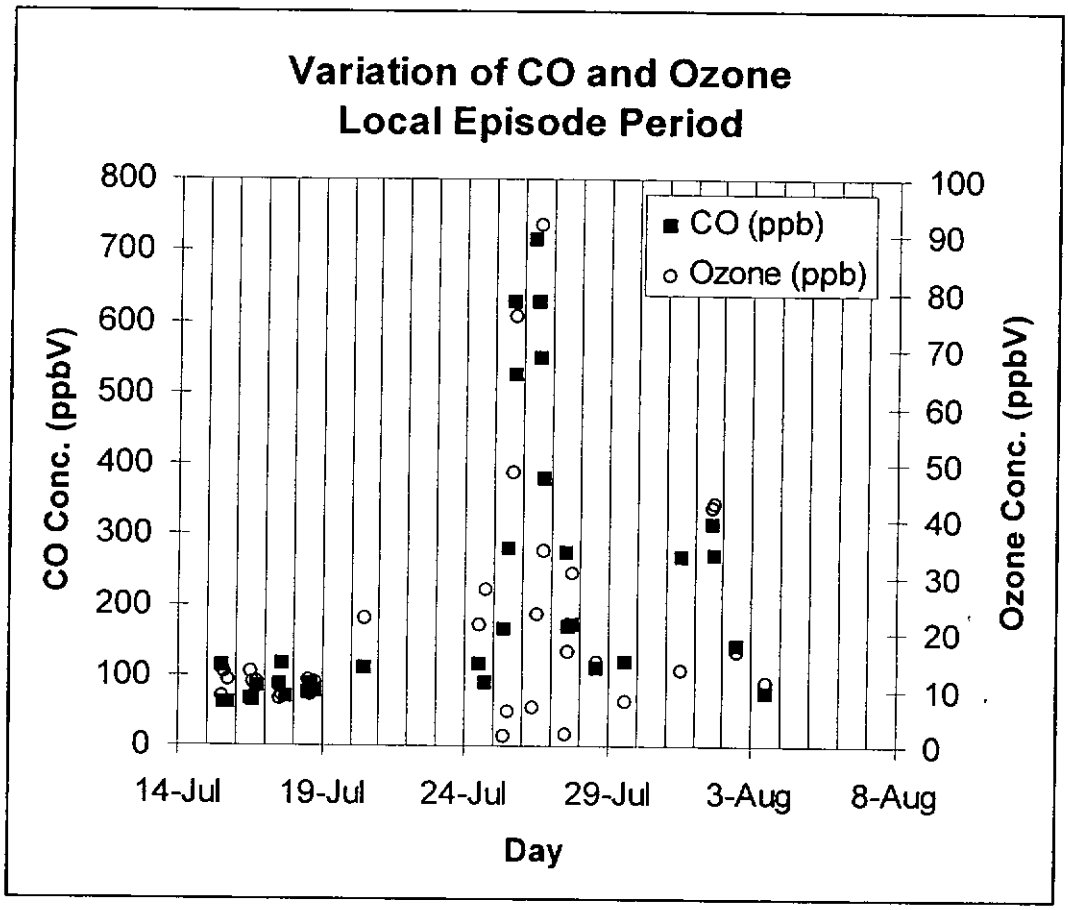

Figure 9.23 : Variation of NMHC during the Local Episode Period (a) C_2 to C_4 and (b) C_5 to C_6

(a) C_2 to C_4 NMHCs

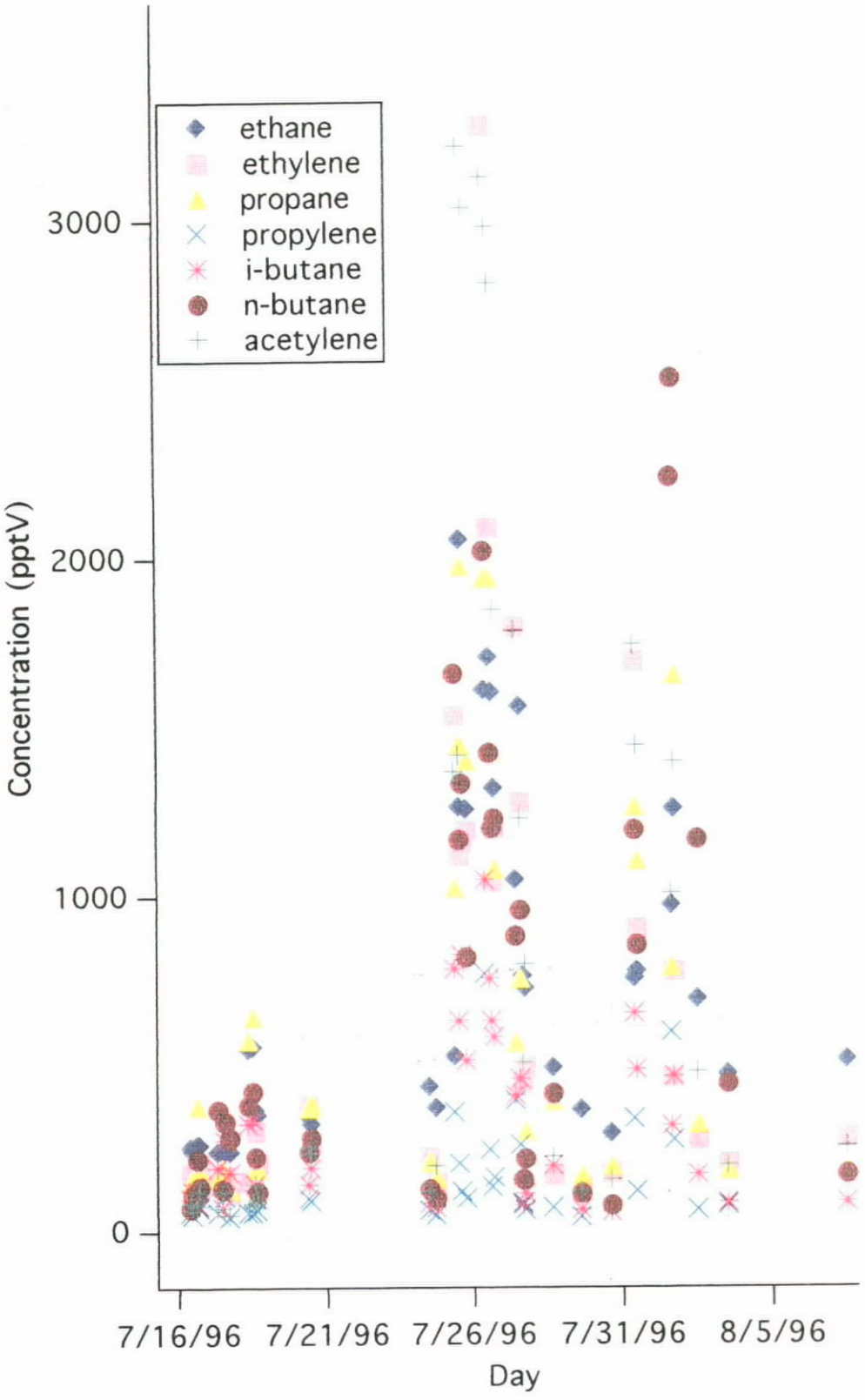

(b) C_5 to C_6 NMHCs

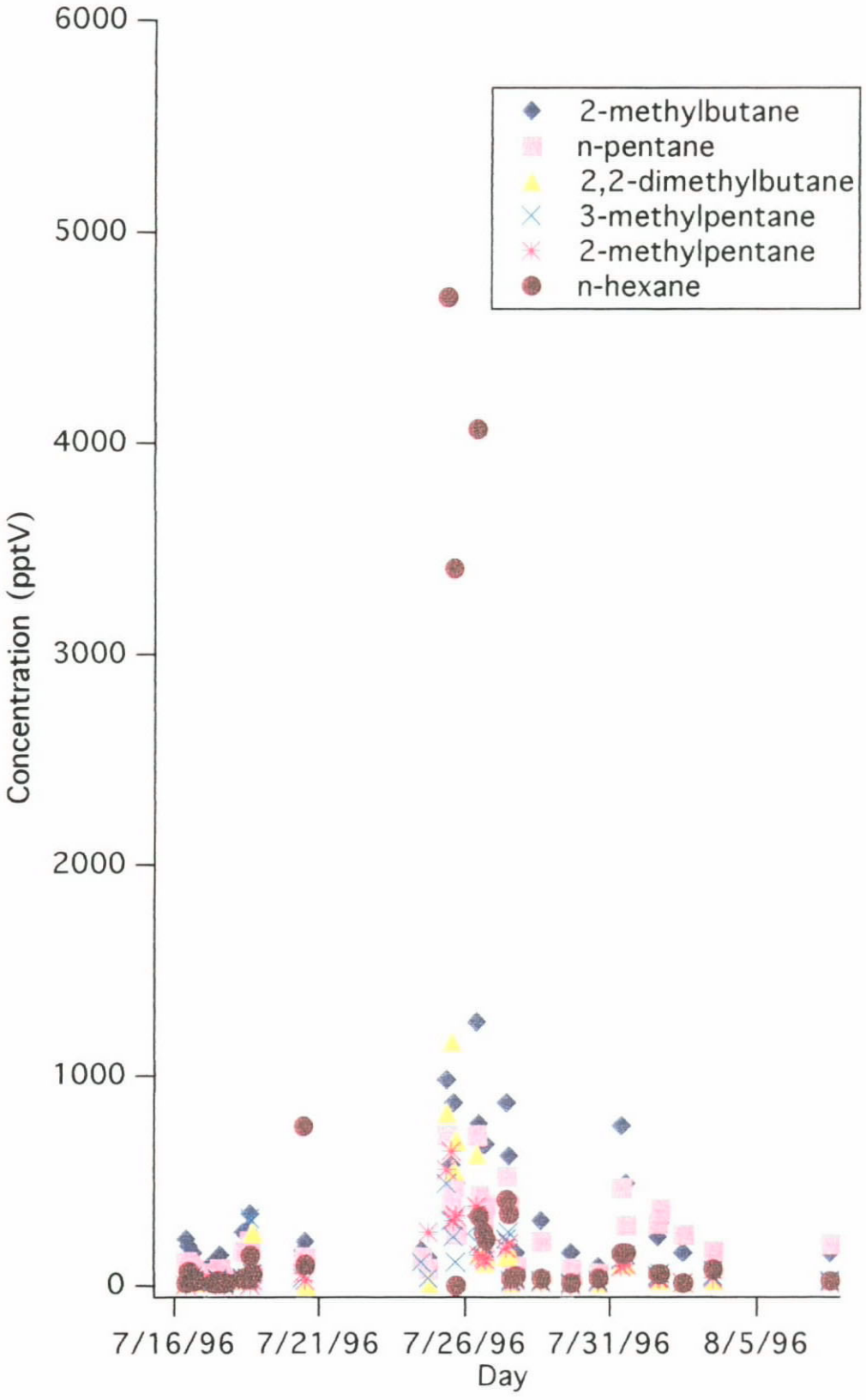

Figure 9.24 : Variation of Surface Wind Directions and Speed During the Local Episode Period

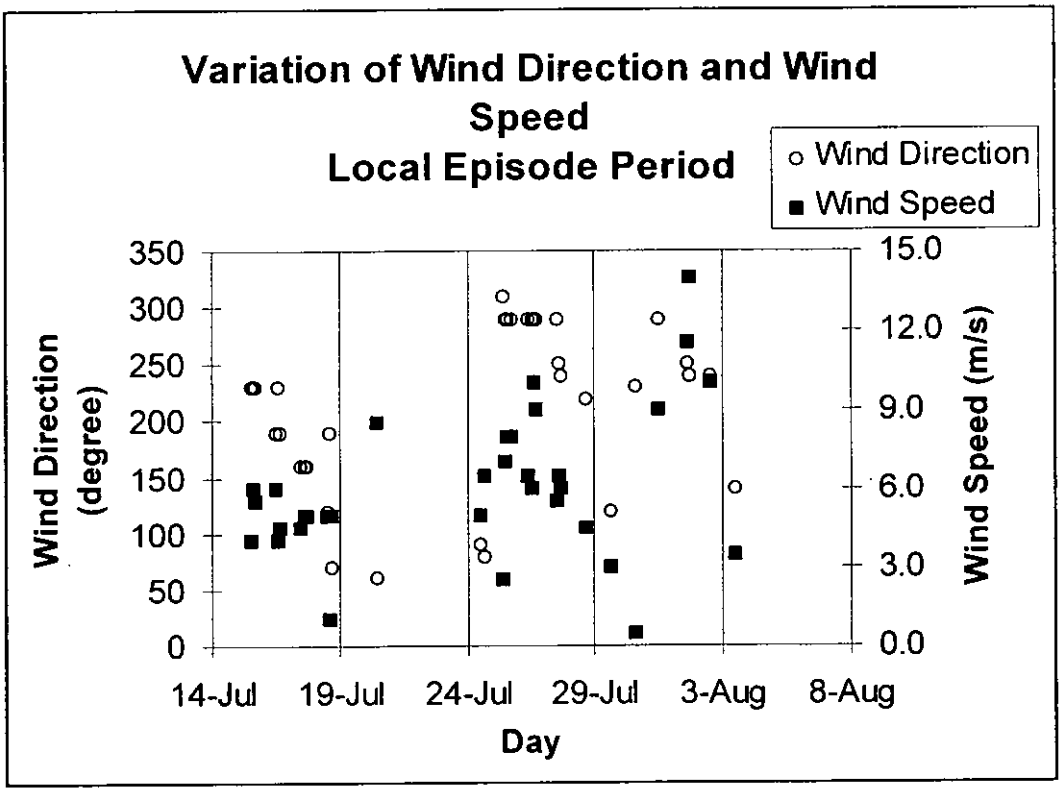

9.2. *Cold Front Episode Days*

Cold fronts are usually characterized by a sudden drop in ambient temperatures and drastically elevated concentrations of NMHCs and other pollutants species. A cold front was observed in 8 January. This cold front passed the South China coast on the morning of 8 January. On the approach of the cold front, easterly surface wind changed to strong northerly, with increasing wind speed from ~8 m/s to a maximum of 14 m/s at noontime (Figure 9.25). Temperature dropped from about 22°C to below 20°C for the following five days (Figure 9.26). Ozone decreased from a concentration of ~50 ppbV to 27 ppbV on the morning of 8 January and returned to 35 to 40 ppbV in the afternoon, while CO increased steadily from ~300 ppbV to ~900 ppbV in the afternoon (Figure 9.27). Peak total NMHC concentration exceeded 40 ppbC, which was 2 times the average level before the arrival of the cold front (Figure 9.27).

On 8th of January, all NMHC showed elevated concentrations, but the magnitude of increase in concentrations was much smaller as compared to the case in local episode days associated with "urban plumes" (Figure 9.28). Acetylene showed the fastest and greatest enhancement in concentration (3.8 times) on the day of arrival of the cold front, whereas ethylene was only slightly enhanced (1.5 times). This could possibly be due to the transport of relatively "aged" air masses to the station and/or the effect of ozone titration in the

morning. This was similar in n-pentane and propylene, which had similar percentage contributions from vehicle exhaust, while lesser enhancement was shown in the latter species. This was most probably due to the faster degradation of short-lived species (n-pentane τ = 5 days; propylene τ = 3 hours) or the difference in emission contribution of individual NMHC in different sources. However, propylene enhancement was greater than that of ethylene (2.4 times for propylene compared to 1.5 times for ethylene). This was a possible contribution of propylene from sources other than vehicle exhaust, such as industrial processes. There might also be the effect of the change in air mass climatology, which led to inhomogenous mixing of the pollutant emissions.

Other NMHCs, including isopentane, 2-methylpentane, 3-methylpentane, and n-hexane, have similar contribution from vehicle (~30-33%) and similar lifetimes (~4-5 days), and as a result, showed similar enhancement (2.5 to 3 times). The observations of the lower enhancement in these NMHCs also suggested that winds from northerly direction did not bring in C_6 hydrocarbons from emission sources located at the northwestern and western directions of the monitoring site as observed in the case of local episode.

In the afternoon of 18 Jan, meteorological conditions turned steady and the surface wind speed was high (14 m/s). Acetylene showed a slightly decrease in concentration and the magnitude of enhancement was 3.6 times as compared to 3.8 times in the morning sample. This was probably the effect of dilution due

to the strong wind[69]. Similar effect should be responsible for the reduced enhancement in concentrations in NMHCs including n-pentane, isopentane, 2-methylpentane, 3-methylpentane, and n-hexane.

In contrast, greater enhancement in concentrations of the following NMHC species was observed: ethylene (1.5 to 4.7 times), propylene (2.4 to 2.8 times), isobutane (1.2 to 1.7 times), and n-butane (1.3 to 1.5 times).

Ethylene showed a much greater enhancement (4.7 times) and the magnitude was even greater than that in acetylene (3.8 times). It was possible that during most of the time in winter, the more photochemically "aged" air masses from the Asian continent were transported to our monitoring station. Ethylene, as a reactive alkene (τ = 2 days), degraded relatively faster than that of acetylene (τ = 23 days). This meant that concentration of ethylene decreased faster in the air masses after a certain degree of photochemical degradation. This would result in a lower background concentration of ethylene relative to that of acetylene in the winter.

During the cold front, strong continental outflow air masses brought the Asian continental emissions, including mostly the vehicle emissions, to the South China coastal regions at high wind speed. The transport time would be much shorter and so these emissions would undergo much less photochemical

processing. Other possible reasons would be the additional effects of reduced temperature on the lower rate of photochemical reactions.

Therefore the magnitude of enhancement in concentration of ethylene was more due to the lower background concentration as well as lesser degree of photochemical processing in the atmosphere. Similar conditions were reflected in the case of propylene, but the lower percentage of contribution from vehicle exhaust resulted in lesser enhancement as compared to that of ethylene.

Figure 9.25 : Variation of Surface Wind Direction and Speed in the Cold Front Period

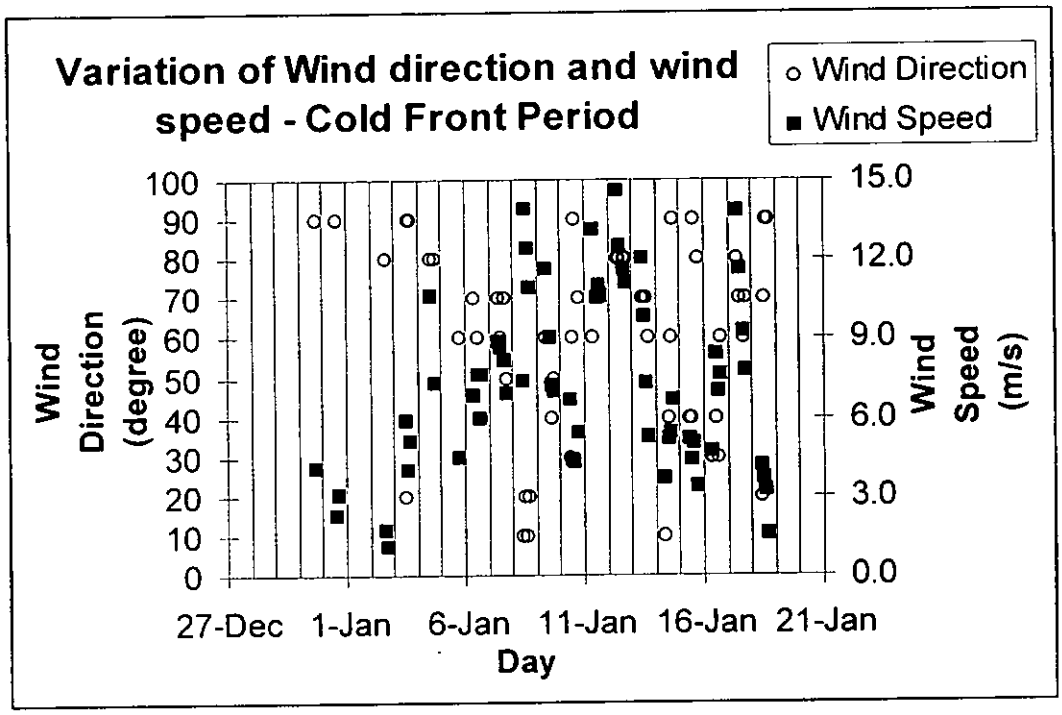

Figure 9.26 : Variation of Temperature in the Cold Front Period

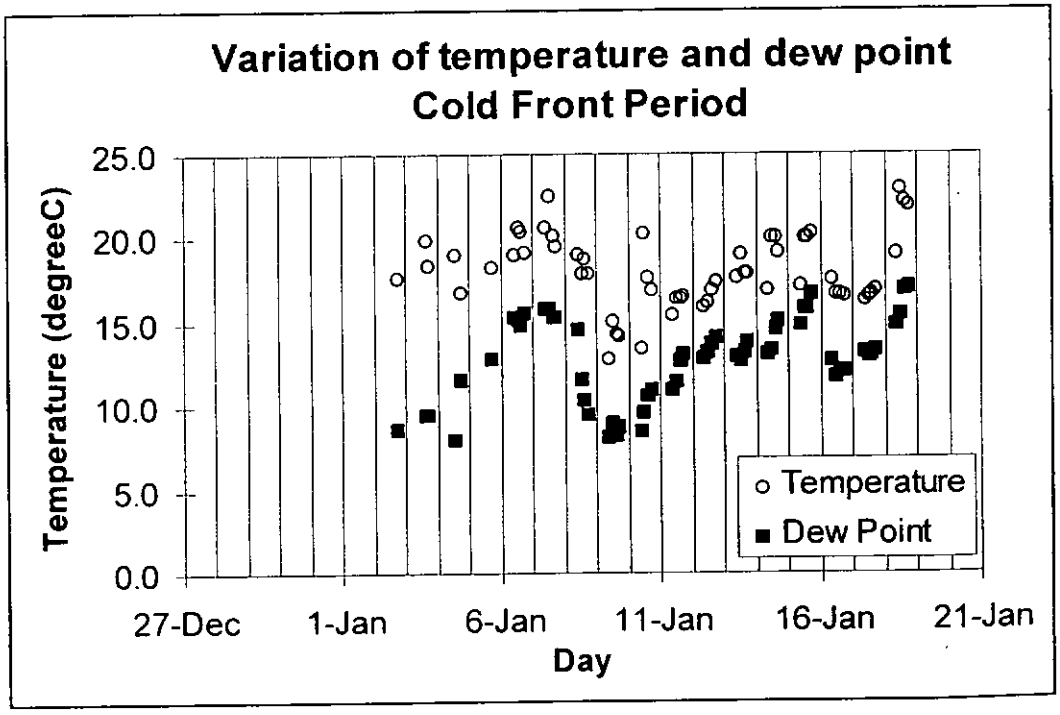

Figure 9.27 : Variation of (a) Total NMHC and (b) CO & O_3 during the Cold Front Period

(a)

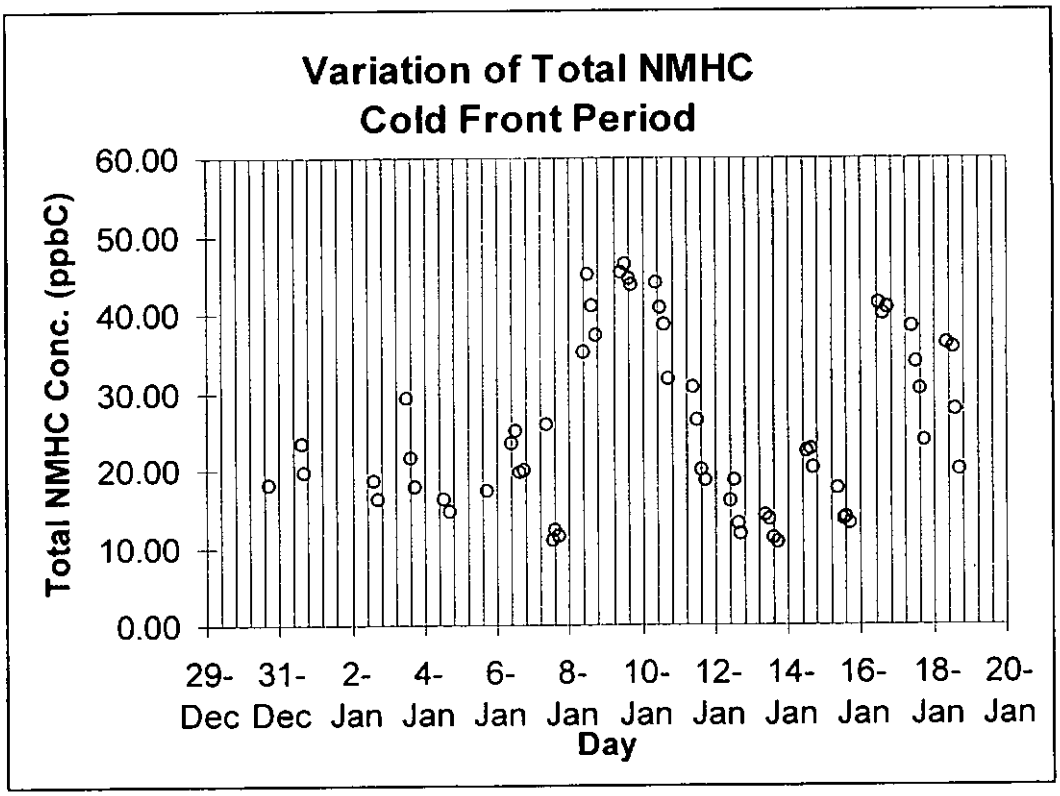

(b)

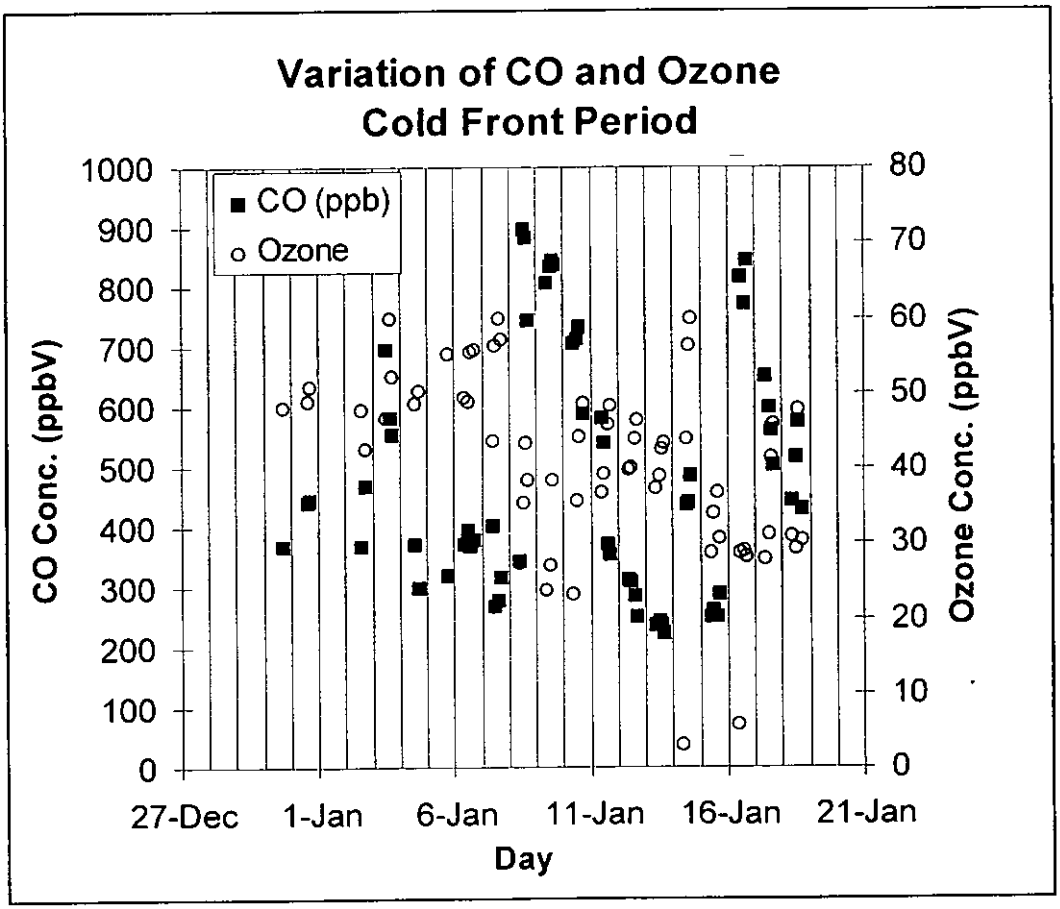

Figure 9.28 : Variation of NMHC during the Cold Front Period (a) C_2 to C_4 and (b) C_5 to C_6

(a) C_2 to C_4 NMHCs

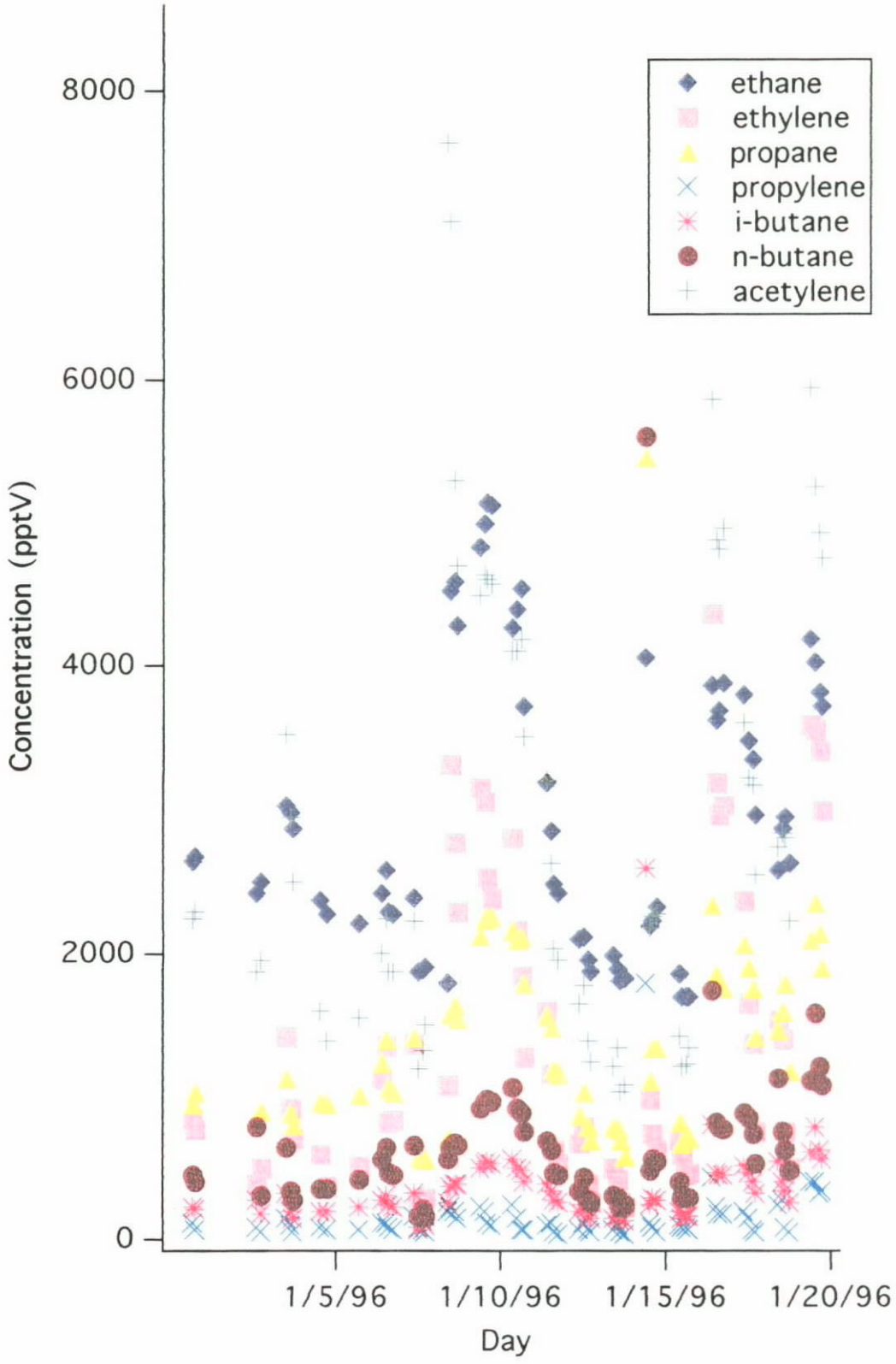

(b) C_5 to C_6 NMHCs

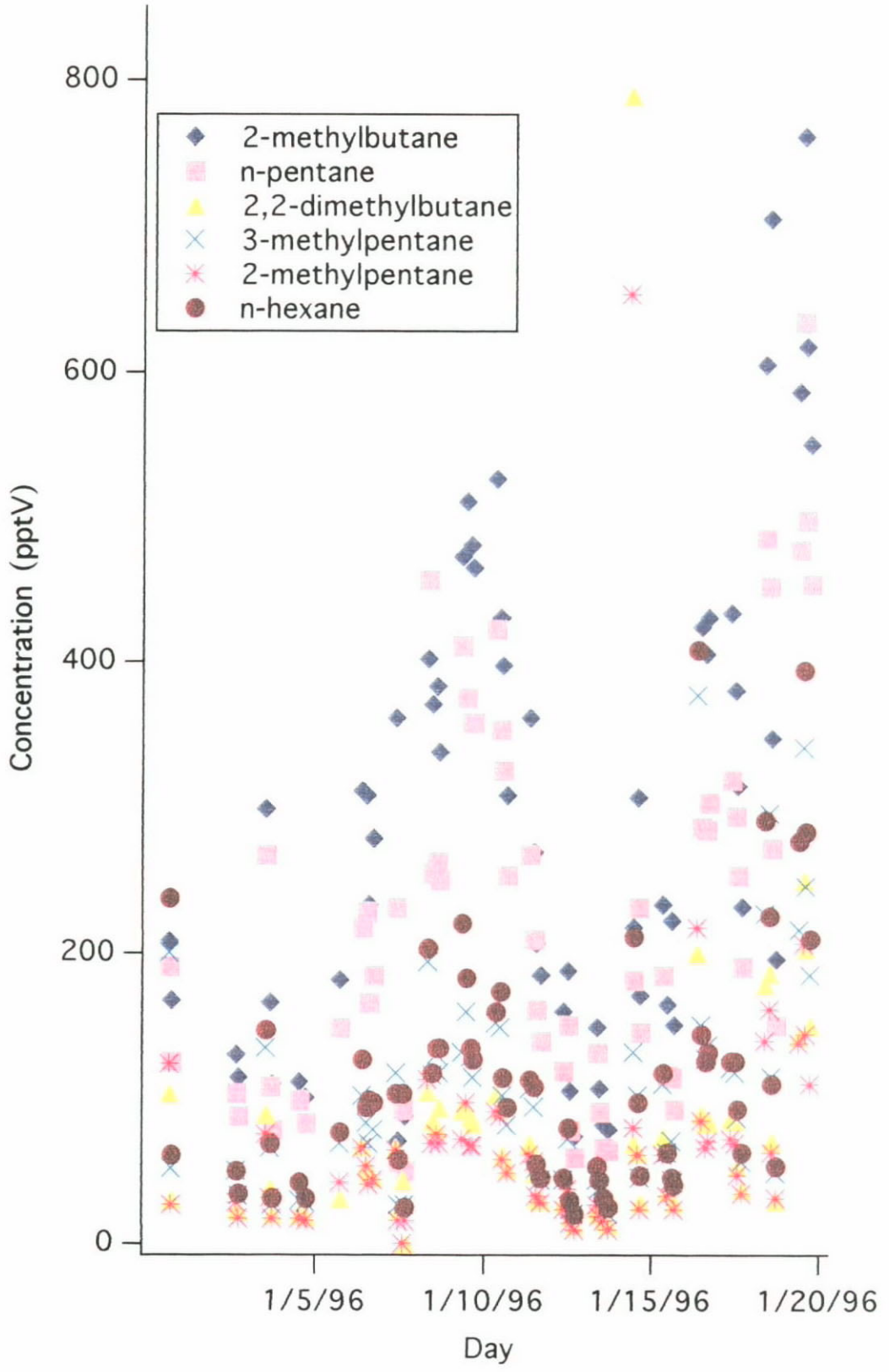

9.3. Comparison with Other Measurements in the Region

A quantitative comparison was made between the NMHC levels measured in Hong Kong and those measured during PEM-West A & B experiments[66,68], which was the most recent NMHC data set gathered in the region near to Hong Kong. The data sets from the PEM-West A & B experiments were based on aircraft expeditions and provided limited time coverage of the period during summer & fall in 1991 and late winter & early spring in 1994, respectively.

The comparison of NMHC levels between the two data sets are shown in Table 9.20. Our data set showed higher NMHC concentrations during Feb-Mar'96 as compared to that during Sep-Oct'96. Similar observations were made during the PEM-West experiments: which demonstrated that more pollutants were transported from the continent to the Pacific[70] by the Asian continental outflow during late winter & early spring (Feb-Mar'94) than in the summer and fall period.

Table 9.20 : Measured NMHC Levels at and near Hong Kong: Comparison between Our Data Set and PEM-West A & B Data Sets

	Our Data Set (Sep & Oct'96) (n=31)				PEM-A Period (Sep & Oct'91) <2km	
Species (pptv)	average	S.D.	median	range	median	range
Ethane	868	339	771	393-1512	634	302-3100
Ethylene	274	153	252	73-894	25	5-5183
Propane	464	257	489	65-1343	44	5-4237
Propylene	59	24	56	20-104	10	<3-1148
iso-Butane	195	160	140	17-678	6	<3-2801
n-Butane	335	300	247	21-1380	9	<3-4805
Acetylene	673	392	606	142-1683	103	16-3327
1-Butene	20	10	19	7-50	4	<3-389
2-methylbutane	202	181	135	11-743	3	<3-4407
n-Pentane	158	137	92	9-440	4	<3-2457
2,2-dimethylbutane	35	40	26	4-202		
3-methylpentane	36	25	30	10-109		
2-methylpentane	23	16	18	4-65		
n-Hexane	30	21	25	3-87	<3	<3-995

* *All concentration in pptV*

	Our Data Set (Feb & Mar'96) (n=65)				PEM-B Period (Feb & Mar'94) <2km	
Species (pptv)	average	S.D.	median	range	median	range
Ethane	2358	922	2554	506-3591	994	153-2658
Ethylene	972	705	768	189-2751		
Propane	1086	552	1193	97-2471	107	0-1112
Propylene	138	79	122	40-410		
iso-Butane	277	143	269	28-755		
n-Butane	491	280	472	45-1456		
Acetylene	1989	1142	2146	175-4118	277	4-1886
1-Butene	44	24	38	11-105		
2-methylbutane	242	135	212	43-774		
n-Pentane	185	111	156	35-664		
2,2-dimethylbutane	45	40	31	9-230		
3-methylpentane	68	54	49	14-292		
2-methylpentane	41	34	28	8-186		
n-Hexane	78	57	59	22-297		

* *All concentration in pptV*

In terms of the reported median values, the levels of major NMHCs like ethane, propane, ethylene and acetylene measured at the Hong Kong ground station were 1-10 times higher than those reported for the PEM-West A and B missions. Even greater difference in measured levels were observed for minor components like n-butane, isobutane, 1-butene, and C_5 alkanes.

There are several reasons for the higher levels of NMHC observed in our data set. The first obvious reason was deduced from the greater difference observed between the data sets in the late winter and early spring period that the continental outflow air masses were bringing a much higher level of NMHCs to Hong Kong, while their impact was expected to lessen in the more distant West and South Pacific due to dilution with clean oceanic air and photo-degradation in the long-range transport process. Secondly, higher NMHC levels were expected to be measured at the ground level compared to sampling carried out at high attitudes during the PEM-West A & B experiments. The lowest sampling height in the PEM-West aircraft expeditions was limited to about 400 m above sea level.

The PEM-West data sets also showed that there was a strong altitudinal gradient of the NMHC levels with higher NMHC levels at lower altitudes. This altitudinal gradient was even greater during the PEM-West B period as compared to the PEM-West A period.

Despite the difference in NMHC levels measured, the two sets of data show the same seasonal variation trends. Our observed data also indicated that the impact of Asian continental outflow was great in the Asian coastal region, especially during the winter and spring seasons.

10. Conclusions

10.1. Summary of Major Findings

A dedicated air sampling and gas chromatographic analysis system was built to measure parts-per-trillion (pptV) to parts-per-billion (ppbV) levels of non-methane hydrocarbons (NMHC) at a coastal rural background air monitoring station in Hong Kong. The accuracy of analysis was successfully validated by inter-laboratory comparison of calibrated NMHC standards and ambient air samples provided by Dr. D.R. Blake, Department of Chemistry, University of California (Irvine), U.S.A. Another dedicated system was built for measurement of atmospheric methane.

NMHCs were measured at a coastal ground station located at Cape D'Aguilar, Hong Kong for the period Oct'95 to Mar'97 on a near daily basis. This is the first annual NMHC data set collected in the South China coastal region. Monthly averages of total C_2-C_6 NMHC concentrations were in the range of 10 - 50 ppbC (on per carbon basis), with alkanes accounting for 60% of the total concentration, which were typical for rural/non-urban environments.

The NMHCs exhibited a strong seasonal variation. This seasonal variability is caused by the change in air mass climatology during different seasons. The seasonal variation of NMHCs is attributed to the dominant influence of outflow of Asian continental air masses in the winter, and inflow of

Pacific maritime air masses in the summer. The origin of air masses reaching Hong Kong was analyzed and classified by 10-day back trajectory calculations.

Relatively high levels of measured NMHCs, characterized by a higher % acetylene content, were associated with continental air masses encountered in Hong Kong. The winter total NMHC concentration had a very good correlation ($r^2 > 0.8$) with acetylene, suggesting that vehicle emission and biomass burning are major contributory sources to NMHC pollution derived from the outflow of Asian continental air masses. Good linear correlations ($r^2 > 0.8$) were also found between signature NMHC species derived from liquefied petroleum gas (LPG) or natural gas, suggesting the co-occurrence of LPG/natural gas leakage as another NMHC contributory source.

Low NMHC concentrations were observed in the summer as compared to that in the winter. The NMHC concentration in the summer data set show no clear correlation among NMHC species of known anthropogenic sources. The low NMHC concentrations may reflect the clean southern hemispheric air being transported to the coastal regions of Asia. This was also supported by the back trajectory analysis showing that maritime air masses from South and West Pacific Ocean could reach Hong Kong in the summer months.

Our data set is in qualitative agreement with the findings of the NASA Pacific Exploratory Missions (PEM-West A & B) which also observed higher

NMHC levels during late winter and early spring, and lower NMHC levels in the summer and early autumn. The PEM-West A & B studies were aircraft-based measurements with flight path stretching a large part of Western Pacific (north to Japan, and south to Singapore and Indonesia), but only of limited time span. In contrast, our data set is based on continuous measurement at a coastal site. Therefore our data set is more comprehensive in providing information on meteorological, micro-meteorological, estimation of emission sources and time span effects on pollution levels at Hong Kong and its neighbouring regions.

The concentrations of NMHCs observed at the monitoring site could be strongly influenced by the changes. More 10 folds increase in total NMHC concentrations was observed on local episode days when surface winds were sweeping urban pollutants direct onto the air monitoring station.

During cold front days in the winter, the measured total NMHC levels were increased by 2 folds due to the greater anthropogenic emission loading in the continental air masses. The chemical composition and characteristics of the continental air masses vary with time of the cold front period. The surface wind speed increased to 14 m/s or higher, contribution from photochemical "less aged" air masses, as indicated by the highest % content of reactive species like propylene and ethylene, were observable in the associated NMHC measurements.

10.2. Suggestions for Future Work

The results presented in this work is a broad overview of the meteorological factors and possible emission sources which determine the NMHC levels measured at the Hong Kong Polytechnic University Air Monitoring Station. This study underlined the need to identify and characterize different air masses transported to Hong Kong. More detailed source emission inventories could be collected for quantitative in-depth analysis of the relative contributions of different emission sources to the NMHCs measured.

Another aspect of work is more detailed and specific characterization of air masses encountered at Hong Kong. A possible approach is principal component analysis, in which the concentrations measured trace gas pollutants, including NMHCs, CO, and O_3, are statistically correlated for commonality associated with a certain type of pollution conditions. Another approach is using the ratios analysis of trace gases, e.g. acetylene/CO or propane/ethane. The magnitude and the relative changes of these ratios may indicate the relative ages of the air masses observed.

By a combination of in-depth analysis, the specific conditions and "fingerprint" pollution profiles associated with different types of air masses will be established. The findings of these studies will contribute to a better understanding of the many factors which influence the pollution and air quality at Hong Kong and its neighbouring regions.

REFERENCES

1. Singh H.B. and Zimmerman P.B. (1992) Atmospheric Distribution and Sources of Nonmethane Hydrocarbons, in Gaseous Pollutants: Characterization and Cycling, edited by Jerome O. Nriagu. pp. 177-235.
2. Steven R.K., Lewis C.W., Lonneman W.A, Rasmussen R.A., Klouda G.A., Ellenson W. and Dattner S.L. (1994) Methods to determine the biogenic contributors to ambient concentrations of volatile organic compounds. Proc. *U.S. EPA/A & WMA Int. Symp. on Measurement of Toxic Related Air Pollutants*, Durham, North Carolina, VIP-39, pp. 847-848. Air & Waste Management Association, Pittsburgh, Pennsylvania.
3. Demerjian K.L., Kerr J.A., and Calvert J.G. (1974) The mechanism of photochemical smog formation, *Adv. Environ. Sci. Technol.*, **4**, 1-262.
4. Robinson E. and Robbins R. (1969) Source, Abundance and Fate of Gaseous Atmospheric Pollutants Supplement. Stanford Research Institute, Menlo Park, CA.
5. Zimmerman P.R., Chatfield R.B., Fishman J., Crutzen P.J., and Hanst P.L. (1978). Estimates on the production of CO and H_2 from the oxidation of hydrocarbon emissions from vegetation. *Geophys. Res. Lett.*, 5, 679-682.
6. Swinnerton J.W. and Linnenbom V.J. (1967) Determination of the C_1-C_4 hydrocarbons in sea water by gas chromatography. *Journal of Gas Chromatography*, 5, 570-573.
7. Lamontagne R.A., Swinnerton J.W., and Linnenbom V.J. (1974) C_1-C_4 hydrocarbons in the North and South Pacific, *Tellus*, 71-77.
8. Swinnerton J.W. and Lamontagne R.A. (1974) Oceanic distribution of low molecular weight hydrocarbons, baseline measurements. *Environ. Sci. and Technol.*, **8**, 657-663.
9. Wagner, J.K., Walters R.A., Maiocco L.J., and Neal D.R. (1986) Development of the 1980 NAPAP emissions inventory. *U.S. Environmental Protection Agency, Official Research Development*, [Rep.] EPA600/7-86-57a.
10. Zimmerman D., Tax W., Smith M., Demmy J., and Battye R. (1988) Anthropogenic emissions data for the 1985 NAPAP inventory. *U.S. Environmental Protection Agency, Official Research Development.* [Rep.] EPA-600/7-88-022.
11. U.S. Environmental Protection Agency (USEPA) (1990). *National Air Pollution Emission Estimates 1940-1988.* USEPA, Washington, DC, EPA-450/4-90-001.
12. Middleton P., and W. Stockwell. (1990) Aggregation and analysis of volatile organic compound emissions for regional modeling. *Atmos. Environ.*, 24A, 1107-1133.

13. National Acid Precipitation Assessment Program (NAPAP) (1990) *NAPAP State of Science and Technology.* U.S. Government Printing Office, Washington, DC, Vol. 1.

14. Altshuller A.P. (1983) National volatile organic substances and their effect on air quality in the United States. *Atmos. Enviorn.* 17, 2131-2165.

15. Duce R.A., Mohnen V.A., Zimmerman P.R., Grosjean D., Cautreels W., Chatfield R., Jaenicke R., Ogren J.A., Pellizzari E.D., and Wallace G.T. (1983) Organic material in the global troposphere. *Rev. Geophys.* 21, 921-952.

16. Lamb B., Guenther A., Gay D., and Westberg H. (1987) A national inventory of biogenic hydrocarbon emissions. *Atmos. Environ.* 21, 1695-1705.

17. National Academy of Sciences (NAS) (1976) *Vapor-Phase Organic Pollutants: Volatile Hydrocarbons and Their Oxidation Products.* National Academy of Sciences Press, Washington, D.C.

18. Ehhalt D.H., Rudolph J., and Schmidt U. (1986) On the importance of light hydrocarbons in multiphase atmospheric systems. In Jaeschke W., ed., *Chemistry of Multiphase Atmospheric Systems.* Springer-Verlag, Berlin, pp. 321-350.

19. Greenberg J.P., Zimmerman P.R., Heidt L., and Pollock W. (1984) Hydrocarbon and carbon monoxide emissions from biomass burning in Brazil. *J. Geophys. Res.* 89, 1350-1354.

20. Hegg D.A., Radke L.F., Hobbs P.W., Rasmussen R.A., and Riggan J.P. (1990) Emissions of some trace gases from biomass fires. *J. Geophys. Res.* 95, 5669-5675.

21. Lobert J.M., Scharffe D.H., Kuhlbusch T.A., Seuwen R., and Crutzen J.P. (1991) Experimental evaluation of biomass burning emissions: Nitrogen and carbon containing compounds. In J.S. Levine, ed., *Global Biomass Burning.* MIT Press, Cambridge, MA.

22. Andreae M.O., Ferek J.R., Bermond F., Byrd K.P., Engstrom R.T., Hardin S., Houmere P.D., Lemarrec F., and Raemdonk H. (1985) Dimethyl sulfide in the marine atmosphere. *J. Geophys. Res.* 90, 12,891-12,900.

23. Bonsang B., Kanakidou M., Lambert G., and Monfray P. (1988) The marine source of C_2-C_5 aliphatic hydrocarbons. *J. Atmos. Chem.* 6, 3-20.

24. Plass, C., Johner F.J., Koppmann R., and Rudolph J. (1989) The latitudinal distribution of NMHC in the Atlantic and their fluxes into the atmosphere. *Physico-Chemical Behavior of Atmospheric Pollutants, Varnese, Italy, September, 1989.*

25. Blake D.R. and Rowland F.S. (1995) Urban Leakage of Liquefied Petroleum Gas and Its Impact on Mexico City Air Quality, *Science,* 269, 953-956.

26. Blake D.R., Smith T.W.Jr., Chen T.Y., Whipple W.J., and Rowland F.S. (1994) Effects of biomass burning on summertime nonmethane hydrocarbon concentrations in the Canadian wetlands, *J. Geophys. Res.*, **99**, D1, 1699-1719.

27. Sigsby J.E., Tejada S., and Ray W. (1987) Volatile organic compound emissions from 46 in-use passenger cars. *Environ. Sci. Technol.* **21**, 466-475.

28. Rasmussen, R.A., and Khalil M.A.K. (1983) Atmospheric benzene and toluene. *Geophys. Res. Lett.* 10, 1096-1099.

29. Ehhalt D.H., Rudolph J., Meixner F., and Schmidt U. (1985) Measurements of selected C_2-C_5 hydrocarbons in the background troposphere: Vertical and latitudinal variations. *J. Atmos. Chem.* 3, 29-52.

30. Kanakidou M., Singh H., Valentin K., and Crutzen P. (1991) A 2-D study of ethane and propane oxidation in the troposphere. *J. Geophys. Res.* **96(ND8)**, 5395-5413, 1991.

31. Singh H.B. (1980) Guidance for the collection and use of ambient hydrocarbon species data in development of ozone control strategies. *U.S. Environ. Prot. Agency, Off. Air Qual. Plann. Stand. [Tech. Rep.]* **EPA 450/14-80-008.**

32. Rudolph J., Khedim A., Bonsang B. (1992) *J. Geophys. Res.*, 97, 6181-6186.

33. Sexton K. and Westberg H. (1984) Nonmethane hydrocarbon composition of urban and rural atmospheres. *Atmos. Environ.*,**18**, 1125-1132.

34. Singh, H.B., Salas L.J., Cantrell B.K., and Redmond R.M. (1985) Distribution of aromatic hydrocarbons in the ambient air. *Atmos. Environ.*, **19**, 1911-1919.

35. Seila R.L., Lonneman W., and Meeks S. (1989) Determination of C_2 to C_{12} ambient air hydrocarbons in 39 U.S. cities, from 1984 through 1986. *U.S. Environ. Prot. Agency, Off. Res. Dev. [Rep.]* **EPA/600/S3-89/058.**

36. Colbeck I. and R.M. Harrison (1985) The concentrations of specific C_2-C_6 hydrocarbons in the air of NW England. *Atmos. Environ.*, **19**, 1899-1904.

37. Nelson P.F. and Quigley S.M. (1982) Non-methane hydrocarbons in the atmosphere of Sydney, Australia. *Environ. Sci. Technol.*, **16**, 650-655.

38. Nelson P.F., Quigley S.M., and Smith M.Y. (1983) Sources of atmospheric hydrocarbons in Sydney: a quantitative determination using a source reconciliation technique. *Atmos. Environ.*, **17**, 439-449.

39. Hov, ϕ., Schmidbauer N., and Oehme M. (1991) C_2-C_5 hydrocarbons in rural South Norway. *Atmos. Environ.*, **25A**, 1981-1999.

40. Greenberg J.P. and Zimmerman P.R. (1984) Nonmethane hydrocarbons in remote tropical, continental and marine atmospheres. *J. Geophys. Res.*, **89**, 4767-4778.

41. Rasmssen R.A. (1972) What do the hydrocarbons from trees contribute to air pollution? *J. Air Pollut. Control Assoc.*, 22, 537-543.

42. Zimmerman P.R. (1979) Testing of hydrocarbon emissions from vegetation, leaf litter and aquatic surfaces and development of a methodology for compiling biogenic emission inventories. *U.S. Environ. Prot. Agency, Off. Air Qual. Plann. Stand. [Tech. Rep.]* EPA-450/4-79-004.

43. Isidorov V.A., Zenkench I.G., and Iofe B.V. (1985) Volatile organic compounds in the atmosphere of forests. *Atmos. Environ.* 19, 1-18.

44. Tingey D. (1981) The effect of environmental factors on the emission of biogenic hydrocarbons from live oak and slash pine. In J. Bufalini and R. Arnts, eds., *Atmospheric Biogenic Hydrocarbonsi.* Ann Arbor Sci. Publ., Ann Arbor, MI, pp. 53-72.

45. Tingey D., Turner D., and Weber U. (1991) Factors controlling the emissions of monterpinesh and other volatile organics. In Sharkey T., Holland E., and Mooney H., eds., *Trace Gas Emissions from Plants.* Academic Press, San Diego, CA.

46. Selia R.L. (1984) Atmospheric volatile hydrocarbon composition at five remote sites in Northwestern North Carolina, In Aneja V., ed., *Environmental Impact of Natural Emissions.* pp. 125-140.

47. Donahue N.M. and Prinn R.G. (1993) In situ nonmethane hydrocarbon measurements on SAGA 3, *J. Geophys. Res.*, **98**, 16,915-16,932.

48. Atlas E., Pollock W., Greenberg J., Heidt L., and Thompson A.M. (1993) Alkyl nitrates, nonmethane hydrocarbons, and halocarbon gases over the equatorial Pacific Ocean during SAGA 3, *J. Geophys. Res.*, **98**, 16,933-16,949.

49. Wallace J.M. (1977) Atmospheric Science: an introductory survey. Academic Press, New York.

50. Harris J.M. and Kahl J.D.W. (1994) An analysis of 10-day Isentropic Flow Patterns for Barrow, Alaska: 1985-1992, *J. Geophys. Res.*, **99, D12**, 25,845-25,855.

51. Harris, J.M., The GMCC atmospheric trajectory program, NOAA Tech. Memo, ERL-ARL-116, 30pp., NOAA Environmental Research Laboratories, Boulder, CO, 1982.

52. Harris, J.M. and B.A. Bodhaine (eds.), Geophysical Monitoring for Climate Change, No. 11: Summary Report 1982, pp. 67-75, NOAA Environmental Research Laboratories, Boulder, CO, 1983.

53. Greenberg J.P., Zimmerman P.R., Pollock W.F., Lueb R.A., and Heidt L.E. (1992) Diurnal variability of atmospheric methane, nonmethane hydrocarbons, and carbon monoxide at Mauna Loa. *J. Geophys. Res.*, 97, D10, 10,395-10,413.

54. Pate B., Jayanty R.K.M., Peterson M.R., Evans G.F. (1992) *J. Air Waste Management Assoc.* 42, 460-462.

55. Jennings W. (1980) Gas chromatography with glass capillary columns, 2nd ed., pp. 215-217, Academic Press, New York.

56. Smith T.W.Jr. (1993) Summertime tropospheric nonmethane hydrocarbon and halocarbon concentrations over central and eastern Canada during ABLE-3B, Ph.D. Dissertation, University of California, Irvine.

57. Chen T.Y. (1996) Three-dimensional distribution of nonmethane hydrocarbons and halocarbons over the Northwestern Pacific and the temporal and spatial variations of oceanic methyl iodide emissions, Ph.D. Dissertation, University of California, Irvine.

58. Westberg H. and Zimmerman P. (1993) Analytical methods used to identify nonmethane organic compounds in ambient atmospheres, in *Measurement Challenges in Atmospheric Chemistry, American Chemical Society, 1993.*

59. Boudries H., Toupance G., and Dutot A.L. (1994) Seasonal variation of atmospheric nonmethane hydrocarbons on the western coast of Brittany, France, *Atmos. Envir.*, 28, 1095-1112.

60. Lindskog A. and Moldanova J. (1994) The influence of the origin, season and time of the day on the distribution of individual NMHC measured at Rörvik, Sweden. *Atmos. Envir.*, 28, 2383-2398.

61. Singh H.B. and Salas L.J. (1982) Measurement of selected light hydrocarbons over the Pacific Ocean: latitudinal and seasonal variations. *Geophy. Res. Lett.* 9, 842-845.

62. Singh H.B., Viezee W. and Salas L.J. (1988) Measurements of selected C_2-C_5 hydrocarbons in the troposphere: latitudinal, vertical, and temporal variations. *J. Geophys. Res.* 93, 15,861-15,878.

63. Chiu T.N. and So C.L. (1986) A geography of Hong Kong, 2nd Edition, Oxford University Press.

64. Xu X.B., Xiang R.B., Ding G.A., and Li X.S. Continental background NMHC concentration, composition, and relation to surface O_3 (Volume and year to be attached), pp.67-81.

65. Whitby R.A. and Altwicker E.R. (1978) Acetylene in the atmosphere: sources, representative ambient concentrations and ratios to other hydrocarbons. *Atmos. Envir.* **12**, 1289-1296.

66. Blake D.R., Chen T.Y., Smith T.W.Jr., Wang C.J.L., Wingenter O.W., Blake N.J. and Rowland F.S. (1996) Three-dimensional distribution of nonmethane hydrocarbons and halocarbons over the northwestern Pacific during the 1991 Pacific Exploratory Mission (PEM-West A). *J. Geophys. Res.* **101, D1**, 1763-1778.

67. Lonneman W.A., Kopczynski S.L., Darley P.E. and Shutterfield F.D. (1974) Hydrocarbon composition of urban pollution. *Envir. Sci. Tech.* **8**, 229-336.

68. Gregory G.L., Merrill J.T., Shipham M.C., Blake D.R., Sachse G.W., and Singh H.B. (1996) Chemical characteristics of tropospheric air over the Pacific Ocean as measured during PEM West-B: Relationship to Asian outflow and trajectory history, *J. Geophys. Res.*, In Press.

69. Wang T., Lam K.S., Lee A.S.Y., Pang S.W., and Tsui W.S. (1997) Meteorological and chemical characteristics of the photochemical ozone episodes observed at Cape D'Aguilar in Hong Kong. *J. App. Met.*, in press.

70. Merrill J.T. (1996) Trajectory results and interpretation for PEM-West A, *J. Geophys. Res.*, **101, D1**, 1679-1690.